A 3D COMPUTER MODEL INVESTIGATION OF BIOFILM DETACHMENT AND PROTECTION MECHANISMS

by

Jason Daniel Chambless

A dissertation submitted in partial fulfillment
of the requirements for the degree

of

Doctor of Philosophy

in

Engineering

MONTANA STATE UNIVERSITY
Bozeman, Montana

April 2008

APPROVAL

of a dissertation submitted by

Jason Daniel Chambless

This dissertation has been read by each member of the dissertation committee and has been found to be satisfactory regarding content, English usage, format, citation, bibliographic style, and consistency, and is ready for submission to the Division of Graduate Education.

Dr. Philip S. Stewart

Approved for the Department of Engineering

Dr. Ronald Larsen

Approved for the Division of Graduate Education

Dr. Carl A. Fox

STATEMENT OF PERMISSION TO USE

In presenting this dissertation in partial fulfillment of the requirements for a doctoral degree at Montana State University, I agree that the Library shall make it available to borrowers under rules of the Library. I further agree that copying of this dissertation is allowable only for scholarly purposes, consistent with "fair use" as prescribed in the U.S. Copyright Law. Requests for extensive copying or reproduction of this dissertation should be referred to ProQuest Information and Learning, 300 North Zeeb Road, Ann Arbor, Michigan 48106, to whom I have granted "the exclusive right to reproduce and distribute my dissertation in and from microform along with the non-exclusive right to reproduce and distribute my abstract in any format in whole or in part."

Jason Daniel Chambless

April 2008

ACKNOWLEDGMENTS

I would like to acknowledge the students, faculty, and staff of the Center for Biofilm Engineering at Montana State University. It was remarkable to be in an environment full of genuinely positive people who thoroughly enjoyed what they were doing and where they worked. The Center is a singularly remarkable place; the relationships and experience I gained there will certainly stay with me forever.

I would like to thank my adviser, Dr. Phil Stewart, for his continued support. His methods were meticulous, his comments on my work were thought-provoking and insightful, and his guidance was invaluable. I consider myself very fortunate to have been chosen to complete this modeling project under his direction.

That fact that I have successfully completed this dissertation, and my graduate program, is largely due to the support of my family and my wife, Anne. Ever since I was very young, I could always count on my parents and family to positively support the goals I set for myself; even when those goals seemed too lofty or foolishly optimistic.

The significance of Anne's role in helping me realize my potential, and her continued encouragement, I could not adequately repay even with a lifetime's worth of gratitude. However, I wholeheartedly look forward to trying.

This work was made possible by grant 5R01GM067245 from the National Institutes of Health.

TABLE OF CONTENTS

TABLE OF CONTENTS - CONTINUED

LIST OF TABLES

LIST OF FIGURES

LIST OF FIGURES - CONTINUED

ABSTRACT

A biofilm is a dense aggregation of microorganisms attached to each other and a supporting surface. Biofilms are ubiquitous in industrial environments and are also frequently recognized as the source of persistent infections. Biofilm invasions and biofilm-induced infections are often difficult or impossible to remedy. This dissertation presents the results of a 3D hybrid computer model, BacLAB, which was used to simulate detachment and protection mechanisms of biofilms in a cellular automata framework.

Protection against antimicrobials afforded by each of four hypothesized protective mechanisms was investigated in order to examine population survival versus antimicrobial exposure time, and the spatial patterns of chemical species and cell types. When compared to each other, the behaviors of the slow penetration, adaptive stress response, substrate limitation, and persister mechanisms produced distinct shapes of killing curves, non-uniform spatial patterns of survival and cell type distribution, and anticipated susceptibility patterns of dispersed biofilm cells.

Detachment is an important process that allows an organism the possibility of traveling to and colonizing a new location. Detachment also balances growth and so determines the net accumulation of biomass on the surface. Three hypothetical mechanisms representing various physical and biological influences of detachment were incorporated into BacLAB. The purpose of this investigation was to characterize each of the mechanisms with respect to four criteria: the resulting biofilm structure, the existence of a steady state, the propensity for sloughing events, and the dynamics during starvation. The results showed that varying the detachment mechanism is a critical determinant of biofilm structure and of the dynamics of biofilm accumulation and loss.

Phenotypic variants, in the form of dormant cells, can often survive an antimicrobial treatment. The existence of these cells, termed persisters, is one hypothetical explanation for biofilm recalcitrance. Four different combinations of random and substrate-dependant persister mechanisms were simulated through the use of the BacLAB model. The purpose of this study was to determine and compare the effects of differing formation and resuscitation strategies on persister-related protection of biofilms. Analysis of the simulations showed that extended periods of dormancy, without regard to the mechanism, were directly responsible for more tolerant biofilms.

CHAPTER 1

INTRODUCTION

A biofilm is a dense aggregation of microorganisms attached to each other and a supporting surface via extracellular polymeric substances of their own secretion (17, 18). Biofilms are ubiquitous in industrial environments such as oil recovery, food processing, and water treatment systems. Biofilms are also recognized as the source of persistent infections resulting in periodontitis (19), chronic lung ailments in cystic fibrosis patients (70), and complications with medical devices such as catheters (57, 59), heart valves (40), and artificial joint replacements (28). Biofilm invasions and biofilm-induced infections are often difficult or impossible to remedy through the use of biocides, antibiotics, or host defenses.

Biofilm models are often called upon to elicit explanations of the phenomena occurring within biofilm-affected industrial equipment. Initially, biofilm models were analytical descriptions of flat "microbial films" used to study the industrially important processes of substrate diffusion (5), substrate uptake (6), and external mass transfer (89). These early models were simple, steady state, one dimensional simulations for the macroscale trends in biofilm-containing systems. [For a thorough treatise on the history of biofilm modeling, see Hunt PhD Dissertation (37).]

Today, models of biofilms are increasingly able to simulate microscale processes. Biofilm models that employ cellular automata (8, 15, 34, 38, 58, 90), individual based modeling (IbM) (48-50, 92), or continuum methods (1, 2, 14, 24, 25) investigate more complex interactions between biofilm components and the surrounding environment.

These models are ideal for the study of cellular-level conjectures on biofilm development, antimicrobial protection, growth, and detachment.

Biofilm Modeling and Antimicrobial Control

Several competing theories attempt to explain biofilm recalcitrance through biofilm activity (13, 63), biofilm inactivity (7), genetic mutation (31), or phenotypic variation (52), among other phenomena. There are a handful of papers describing neutralization of an antimicrobial agent by a reaction as it diffuses into the biofilm (3, 22, 33, 77). The biofilm is said to consume the antimicrobial agent in the same manner that it would consume a substrate. This consumption could allow biofilms to decrease the concentration of the antimicrobial to a level that would be ineffective in the deeper regions of the biofilm.

Bacteria are equipped with a host of stress responses that allow them to cope with environmental adversity (41, 55). It could be possible that these same protective mechanisms are utilized by biofilms. An example of a stress response that is of obvious interest in the context of antimicrobials is the expression of drug efflux pumps (10, 63). Another example of a stress response, which induces alterations in the *hipA* gene, is also widely studied due to its protective effects (16, 32, 46).

The possibility that substrate limitation within a biofilm creates regions of inactive and less susceptible cells remains an attractive explanation for the recalcitrance of biofilms to antimicrobial agents. It is clear that gradients in substrate concentrations exist within biofilms (22). These concentration gradients give rise to corresponding

gradients in microbial growth rate and activity as observed by researchers using fluorescent probes and reporter genes (72, 80).

Models of Antimicrobial Control

As might be expected, the ample interest in defining the characteristics that allow a biofilm to survive antimicrobial treatments has lead to a number of models of biofilm protection. Biofilm models can test conjectures of biofilm protection and tolerance stemming from antimicrobial treatment studies. One of the first was a biofilm accumulation model by Stewart (74) that incorporated two mechanisms of protection into a one-dimensional, mass balance model of growth in a chemostat. The two mechanisms, substrate limited protection and antimicrobial depletion due to reaction with the biofilm, resulted in reduced susceptibility to antimicrobials, especially as the areal cell density increased. In a later work, Stewart (76) showed that antimicrobial depletion due to reaction with biofilm components, which created antimicrobial gradients within the biofilm, also provided protection by reducing the bulk concentration of the antimicrobial.

Likewise, Dibdin, et al. (23) used a similar model to demonstrate the protection provided by the release of enzymes (beta-lactamases) from sacrificial cells at the surface of a *Pseudomonas aeruginosa* biofilm. The enzymes shielded the biofilm by inactivating beta-lactam antimicrobials. The results predicted a stratified biofilm with an outer layer of dead cells and an inner layer of surviving cells.

In one of the first multi-mechanism studies of biofilm protection, Dodds, et al. (26) used a one-dimensional mass balance model to test three hypothetical protection schemes: 1) cells deep within the biofilm are more resistant due to assumed substrate

limitation, 2) biofilm constituents react with the antimicrobial in stoichiometric amounts until the biofilm and/or antimicrobial is consumed, and 3) biofilm constituents react with the antimicrobial catalytically and only the antimicrobial is consumed completely. The authors used the results to predict which mechanism could be responsible for behaviors of particular biofilms challenged by particular antimicrobials at specific times in the biofilm's growth cycle.

Biofilm Modeling and Detachment Processes

The motivation behind research on biofilm detachment varies widely. Detachment studies can focus on discovering new approaches for controlling detrimental biofilms (84), improving biological reactor design for treating wastewater (28, 30, 59, 85), or developing insight into the metastasis of infections within the human body (29, 44, 90).

Models of Detachment Processes

The absence of a single pathway to understanding biofilm detachment is reflected in the wide variety of mathematical submodels that have been proposed to describe detachment. The earliest detachment models were those based on concepts of fluid shear (61, 64) in which the rate of detachment increases with the distance above the substratum (11, 82, 88). A common form assumes that detachment rate is proportional to the square of the height above the substratum, a functionality that has the practical advantage of ensuring a steady state (75). A few biofilm models have made detachment rates dependent on the local concentration of a metabolic substrate or product; several studies specifically link detachment to nutrient deprivation (39, 54). Finally, some

multidimensional biofilm models have prescribed an erosive detachment mechanism in which individual cells are lost from the surface of the biofilm (35, 51).

Biofilm modeling in an industrial setting is concerned with several different processes across a wide spectrum of uses. Bioreactors of many varieties depend on, or are affected by, biofilms. Numerous modeling studies are primarily concerned with how biofilm detachment influences the overall performance of a reactor (56, 62, 68, 79, 81); but they can also be used to elaborate on unexplained phenomena (27, 83) or describe how biofilm detachment affects downstream processes (42).

Along with general bioreactors, wastewater treatment (12, 36, 65), membrane reactor (60), and biofiltration systems (53, 66, 86) can be designed, evaluated, or optimized with biofilm detachment-related model studies.

Biofilm Modeling and Persister Protection

Another, more recent use of biofilm models is attempting to explain cell variants within biofilms that tolerate antimicrobial treatments, but do not pass this tolerance to their progeny. Phenotypic variants, often in the form of dormant cells that survive an antimicrobial treatment (69), can make up 0.1% to 1% of a biofilm population (33, 43). The existence of these cells, termed persisters, has been hypothesized to explain several characteristics of biofilm recalcitrance that cannot be adequately addressed with any other single survival mechanism.

Such a phenotypic state is suggested by experiments with young biofilms that display resistance even though they are too thin to pose a barrier to the penetration of either an antimicrobial agent or of metabolic substrates (13, 20). Another indication that

biofilms may harbor a subpopulation of resistant cells comes from experiments in which most, but not all, of the biofilm is rapidly killed by an antimicrobial (4). The survivors, which may number one percent or less of the original population, persist despite continued exposure to the antimicrobial (4, 71).

Over the past few years, researchers have developed a number of different explanations for the rise of persister protection in biofilms. Originally designed to be a study of drug efflux pumps in bacteria, the article by Brooun, et al. (10) renewed the interest in the persister cells that were first described by Bigger in penicillin treatments of staphylococcal infections (9). Since then, myriad different explanations for the persister cell's tolerance have been submitted. Debbia, et al. (21) posited that persisters were resilient during antimicrobial treatments because they, unlike live cells that continued utilizing substrate for growth, concentrated all their efforts on repairing spontaneous errors in DNA synthesis caused by the antimicrobial. Such a hypothesis could explain why the persister resisted growth-targeted antimicrobials, as well as the reason that the resistance was not heritable. In a similar vein, Sufya, et al. (78) proposed that persisters (and biofilm tolerance in general) could be a result of substrate starved, slow growing cells in the lower regions of the biofilm. This proposal was suggested when the researchers observed small pockets of surviving cells in close proximity to each other, deep within the biofilm.

However, what of antimicrobials that did not solely target actively growing cells? The idea of a truly dormant state that did not depend on the existence of an antimicrobial or require starvation was described in Korch, et al. (47). They suggested that the over-

expression of certain genes in toxin-antitoxin (TA) modules lead to the dormant persister state. However, a few months prior to the article by Korch, Vazquez-Laslop, et al. (87) reported that an increased persister population was induced by cells that ectopically expressed proteins entirely unrelated to TA modules.

Models of Persister Protection

The riddle of persister protection is an ideal fit for conjecture-based biofilm modeling. Several researchers have attempted to explain the rise, existence, and protective effects of a persister, or "protected", population within biofilms through modeling studies. In 2005, Szomolay, et al. (80) hypothesized that reaction-diffusion-limited penetration of antimicrobial agents caused ineffective exposure deep within biofilm colonies, leading to an adaptive cell state that survived the antimicrobial treatment.

Wiuff, et al. (91) examined multiple hypotheses regarding biofilm recalcitrance, one of which hypothesized a phenotypic variant whose resistance was not heritable by the next generation. The study demonstrated the protective effects of such a variant on a biofilm population.

A 2005 article provided one of the first models for persister formation based on substrate depletion (67). Persister cell formation was proportional to the total live cell concentration, and reversion was proportional to the local substrate concentrations. The study concluded that substrate depletion could account for the accumulation of persisters in the depths of the biofilm, leading to greater protection than that afforded to planktonic cultures.

In a recently published article, Klapper, et al. (45) took a new look at tolerance with the knowledge that asymmetric cell division creates a new daughter cell, but leaves the mother cell unchanged (73). The older (senescent), mother cells were hypothesized to be persister cells. The core finding of this work was that if antimicrobial agents become less effective as cells age, a modeled biofilm can successfully exhibit several of the experimentally observed persister-related characteristics.

Scope of this Dissertation

The scope of this dissertation is the ongoing adaptation of an existing 3D computer model framework of biofilm dynamics to investigate mechanisms related to biofilm development and recalcitrance. The original hybrid cellular automata model described by Hunt (37) has been modified to include three new detachment mechanisms, three new antimicrobial protection mechanisms, and three new mechanisms of persister protection. The focus of this dissertation is the analysis of qualitative behaviors resultant from hypothetical conjectures; only minor attention is given to the predictive ability of the mathematical model. The original goal for the development of this inherently visual, rule-based model still drives our current research: to serve as a vehicle for dialogue between engineers, mathematicians, biologists, medical scientists, and clinicians.

Existing Model Description

The computer model, BacLAB, used in this dissertation has been described in detail elsewhere (38). BacLAB is a hybrid model where the distribution of the soluble components is modeled using discretized differential equations describing simultaneous

reaction and diffusion, while the individual microorganisms that compose the biofilm are modeled discretely using a cellular automata (CA) algorithm. The cellular automaton (CA) component of the model is a Markov process that is discrete in time, space, and state. The cellular automata model is written in C++ and the Fast Fourier Transform solution to the reaction diffusion equation is written in Fortran. A cellular automaton is an independent unit, here equated to a microbial cell and its associated matrix material, which follows certain behavioral rules. The resulting aggregate behavior of the biofilm is therefore emergent from the local interactions between these individually minded bacteria. The cellular automata model produces realistic, structurally heterogeneous biofilms. Furthermore, it allows the artificial biofilm structure to evolve as a self-organization process, emulating how bacterial cells organize themselves into biofilms. Two advantages to the hybrid approach are the ability to separate different biofilm processes according to their natural time scales, and that the aggregate behavior of the biofilm is emergent from the local interactions between individual microorganisms.

The model integrates processes of substrate utilization, microbial growth, advective displacement of biomass, phenotypic switching, antimicrobial action, and detachment into the CA framework.

In BacLAB, a biofilm cell can occupy fixed nodes on a regular 3D grid. When a cell has consumed sufficient substrate to divide, a daughter cell is generated and placed in an adjoining node. Growth can lead to the displacement of neighboring cells when there is no empty adjoining node to receive the daughter. This displacement is analogous to the process of biomass advection as articulated by Wanner and Gujer (88).

A cell can detach, in which case it is removed entirely from the model space. Detachment from the model space is accomplished via mechanisms functionally dependant on the local substrate concentrations, the height of the bacterial cell above the substratum, or the number of empty nodes surrounding the bacterial cell. The mechanism employed depends on the specific study in question. Detachment also occurs when a biofilm cell (or cluster of cells) no longer has an unbroken chain of occupied automata nodes leading back to the substratum. As a result, the cell (or cluster) is removed from the model space and considered to have detached. In this way it is possible for a single detaching cell to precipitate the release of an aggregate of cells (i.e. sloughing).

Neither fluid flow nor extracellular polymeric substances (EPS) were explicitly modeled within BacLAB, however the detachment mechanisms make use of properties resultant from an assumed existence of both. An artificial boundary layer exists at 49μm above the highest cell in the model space, which causes gradients to develop in diffusible materials.

The current dissertation is concerned exclusively with development and adaptation of the CA portion of the model, and no efforts were made to alter the Fortran-based Fast Fourier Transform solution to the reaction-diffusion equation. A thorough treatment of this aspect of the model can be found in Hunt, et al. (38).

Research Objectives

- Theoretically investigate the level of protection against antimicrobials afforded by the hypothetical slow antimicrobial penetration, adaptive stress response, substrate

limitation, and persister protection mechanisms by examining population survival and spatial patterns of survival versus antimicrobial exposure time.

- Theoretically characterize three hypothetical biofilm detachment mechanisms with respect to resulting biofilm structure, existence of a steady state, propensity for sloughing events, and behavior during substrate starvation.
- Theoretically determine and compare the effects of differing persister cell switching methods on persister-related biofilm protection by examining the resulting structures, live and persister areal cell densities, and persister cell locations.

References

1. Alpkvist, E., and I. Klapper. 2007. A multidimensional multispecies continuum model for heterogeneous biofilm development. Bull Math Biol 69:765-89.

2. Alpkvist, E., C. Picioreanu, M. C. van Loosdrecht, and A. Heyden. 2006. Three-dimensional biofilm model with individual cells and continuum EPS matrix. Biotechnol Bioeng 94:961-79.

3. Anderl, J. N., M. J. Franklin, and P. S. Stewart. 2000. Role of antibiotic penetration limitation in *Klebsiella pneumoniae* biofilm resistance to ampicillin and ciprofloxacin. Antimicrob Agents Chemother 44:1818-24.

4. Anderl, J. N., J. Zahller, F. Roe, and P. S. Stewart. 2003. Role of nutrient limitation and stationary-phase existence in *Klebsiella pneumoniae* biofilm resistance to ampicillin and ciprofloxacin. Antimicrob Agents Chemother 47:1251-6.

5. Atkinson, B., and I. S. Daoud. 1970. Diffusion effects within microbial films. Transactions of the Institution of Chemical Engineers and the Chemical Engineer 48:T245.

6. Atkinson, B., and I. J. Davies. 1974. Overall rate of substrate uptake (reaction) by microbial films P1. Biological rate equation. Transactions of the Institution of Chemical Engineers 52:248-259.

7. Balaban, N. Q., J. Merrin, R. Chait, L. Kowalik, and S. Leibler. 2004. Bacterial persistence as a phenotypic switch. Science 305:1622-1625.

8. Barker, G. C., and M. J. Grimson. 1993. A cellular automaton model of microbial growth. Binary 5:132-137.

9. Bigger, J. W. 1944. Treatment of staphylococcal infections with penicillin. Lancet 2:497-500.

10. Brooun, A., S. Liu, and K. Lewis. 2000. A dose-response study of antibiotic resistance in *Pseudomonas aeruginosa* biofilms. Antimicrob Agents Chemother 44:640-6.

11. Bryers, J. D. 1984. BIOFILM FORMATION AND CHEMOSTAT DYNAMICS - PURE AND MIXED CULTURE CONSIDERATIONS. Biotechnology and Bioengineering 26:948-958.

12. Chen, L. M., and L. H. Chai. 2005. Mathematical model and mechanisms for biofilm wastewater treatment systems. World Journal of Microbiology & Biotechnology 21:1455-1460.

13. Cochran, W. L., G. A. McFeters, and P. S. Stewart. 2000. Reduced susceptibility of thin *Pseudomonas aeruginosa* biofilms to hydrogen peroxide and monochloramine. J Appl Microbiol 88:22-30.

14. Cogan, N. G. 2007. Two-Fluid Model of Biofilm Disinfection. Bull Math Biol.

15. Colasanti, R. L. 1992. Cellular automata models of microbial colonies. Binary 4:191-193.

16. Correia, F. F., A. D'Onofrio, T. Rejtar, L. Li, B. L. Karger, K. Makarova, E. V. Koonin, and K. Lewis. 2006. Kinase activity of overexpressed HipA is required for growth arrest and multidrug tolerance in *Escherichia col*i. J Bacteriol 188:8360-7.

17. Costerton, J. W., and P. S. Stewart. 2001. Battling biofilms. Sci Am 285:74-81.

18. Costerton, J. W., P. S. Stewart, and E. P. Greenberg. 1999. Bacterial biofilms: a common cause of persistent infections. Science 284:1318-22.

19. Darveau, R. P., A. Tanner, and R. C. Page. 1997. The microbial challenge in periodontitis. Periodontol 2000 14:12-32.

20. Das, J. R., M. Bhakoo, M. V. Jones, and P. Gilbert. 1998. Changes in the biocide susceptibility of *Staphylococcus epidermidis* and *Escherichia coli* cells associated with rapid attachment to plastic surfaces. J Appl Microbiol 84:852-8.

21. Debbia, E. A., S. Roveta, A. M. Schito, L. Gualco, and A. Marchese. 2001. Antibiotic persistence: the role of spontaneous DNA repair response. Microb Drug Resist 7:335-42.

22. Debeer, D., P. Stoodley, F. Roe, and Z. Lewandowski. 1994. Effects of biofilm structures on oxygen distribution and mass-transport. Biotechnology and Bioengineering 43:1131-1138.

23. Dibdin, G. H., S. J. Assinder, W. W. Nichols, and P. A. Lambert. 1996. Mathematical model of beta-lactam penetration into a biofilm of *Pseudomonas aeruginosa* while undergoing simultaneous inactivation by released beta-lactamases. J Antimicrob Chemother 38:757-69.

24. Dillon, R., and L. Fauci. 2000. A microscale model of bacterial and biofilm dynamics in porous media. Biotechnol Bioeng 68:536-47.

25. Dockery, J., and I. Klapper. 2002. Finger formation in biofilm layers. Siam Journal on Applied Mathematics 62:853-869.

26. Dodds, M. G., K. J. Grobe, and P. S. Stewart. 2000. Modeling biofilm antimicrobial resistance. Biotechnol Bioeng 68:456-65.

27. Ebrahimi, S., C. Picioreanu, J. B. Xavier, R. Kleerebezem, M. Kreutzer, F. Kapteijn, J. A. Moulijn, and M. C. M. van Loosdrecht. 2005. Biofilm growth pattern in honeycomb monolith packings: Effect of shear rate and substrate transport limitations. Catalysis Today 105:448-454.

28. Eker, S., and F. Kargi. 2006. Biological treatment of para-chlorophenol containing synthetic wastewater using rotating brush biofilm reactor. Journal of Hazardous Materials 135:365-371.

29. Fux, C. A., S. Wilson, and P. Stoodley. 2004. Detachment characteristics and oxacillin resistance of *Staphyloccocus aureus* biofilm emboli in an in vitro catheter infection model. J Bacteriol 186:4486-91.

30. Gonzalez-Brambila, M., O. Monroy, and F. Lopez-Isunza. 2006. Experimental and theoretical study of membrane-aerated biofilm reactor behavior under different modes of oxygen supply for the treatment of synthetic wastewater. Chemical Engineering Science 61:5268-5281.

31. Halme, A., S. Bumgarner, C. Styles, and G. R. Fink. 2004. Genetic and epigenetic regulation of the FLO gene family generates cell-surface variation in yeast. Cell 116:405-15.

32. Harrison, J. J., H. Ceri, N. J. Roper, E. A. Badry, K. M. Sproule, and R. J. Turner. 2005. Persister cells mediate tolerance to metal oxyanions in *Escherichia coli*. Microbiology 151:3181-95.

33. Harrison, J. J., R. J. Turner, and H. Ceri. 2005. Persister cells, the biofilm matrix and tolerance to metal cations in biofilm and planktonic *Pseudomonas aeruginosa*. Environ Microbiol 7:981-94.

34. Hermanowicz, S. W. 1998. A model of two-dimensional biofilm morphology. Water Science and Technology 37:219-222.

35. Hermanowicz, S. W. 2001. A simple 2D biofilm model yields a variety of morphological features. Math Biosci 169:1-14.

36. Horn, H., H. Reiff, and E. Morgenroth. 2003. Simulation of growth and detachment in biofilm systems under defined hydrodynamic conditions. Biotechnol Bioeng 81:607-17.

37. Hunt, S. M. 2004. Theoretical investigation of biofilm detachment and protection from killing using a bacterium level automata model. PhD Dissertation, Montana State University.

38. Hunt, S. M., M. A. Hamilton, J. T. Sears, G. Harkin, and J. Reno. 2003. A computer investigation of chemically mediated detachment in bacterial biofilms. Microbiology 149:1155-63.

39. Hunt, S. M., E. M. Werner, B. Huang, M. A. Hamilton, and P. S. Stewart. 2004. Hypothesis for the role of nutrient starvation in biofilm detachment. Appl Environ Microbiol 70:7418-25.

40. Hyde, J. A., R. O. Darouiche, and J. W. Costerton. 1998. Strategies for prophylaxis against prosthetic valve endocarditis: a review article. J Heart Valve Dis 7:316-26.

41. Kaldalu, N., R. Mei, and K. Lewis. 2004. Killing by ampicillin and ofloxacin induces overlapping changes in *Escherichia coli* transcription profile. Antimicrob Agents Chemother 48:890-6.

42. Kapellos, G. E., T. S. Alexiou, and A. C. Payatakes. 2007. Hierarchical simulator of biofilm growth and dynamics in granular porous materials. Advances in Water Resources 30:1648-1667.

43. Keren, I., N. Kaldalu, A. Spoering, Y. Wang, and K. Lewis. 2004. Persister cells and tolerance to antimicrobials. FEMS Microbiol Lett 230:13-8.

44. Khardori, N., and M. Yassien. 1995. Biofilms in device-related infections. J Ind Microbiol 15:141-7.

45. Klapper, I., P. Gilbert, B. P. Ayati, J. Dockery, and P. S. Stewart. 2007. Senescence can explain microbial persistence. Microbiology 153:3623-3630.

46. Korch, S. B., T. A. Henderson, and T. M. Hill. 2003. Characterization of the hipA7 allele of *Escherichia coli* and evidence that high persistence is governed by *(p)ppGpp* synthesis. Molecular Microbiology 50:1199-1213.

47. Korch, S. B., and T. M. Hill. 2006. Ectopic overexpression of wild-type and mutant hipA genes in *Escherichia coli*: effects on macromolecular synthesis and persister formation. J Bacteriol 188:3826-36.

48. Kreft, J. U. 2004. Biofilms promote altruism. Microbiology 150:2751-60.

49. Kreft, J. U., G. Booth, and J. W. Wimpenny. 1998. BacSim, a simulator for individual-based modelling of bacterial colony growth. Microbiology 144 (Pt 12):3275-87.

50. Kreft, J. U., C. Picioreanu, J. W. Wimpenny, and M. C. van Loosdrecht. 2001. Individual-based modelling of biofilms. Microbiology 147:2897-912.

51. Laspidou, C. S., and B. E. Rittmann. 2004. Modeling the development of biofilm density including active bacteria, inert biomass, and extracellular polymeric substances. Water Res 38:3349-61.

52. Lewis, K. 2001. Riddle of biofilm resistance. Antimicrob Agents Chemother 45:999-1007.

53. Liang, C. H., and P. C. Chiang. 2007. Mathematical model of the non-steady-state adsorption and biodegradation capacities of BAC filters. J Hazard Mater 139:316-22.

54. Luna, E., G. Dominguez-Zacarias, C. P. Ferreira, and J. X. Velasco-Hernandez. 2004. Detachment and diffusive-convective transport in an evolving heterogeneous two-dimensional biofilm hybrid model. Phys Rev E Stat Nonlin Soft Matter Phys 70:061909.

55. Massey, R. C., A. Buckling, and S. J. Peacock. 2001. Phenotypic switching of antibiotic resistance circumvents permanent costs in *Staphylococcus aureus*. Curr Biol 11:1810-4.

56. McCarty, P. L., and T. E. Meyer. 2005. Numerical model for biological fluidized-bed reactor treatment of perchlorate contaminated groundwater. Environ Sci Technol 39:850-8.

57. Morris, N. S., D. J. Stickler, and R. J. McLean. 1999. The development of bacterial biofilms on indwelling urethral catheters. World J Urol 17:345-50.

58. Noguera, D. R., G. Pizarro, D. A. Stahl, and B. E. Rittmann. 1999. Simulation of multispecies biofilm development in three dimensions. Water Science and Technology 39:123-130.

59. Odegaard, H. 2006. Innovations in wastewater treatment: the moving bed biofilm process. Water Sci Technol 53:17-33.

60. Pavasant, P., L. M. F. dosSantos, E. N. Pistikopoulos, and A. G. Livingston. 1996. Prediction of optimal biofilm thickness for membrane-attached biofilms growing in an extractive membrane bioreactor. Biotechnology and Bioengineering 52:373-386.

61. Peyton, B. M., and W. G. Characklis. 1993. A statistical-analysis of the effect of substrate utilization and shear-stress on the kinetics of biofilm detachment. Biotechnology and Bioengineering 41:728-735.

62. Plattes, M., D. Fiorelli, S. Gille, C. Girard, E. Henry, F. Minette, O. O'Nagy, and P. M. Schosseler. 2007. Modelling and dynamic simulation of a moving bed bioreactor using respirometry for the estimation of kinetic parameters. Biochemical Engineering Journal 33:253-259.

63. Ramage, G., S. Bachmann, T. F. Patterson, B. L. Wickes, and J. L. Lopez-Ribot. 2002. Investigation of multidrug efflux pumps in relation to fluconazole resistance in *Candida albicans* biofilms. J Antimicrob Chemother 49:973-80.

64. Rittmann, B. E. 1982. The effect of shear-stress on biofilm loss rate. Biotechnology and Bioengineering 24:501-506.

65. Rittmann, B. E., D. Stilwell, J. C. Garside, G. L. Amy, C. Spangenberg, A. Kalinsky, and E. Akiyoshi. 2002. Treatment of a colored groundwater by ozone-biofiltration: pilot studies and modeling interpretation. Water Res 36:3387-97.

66. Rittmann, B. E., D. Stilwell, and A. Ohashi. 2002. The transient-state, multiple-species biofilm model for biofiltration processes. Water Res 36:2342-56.

67. Roberts, M. E., and P. S. Stewart. 2005. Modelling protection from antimicrobial agents in biofilms through the formation of persister cells. Microbiology 151:75-80.

68. Seok, J. 2003. Hybrid adaptive optimal control of anaerobic fluidized bed bioreactor for the de-icing waste treatment. J Biotechnol 102:165-75.

69. Shah, D., Z. Zhang, A. Khodursky, N. Kaldalu, K. Kurg, and K. Lewis. 2006. Persisters: a distinct physiological state of *E. coli*. BMC Microbiol 6:53.

70. Singh, P. K., A. L. Schaefer, M. R. Parsek, T. O. Moninger, M. J. Welsh, and E. P. Greenberg. 2000. Quorum-sensing signals indicate that cystic fibrosis lungs are infected with bacterial biofilms. Nature 407:762-4.

71. Spoering, A. L., and K. Lewis. 2001. Biofilms and planktonic cells of *Pseudomonas aeruginosa* have similar resistance to killing by antimicrobials. J Bacteriol 183:6746-51.

72. Sternberg, C., B. B. Christensen, T. Johansen, A. Toftgaard Nielsen, J. B. Andersen, M. Givskov, and S. Molin. 1999. Distribution of bacterial growth activity in flow-chamber biofilms. Appl Environ Microbiol 65:4108-17.

73. Stewart, E. J., R. Madden, G. Paul, and F. Taddei. 2005. Aging and death in an organism that reproduces by morphologically symmetric division. PLoS Biol 3:e45.

74. Stewart, P. S. 1994. Biofilm accumulation model that predicts antibiotic resistance of *Pseudomonas aeruginosa* biofilms. Antimicrob Agents Chemother 38:1052-8.

75. Stewart, P. S. 1993. A model of biofilim detachment. Biotechnology and Bioengineering 41:111-117.

76. Stewart, P. S. 1996. Theoretical aspects of antibiotic diffusion into microbial biofilms. Antimicrob Agents Chemother 40:2517-22.

77. Stewart, P. S., J. Rayner, F. Roe, and W. M. Rees. 2001. Biofilm penetration and disinfection efficacy of alkaline hypochlorite and chlorosulfamates. J Appl Microbiol 91:525-32.

78. Sufya, N., D. G. Allison, and P. Gilbert. 2003. Clonal variation in maximum specific growth rate and susceptibility towards antimicrobials. J Appl Microbiol 95:1261-7.

79. Suzuki, Y., M. Takahashi, M. Haesslein, and C. F. Seyfried. 1999. Development of simulation model for a combined activated-sludge and biofilm process to remove nitrogen and phosphorus. Water Environment Research 71:388-397.

80. Szomolay, B., I. Klapper, J. Dockery, and P. S. Stewart. 2005. Adaptive responses to antimicrobial agents in biofilms. Environ Microbiol 7:1186-91.

81. Tartakovsky, B., and S. R. Guiot. 1997. Modeling and analysis of layered stationary anaerobic granular biofilms. Biotechnology and Bioengineering 54:122-130.

82. Trulear, M. G., and W. G. Characklis. 1982. Dynamics of biofilm processes. Journal Water Pollution Control Federation 54:1288-1301.

83. Tsuno, H., T. Hidaka, and F. Nishimura. 2002. A simple biofilm model of bacterial competition for attached surface. Water Res 36:996-1006.

84. van der Borden, A. J., H. C. van der Mei, and H. J. Busscher. 2005. Electric block current induced detachment from surgical stainless steel and decreased viability of Staphylococcus epidermidis. Biomaterials 26:6731-5.

85. van Loosdrecht, M. C., and S. Salem. 2006. Biological treatment of sludge digester liquids. Water Sci Technol 53:11-20.

86. Vayenas, D. V., and G. Lyberatos. 1994. A novel model for nitrifying trickling filters. Water Research 28:1275-1284.

87. Vazquez-Laslop, N., H. Lee, and A. A. Neyfakh. 2006. Increased persistence in *Escherichia coli* caused by controlled expression of toxins or other unrelated proteins. J Bacteriol 188:3494-7.

88. Wanner, O., and W. Gujer. 1986. A multispecies biofilm model. Biotechnology and Bioengineering 28:314-328.

89. Williamson, K., and P. L. McCarty. 1976. A model of substrate utilization by bacterial films. J Water Pollut Control Fed 48:9-24.

90. Wilson, S., M. A. Hamilton, G. C. Hamilton, M. R. Schumann, and P. Stoodley. 2004. Statistical quantification of detachment rates and size distributions of cell clumps from wild-type (PAO1) and cell signaling mutant (JP1) *Pseudomonas aeruginosa* biofilms. Appl Environ Microbiol 70:5847-52.

91. Wiuff, C., R. M. Zappala, R. R. Regoes, K. N. Garner, F. Baquero, and B. R. Levin. 2005. Phenotypic tolerance: antibiotic enrichment of noninherited resistance in bacterial populations. Antimicrob Agents Chemother 49:1483-94.

92. Xavier, J. B., C. Picioreanu, S. A. Rani, M. C. van Loosdrecht, and P. S. Stewart. 2005. Biofilm-control strategies based on enzymic disruption of the extracellular polymeric substance matrix--a modelling study. Microbiology 151:3817-32.

CHAPTER 2

A 3D COMPUTER MODEL OF FOUR HYPOTHETICAL MECHANISMS PROTECTING BIOFILMS FROM ANTIMICROBIALS

Reproduced with permission from Chambless, J. D., S. M. Hunt, and P. S. Stewart. 2006. A three-dimensional computer model of four hypothetical mechanisms protecting biofilms from antimicrobials. Applied and Environmental Microbiology 72:2005-2013.

Summary

Four hypothetical mechanisms of biofilm protection against antimicrobials were incorporated into a three-dimensional model of biofilm growth and development. The model integrated processes of substrate utilization, diffusion, growth, cell migration, death, and detachment in a cellular automata framework. When compared to simulations of unprotected biofilms, each of the protective mechanisms provided some tolerance to antimicrobial action. When compared to each other, the behaviors of the four different protective mechanisms produced distinct shapes of killing curves, non-uniform spatial patterns of survival and cell type distribution, and anticipated susceptibility patterns of dispersed biofilm cells. The differences between the protective mechanisms predicted in these simulations could guide the design of experiments to discriminate antimicrobial tolerance mechanisms in biofilms. Each of the mechanisms could be a plausible avenue of biofilm protection.

Introduction

Microorganisms within biofilms have a remarkable tolerance to killing by antimicrobial agents (21,26,39). The reduced susceptibility of bacteria and yeast in biofilms is recognized as an important factor in the persistence of some chronic infections and the troublesome recurrence of fouling in industrial systems. While the phenomenon of reduced antimicrobial and biocide susceptibility in biofilms is well documented, the mechanisms of this resistance are incompletely understood (21,26,39,41). Four leading hypotheses explaining the reduced susceptibility of biofilms, diagrammed in Figure 2-1, are poor antimicrobial penetration, deployment of adaptive stress responses, physiological heterogeneity in the biofilm population, and the presence of phenotypic variants or persister cells (12,21,38). It seems likely that a combination of these factors determines the overall protection in the biofilm (6,21,38,39).

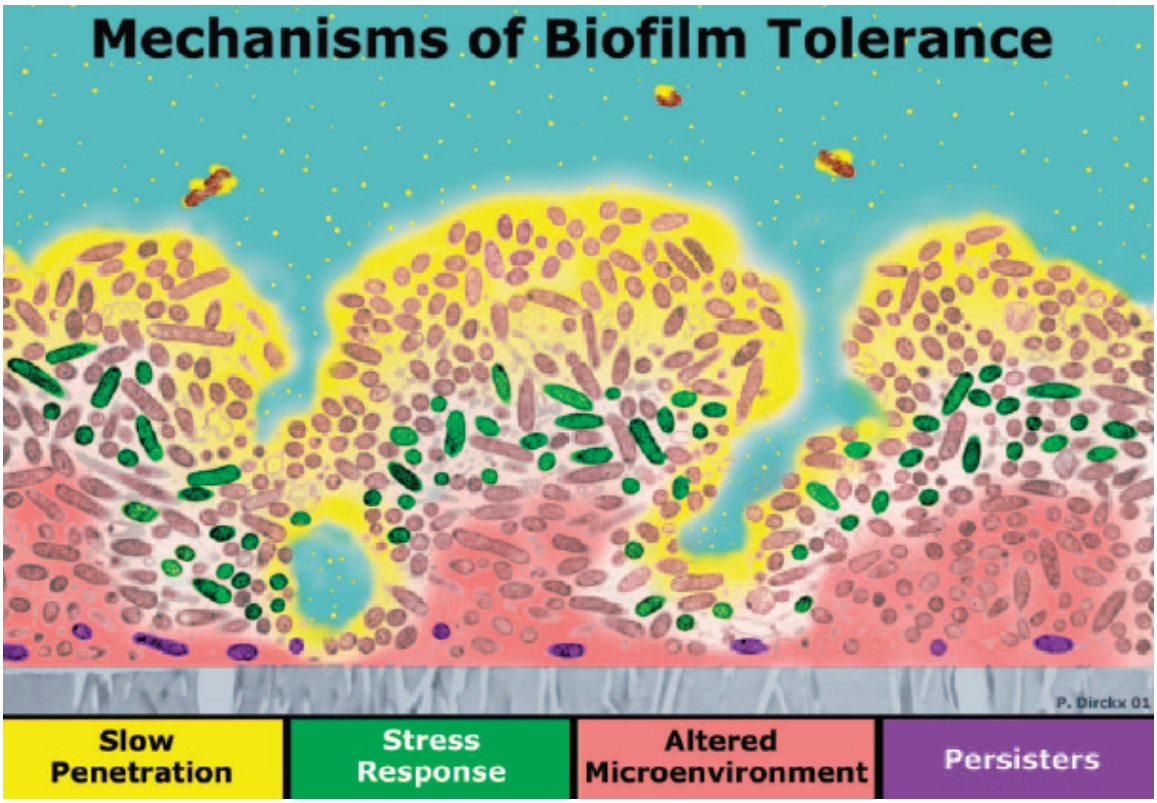

Figure 2-1. Four possible mechanisms of biofilm antibiotic resistance. The biofilm is shown in cross section with the attachment surface (gray) at the bottom and the aqueous phase containing the antibiotic (yellow) at the top. In zones of nutrient depletion (red), antibiotic action may be antagonized. Some bacteria may activate stress responses (green), while others may differentiate into a protected phenotype (purple).

There are a handful of papers describing neutralization of an antimicrobial agent by a reaction as it diffuses into the biofilm (1,13,42). The biofilm is said to consume the antimicrobial agent in the same manner that it would consume a substrate. This consumption could allow biofilms to decrease the concentration of the antimicrobial to a level that would be ineffective in the deeper regions of the biofilm. However, such a protective mechanism would be expected to only be present in thicker biofilms. Also, antimicrobial agents that do not react with or bind to the biofilm can be expected to

penetrate over a matter of seconds or minutes (37). Examples of several antimicrobial agents that penetrate biofilms but fail to kill the sessile microorganisms at the observed rate of their planktonic counterparts are plentiful (1,8,14,33,43,49).

Bacteria are equipped with a host of stress responses that allow them to cope with environmental adversity. It could be possible that these same protective mechanisms are utilized by biofilms. The most compelling version of this second mechanism of biofilm protection is that stress response defenses are induced in biofilm bacteria when facing an environmental challenge, just as they are in bacteria in aqueous suspension. The difference between a free-floating and biofilm-embedded cell is that the biofilm bacteria are sufficiently protected by other defenses, such as retarded antimicrobial penetration or slow growth, allowing the biofilm cells to respond to an antimicrobial challenge that overwhelms planktonic cells. An example of a stress response that is of obvious interest in the context of antimicrobials is the expression of drug efflux pumps.

The possibility that substrate limitation within a biofilm creates regions of inactive and less susceptible cells remains an attractive explanation for the recalcitrance of biofilms to antimicrobial agents. It is clear that gradients in substrate concentrations exist within biofilms (13). These concentration gradients give rise to corresponding gradients in microbial growth rate and activity as observed by researchers using fluorescent probes and reporter genes (35,44,47). Since antimicrobials are thought to be more effective in killing actively growing cells, it seems reasonable that in substrate-limited regions of a biofilm the microorganisms could better tolerate the presence of an antimicrobial agent by virtue of their inactivity. However, one would expect that as

growing cells within the biofilm are killed, substrate would penetrate into regions that were previously substrate depleted. Thus, dormant microorganisms might lose their tolerance for the antimicrobial agent as substrate becomes available.

A fourth mechanism of antimicrobial resistance in biofilms invokes the possibility of a unique, and highly protected, phenotypic state that is adopted by a subpopulation of microorganisms in a biofilm (26,41). This is conceptualized as a true differentiation of the cell akin to spore formation that requires the expression of specific sets of genes. Cells in this special state have been termed persisters. Such a phenotypic state is suggested by experiments with young biofilms that display resistance even though they are too thin to pose a barrier to the penetration of either an antimicrobial agent or of metabolic substrates (7,11). Another indication that biofilms may harbor a subpopulation of resistant cells comes from experiments in which most, but not all, of the biofilm is rapidly killed by an antimicrobial (2,18). The survivors, which may number one percent or less of the original population, persist despite continued exposure to the antimicrobial (2,34).

Computer models of biofilm dynamics complement experimental investigations and thus are valuable tools in the exploration of biofilm phenomena. Models can be used to test conjectures or make predictions about how specific processes affect biofilm structure or function. Theoretical explorations are particularly attractive because often there are multiple mechanisms at work that are difficult to separate experimentally. We have been interested in using biofilm models to explore the degree of protection from killing by antimicrobials that can be realized by specific tolerance mechanisms. Several

previous studies have described biofilm models that incorporate antimicrobial action (8,14,15,23,28,36,40,44). Using a three-dimensional computer model of biofilm dynamics, we have investigated the levels of protection against antimicrobials afforded by each of four hypothesized protective mechanisms. The purpose of this study was to characterize the predicted features of four different protective mechanisms when incorporated into a multidimensional computer model of biofilm dynamics. We sought in particular to examine population survival versus antimicrobial exposure time and the spatial patterns of chemical species and cell types within the biofilm during or after antimicrobial treatment.

Materials and Methods

The computer model, BacLAB, used in this study has been described in detail elsewhere (21). This model uses a hybrid modeling approach in which all soluble components are modeled using discretized differential equations while the individual microorganisms that compose the biofilm are modeled discretely using a cellular automata algorithm. A cellular automaton is an independent unit, here equated to a bacterial cell, which follows certain behavioral rules. The resulting aggregate behavior of the biofilm is therefore emergent from the local interactions between these individually minded bacteria. The cellular automata model produces realistic, structurally heterogeneous biofilms (4,9,18,24,28,29,47). Furthermore, it allows the artificial biofilm structure to evolve as a self-organization process, emulating how bacterial cells organize themselves into biofilms. Two advantages to the hybrid approach are the ability to separate different biofilm processes according to their natural time scale, and that the

aggregate behavior of the biofilm is emergent from the local interactions between individual microorganisms. Some of the processes simulated by the computer model include diffusion of soluble components into the biofilm, substrate and antimicrobial consumption, microbial growth, and biofilm detachment resulting from nutrient starvation. Parameter values are summarized in Table 2-1, and a visual representation of a typical BacLAB biofilm simulation is provided in Figure 2-2. Please note that the parameters described in Table 2-1 do not represent any specific bacterial species; however, these parameters are the same order of magnitude for a typical bacterial species.

Table 2-1. Summary of parameters used in BacLAB model.

Parameter	Symbol	Value	Unit(s)
Maximum specific growth rate	$\mu_{S,max}$	0.3	h^{-1}
Time step	Δt	1.0	h
Bulk substrate concentration	$C_{S,bulk}$	8.0	$g\ m^{-3}$
Diffusivity of substrate in the aqueous phase (including the liquid, channels and voids)	$D_{S,aq}$	$7.20 \cdot 10^{-6}$	$m^2\ h^{-1}$
Relative effective diffusivity of substrate in biofil	$D_{S,e} / D_{S,aq}$	0.55	
Local nutrient concentration threshold	$C_{S,min}$	1.0	$g\ m^{-3}$
Substrate Monod half saturation coefficient	K_S	0.1	$g\ m^{-3}$
Average cell mass	m_{avg}	$1.75 \cdot 10^{-13}$	g
Number of initial colonies	N_c	28	
Number of nodes in x-direction	N_x	300	
Number of nodes in y-direction	N_y	300	
Radius of initial colonies	R_c	$8.55 \cdot 10^{-6}$	m
Duration of time below $C_{S,min}$ before detachment	t_{detach}	24	h
Biomass yield (g_X) per gram of substrate (g_S)	Y_{XS}	0.24	$g_X\ g_S^{-1}$

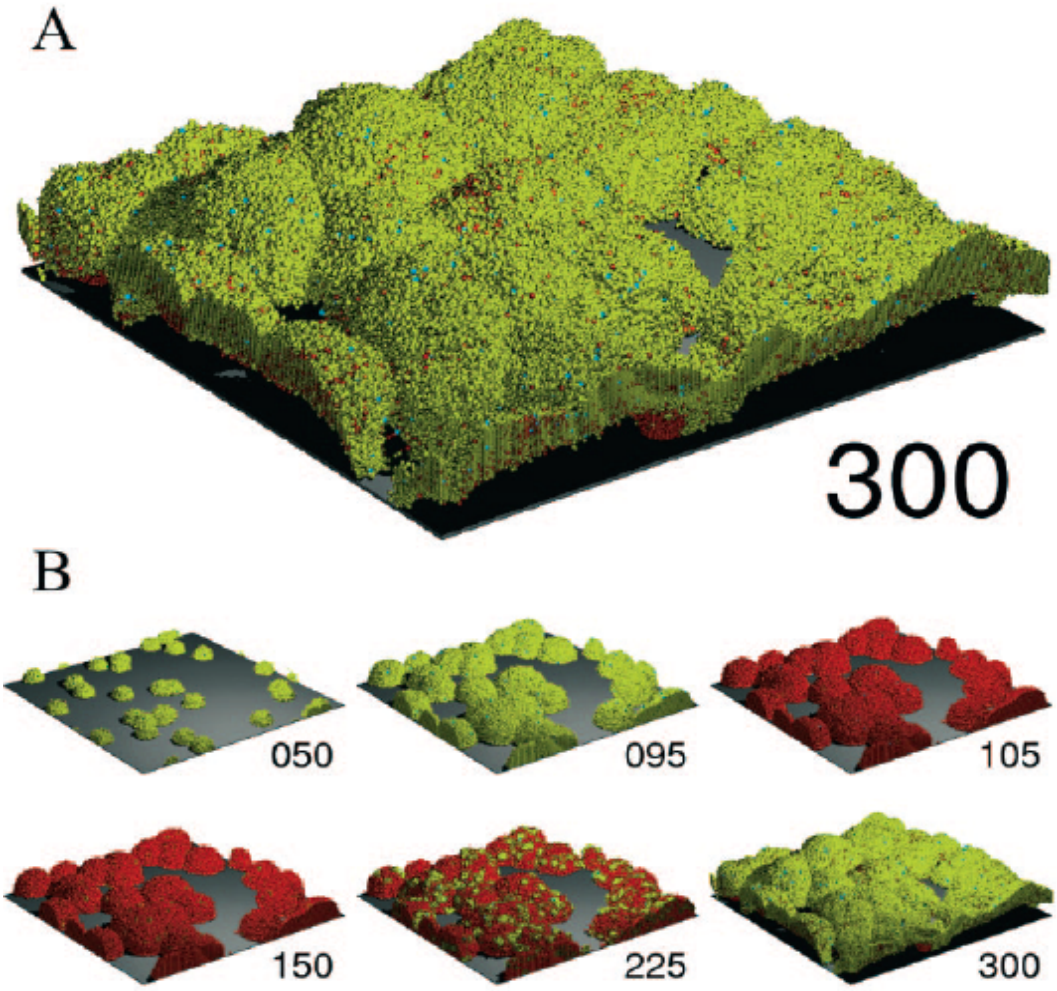

Figure 2-2. Visual 3D representation of BacLAB model (A) showing a biofilm with live (green), dead (red), and persister (blue) cells at hour 300 (150 hours after the completion of a 50-hour antimicrobial treatment) and (B) through the course of a 300 hour simulation in which the persister protection mechanism is active. Biofilm formation begins with the development of independent cell clusters that merge over time. Antimicrobial treatment initiated at 100 h rapidly kills most of the live cells, but persister cells survive. When persister cells eventually resuscitate, they give rise to new growth that begins in clonal pockets but rapidly extends throughout the biofilm. A video of this simulation can be viewed here: www.erc.montana.edu/Res-Lib99-SW/Movies/Database/MD_DisplayScript.asp.

Two sets of simulations were performed for each of the four protective mechanisms: (1) Protected with a continuous antimicrobial treatment initiated at hour 100

and lasting 50 hours, (2) Unprotected with a continuous antimicrobial treatment initiated at hour 100 and lasting 50 hours.

For all unprotected studies the probability of killing due to the presence of the antimicrobial agent was 0.6838 for a 1 hour interval. This value was calculated so as to provide a 6 log reduction in non-growing suspended cell cultures in a 12 hour treatment period by solving the following equality

$$(1-P)^{12} = 10^{-6} \tag{2-1}$$

where P is the probability of killing. Therefore, the probability that a cell will survive a 12 hour treatment is one in a million. At each time step that the antimicrobial agent is present, every cell in the simulation generates a random number from a uniform distribution on the interval [0, 1]. If the random number is less than or equal to the probability of killing (0.6838), the cell dies and remains metabolically inactive for the remainder of the simulation or until it detaches from the biofilm. If the random number is greater than 0.6838, the cell continues to function normally.

The slow penetration, stress response, and persister mechanisms use the same probability for killing of live cells as is found in the unprotected simulations. In order to provide a form of protection, the slow penetration and stress response mechanisms include restrictions on when this probability equation is active as a result of the barrier to antimicrobial diffusion. For the persister mechanism, no restrictions are placed on this probability since the protection stems from the inclusion of the spore-like persister cells. The substrate limitation mechanism is different from each of these mechanisms and the

unprotected simulations in that the probability for killing is altered so that it is directly proportional to the local substrate concentration.

In the simulations where the slow penetration mechanism is active, both live and dead biofilm cells consume the antimicrobial as it diffuses into the biofilm. The parameters for antimicrobial diffusion and consumption are shown in Table 2-2.

Table 2-2. BacLAB parameters for use in antimicrobial diffusion and consumption.

Parameter	Symbol	Value	Unit(s)
Maximum specific reaction rate of antimicrobial	$k_{A,\,max}$	2.5	$g_A\ g_S^{-1}\ h^{-1}$
Bulk antimicrobial concentration	$C_{A,\,bulk}$	10.0	$g\ m^{-3}$
Diffusivity of the antimicrobial in the aqueous phase (including the liquid, channels and voids)	$D_{A,aq}$	$1.44 \cdot 10^{-6}$	$m^2\ h^{-1}$
Relative effective diffusivity of the antimicrobial in biofilm	$D_{A,e} / D_{A,aq}$	0.25	
Antibiotic Monod half saturation coefficient	K_A	1.0	$g\ m^{-3}$

In the aqueous environment being modeled, the bulk liquid is well-mixed, but imposes no shear-stress on the biofilm. The antimicrobial is transported solely by diffusion in the biofilm. The local concentrations are a result of molecular diffusion and reaction (consumption or production) with the bacteria. The diffusional time constant is approximately 100 times smaller than that for bacterial cell division (28). Thus, molecular diffusion can be assumed to be at steady state with respect to the bacterial growth.

Since the antimicrobial is steadily being depleted, there will exist an antimicrobial concentration at which it is no longer effective against the biofilm cells. This concentration, otherwise known as the minimum inhibitory concentration (MIC), is set at

1.0 g m^{-3}. It follows that, as the thickness of a biofilm increases, so too does its chance of thwarting an antimicrobial challenge.

The stress response mechanism includes the same rules that are used for slow penetration protection, diffusion and consumption of the antimicrobial based on the parameters shown in Table 2-2 and no killing below the MIC of 1.0 g m^{-3}, but with one variation: if the antimicrobial concentration is greater than or equal to one-tenth the MIC, and the cell has not been killed by the antimicrobial, then the cell has some probability of switching to an adapted state. This probability is 0.06838, ten percent of the probability of death. In the adapted state the cell acquires an absolute resistance to the effects of the antimicrobial, and continues its cellular functions uninhibited by the antimicrobial.

For the substrate limitation mechanism, the antimicrobial efficacy was simulated to be proportional to the amount of substrate available to the microorganism. That is,

$$P = \frac{P_{MAX}}{C_{S0}} \cdot C_S \tag{2-2}$$

where P_{MAX} is the maximum probability of killing and equal to the probability of killing used in the base case simulations, C_{S0} is the substrate concentration in the bulk fluid, and C_S is the local substrate concentration at a particular cell. Thus cells in substrate rich regions of the biofilm have the lowest antimicrobial tolerance, whereas cells in substrate depleted regions are expected to be tolerant to antimicrobial killing.

When simulating the persister mechanism, the protection stems from the random conversion of live cells to persister cells. Persister cells are non-growing, spore-like cells that are nearly impervious to antimicrobial effects. Persisters are constantly being

formed, with no regard to the presence or absence of an antimicrobial. The probability of a live cell converting to a persister cell is 0.0015 and the probability of a persister cell converting back to a live cell is 0.15. These values were chosen to yield a persister population of approximately one percent. The probability that a persister cell would be killed by an antimicrobial is 0.0034, making it 200-fold more resistant to the antimicrobial than a normal live cell.

We did not conduct a full sensitivity analysis of the model to the values of key parameters. It was rather our intent to illustrate the qualitative behaviors predicted when certain biological and physical phenomena were simulated.

All simulations progressed through a 300 hour experiment: 100 hours of initial attachment and unchallenged growth, a 50-hour antimicrobial treatment, and 150 hours of recovery.

Results and Discussion

The computer model used in this investigation simulated biofilm development over 300 hours, along with the response to a 50-hour continuous antimicrobial treatment for both unprotected and protected biofilms. Because there are stochastic components of the model, simulation results vary slightly from run to run even when the same parameter settings and initial conditions are used. We therefore ran each simulation case six times.

We selected a value for the antimicrobial kill rate that corresponded to a 6 log reduction in viable cell numbers after a 12 hour exposure of planktonic cells to the antimicrobial agent in the absence of cell growth. Even with the inclusion of biofilm growth during an antimicrobial treatment, we anticipated that each of the unprotected

biofilms would be eradicated by a 50-hour treatment. In all cases, this was indeed the result. All of the unprotected biofilms were killed completely by the 15th hour of the antimicrobial treatment.

With regard to the protected biofilms, Table 2-3 summarizes the log reductions produced by the 50-hour antimicrobial treatment.

Table 2-3. Log reductions of live cells for each protective mechanism after a 50-hour antimicrobial treatment.

Simulations	Slow Penetration*	Adaptation	Substrate	Persisters
1	> 5.93	1.59	0.59	5.93
2	> 5.91	1.56	0.68	5.92
3	> 5.89	1.50	0.57	5.90
4	> 5.93	1.41	0.75	5.86
5	> 5.93	1.54	0.51	5.30
6	> 5.93	1.57	0.54	5.92
Average	**> 5.92**	**1.53**	**0.61**	**5.80**
Standard Deviation	**----**	**0.06**	**0.09**	**0.25**

*No live cells remained at the end of the antimicrobial treatment in each of the slow penetration simulations

Slow Penetration

The kill curve for the slow penetration investigations and the corresponding base case simulations are shown in Figure 2-3. The survival curve is highly non-linear. Retarded antimicrobial penetration provided the biofilm good protection up until around 15 hours after the onset of treatment. If this had been only a 12 hour treatment, then the biofilm would have easily survived due to the protection of slow penetration. After this time, however, viability takes a sharp turn downwards as the diffusion of the

antimicrobial outpaces the neutralization by the bacteria. This imbalance leads to the complete disinfection of the biofilm colony 15 to 20 hours before the end of the 50-hour treatment.

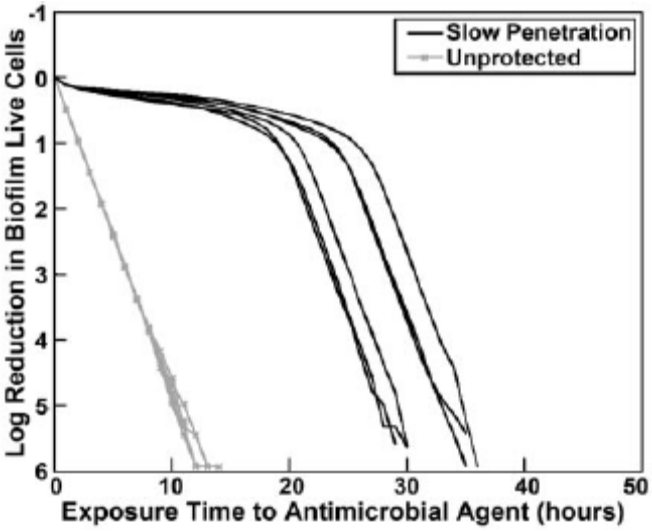

Figure 2-3. Log reduction of biofilm live cells during a 50-hour antimicrobial treatment for unprotected biofilms (x) and biofilms protected by the slow penetration mechanism (black). The biofilms without protection are completely eradicated after 13 hours, while the protected biofilms are able to withstand the antimicrobial for 30 to 35 hours.

When the slow penetration mechanism is active, both live and dead biofilm cells consume the antimicrobial. The effects of this consumption are evident in the antimicrobial concentration profile in the biofilm ten hours after the treatment began, shown in Figure 2-4. The concentration of antimicrobial agent is reduced in and around the biofilm clusters, even in the fluid where there is no consumption of the antimicrobial. This is because the stagnant fluid outside the biofilm poses a resistance to diffusive mass transfer. There are bands of live cells at the bottoms of the larger biofilm clusters, where the antimicrobial concentration is less than ten percent of its bulk concentration. The

separation between live and dead cells is distinct as there are few live cells above the 1.0 g m^{-3} concentration and almost no dead cells below this concentration.

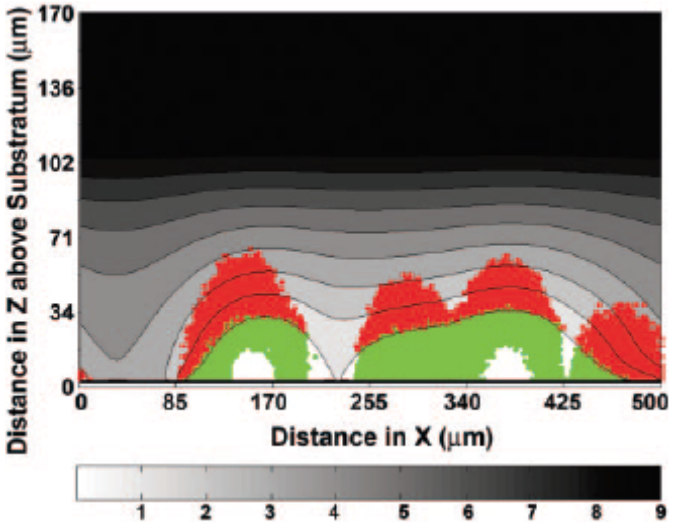

Figure 2-4. Concentration profile for the antimicrobial in a slow penetration simulation after hour 110, 10 hours after antimicrobial introduction. The image is a two-dimensional cross section of the biofilm with the substratum at bottom and the bulk fluid at top. The isoline represents antimicrobial concentrations in g m^{-3}. The figure shows a clear separation of live (green) and dead (red) cells at an antimicrobial concentration of 1.0 g m^{-3}. The applied antimicrobial concentration was 10 g m^{-3}. This concentration occurs above the domain plotted here.

The results of these simulations are most likely highly dependent on the choice of parameter values (Table 2-2). If the antibiotic consumption rate ($k_{A,max}$) were increased, the biofilm would stand a greater chance of surviving the treatment. There would seem to be a critical consumption rate that, once passed, would allow the biofilm to consume the antimicrobial quickly enough that no investigations would see the eradication of the biofilm. This assumption was not tested for the current publication. This concept has been discussed in previous studies of beta-lactam penetration (14,27).

It is interesting to consider the fate of a biofilm that is disaggregated, then exposed to an antimicrobial agent. In the case of the slow penetration mechanism, the

inherent susceptibility of all the cells in a biofilm is identical to their planktonic counterparts. The only difference is that the antimicrobial concentrations experienced by the biofilm population are heterogeneous and lower than those experienced by a planktonic population. If slow penetration is the sole basis for biofilm tolerance, we would anticipate that dispersal of a biofilm would immediately and completely restore its full planktonic susceptibility. This behavior has been reported in some studies (2,16,42,45).

Stress Response

When slow penetration is combined with an adaptive stress response, greater protection is predicted by the model (compare Figure 2-5 to Figure 2-3). In this case, the antimicrobial fails to eradicate the biofilm. This is due to the transformation of live cells into adapted cells, which are immune to the antimicrobial agent. The adapted cells continue to grow and out-compete other cell types in the antimicrobial-treated biofilm community. By the end of the simulation, there are no non-adapted live cells remaining.

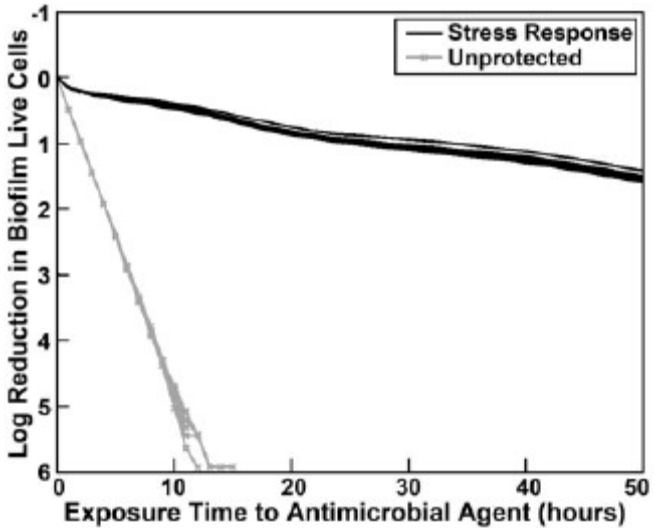

Figure 2-5. Log reduction of biofilm live cells during a 50-hour antimicrobial treatment for unprotected biofilms (x) and biofilms protected by the stress response and slow penetration mechanisms (black). The biofilms without protection are completely eradicated after 15 hours, while the protected biofilms are able to withstand the antimicrobial throughout the treatment time with an average log reduction of 1.53 ± 0.06.

It is evident from the representative antimicrobial concentration profile shown in Figure 2-6 that incomplete penetration of the antimicrobial limits killing to the uppermost layers of the biofilm. There is a sharp delineation between live and dead cells corresponding to the isoline of antimicrobial concentration equal to 1.0 g m^{-3}. The gradient in antimicrobial concentration allows cells in the lower regions of the biofilm to adapt and convert from the live cell state to the adapted cell state (yellow cells in Figure 2-6). This transformation occurs with a fixed probability wherever the antimicrobial concentration is greater than 0.1 g m^{-3}.

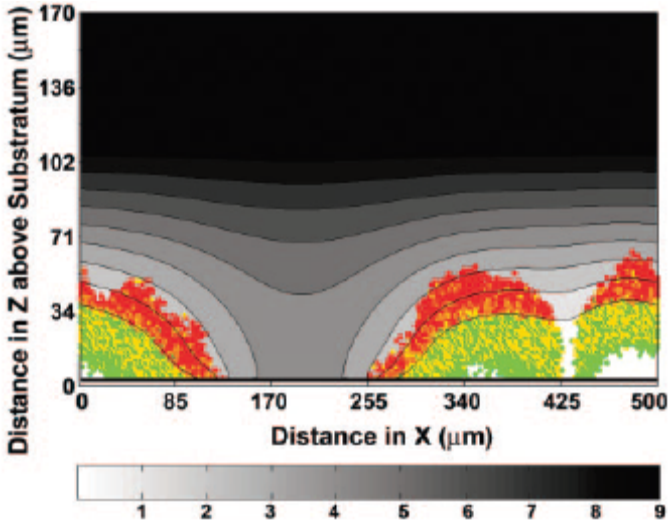

Figure 2-6. Concentration profile for the antimicrobial in a stress response simulation after hour 110, 10 hours after antimicrobial introduction. The image is a two-dimensional cross section of the biofilm with the substratum at bottom and the bulk fluid at top. The isoline represents antimicrobial concentrations in g m^{-3}. The applied antimicrobial concentration was 10 g m^{-3}. This concentration occurs above the domain plotted here. A small band of only live cells is also evident near the bottom of the biofilm. This corresponds to an antimicrobial concentration less than 0.1 g m^{-3}. Above this band, adaptive cells (yellow) are formed.

The particular outcome simulated here is dependent on the choice of parameter values (Table 2-2). The threshold concentration for implementation of the stress response (here 0.1 g m^{-3}) is critical. When this value is less than the concentration required for killing, then there will exist a window of antimicrobial concentrations (here 0.1 to 1.0 g m^{-3}) in which adaptation is relatively favorable. Note that adaptation can still occur at concentrations above the killing threshold concentration, but in this situation there is a race between the transformation of live cells to dead cells (killing) and the transformation of live cells to adapted cells (adaptation). The essential property of the adapted cell state is its invulnerability to killing, which allows these cells, even if generated in only small numbers, to eventually dominate the biofilm population.

One of the predictions implicit in the simulation of the stress response mechanism is that the adapted cells in an antimicrobial-treated biofilm should retain their antimicrobial tolerance for some time even if dispersed from the biofilm. Adapted cells may revert to the unadapted state if grown in the absence of the antimicrobial agent, but this process presumably requires some time. A biofilm population that is disaggregated and immediately challenged with antimicrobial agent would be expected to contain some adapted cells and therefore exhibit a susceptibility intermediate between a normal (unadapted) planktonic population and an intact biofilm. This has been observed in some experimental studies (3,18,20,28). While this investigation did not incorporate the process of adapted cells returning to an unadapted state, this would be a straightforward modification.

Substrate Limitation

When substrate-limited killing is simulated, the biofilm is well-protected (Figure 2-7). Since cells in the outer layers of the biofilm are killed (Figure 2-8), and these dead cells no longer consume substrate, substrate should permeate into the biofilm, feeding the inner layers and making them vulnerable to the action of the antimicrobial. This process is not particularly rapid, as Figure 2-7 attests. This result of prolonged tolerance afforded by the substrate limitation mechanism is in agreement with the predictions of a previous study conducted with a one-dimensional biofilm model (28). Please note that the simulations and results described here and in the next section do not incorporate the slow penetration protection used in the two previous cases.

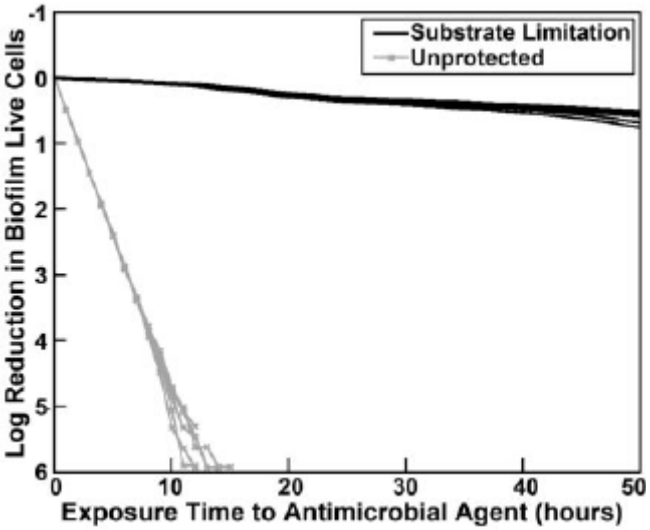

Figure 2-7. Log reduction of biofilm live cells during a 50-hour antimicrobial treatment for unprotected biofilms (x) and biofilms protected by the substrate limitation mechanism (black). The biofilms without protection are completely eradicated after 15 hours, while the protected biofilms are able to withstand the antimicrobial throughout the treatment time with an average log reduction of 0.61 ± 0.09.

According to the substrate limitation mechanism, cells in substrate-rich regions of the biofilm will have the greatest antimicrobial susceptibility, whereas cells in substrate-depleted regions are expected to be relatively tolerant to antimicrobial killing. This behavior is evident in the substrate concentration profile shown in Figure 2-8, which reveals domination of live cells in the innermost, and nutrient-limited, layers of the biofilm. Dead cells are localized preferentially at the surface layers of the biofilm, where substrate concentrations are highest. The stratification of live and dead cells is not as sharp as predicted by the slow penetration and stress response mechanisms. Surviving cells can be found at the outermost reaches of the biofilm and dead cells can be found deep in the biofilm interior.

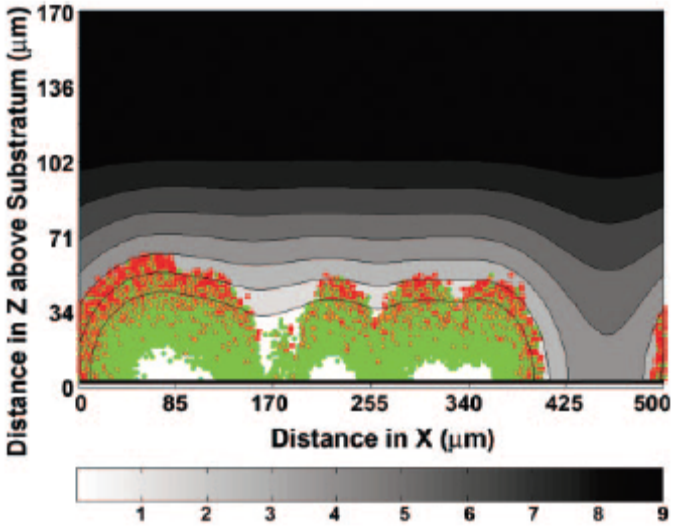

Figure 2-8. Concentration profile for the substrate in a substrate limitation simulation after hour 110, 10 hours after antimicrobial introduction. The image is a two-dimensional cross section of the biofilm with the substratum at bottom and the bulk fluid at top. The isoline represents substrate concentrations in g m^{-3}. The majority of dead cells (red) are concentrated at the tops of the biofilms, where substrate is at its local maximum. Few dead cells are found deep within the biofilm, where the local substrate concentrations can fall below 0.1 g m^{-3}. The applied substrate concentration was 10 g m^{-3}. This concentration occurs above the domain plotted here.

If cells were dispersed from a biofilm protected by substrate limitation, how susceptible would they be to antimicrobial challenge? If the biofilm were dispersed into a substrate-replete medium, susceptibility should approach the typical planktonic state. The awakening from a non-growing, starved state to a state of rapid growth may require some time, so susceptibility may not be restored instantly. This could explain the occasional observation of intermediate susceptibility of dispersed biofilm cells (3,18,20,28). An interesting experiment would be to disperse biofilm cells into a substrate-limited medium (or medium lacking substrate altogether) and then apply the antimicrobial challenge. If substrate limitation is the sole protective mechanism, then

these cells should retain the full level of tolerance exhibited by the intact biofilm. There are very few examples of this kind of experiment, and the data are inconclusive.

Persisters

The time course of killing of cells in a biofilm protected by persister formation is distinct from the patterns exhibited by the other three protective mechanisms (Figure 2-9). Most of the biofilm consists of cells whose intrinsic susceptibility is the same as a planktonic cell. Thus, the majority of the biofilm population is rapidly killed. The persister subpopulation, which constitutes approximately one percent of the biofilm initially, is very slowly killed. The rate of killing of the persister cells is controlled by the slow, random reversion of these cells to the live cell state. As persisters convert to live cells, they become vulnerable to the antimicrobial. This mechanism leads to a bilinear kill curve in which rapid killing of most of the biofilm is followed by very slow killing of the small remainder of the population. The noise at the bottom of the curve comes from the stochastic conversion and resuscitation of live and persister cells, respectively.

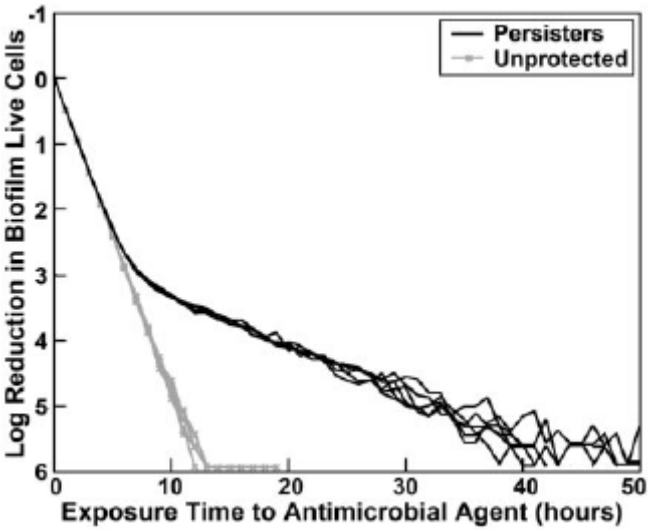

Figure 2-9. Log reduction of biofilm live cells during a 50-hour antimicrobial treatment for unprotected biofilms (x) and biofilms protected by the persister mechanism (black). The biofilms without protection are completely eradicated after 11 to 19 hours, while the protected biofilms are able to withstand the antimicrobial for 40 to 50 hours with an average log reduction of 5.80 ± 0.25.

The pattern of survival and regrowth inside a biofilm protected by persister formation is also distinct from the patterns predicted for the other three protective mechanisms (Figure 2-10). Regrowth of the biofilm, germinating from isolated persister cells, occurs in randomly located clonal pockets. The lone persister in the second panel of Figure 2-10 (circled in yellow) resuscitated to the live cell state and began to grow, effectively reseeding the biofilm. This spatial pattern is qualitatively different from the stratified patterns of killing observed with the other protective mechanisms. It is worth reiterating that this result occurs within an environment free of convective mixing of biomass.

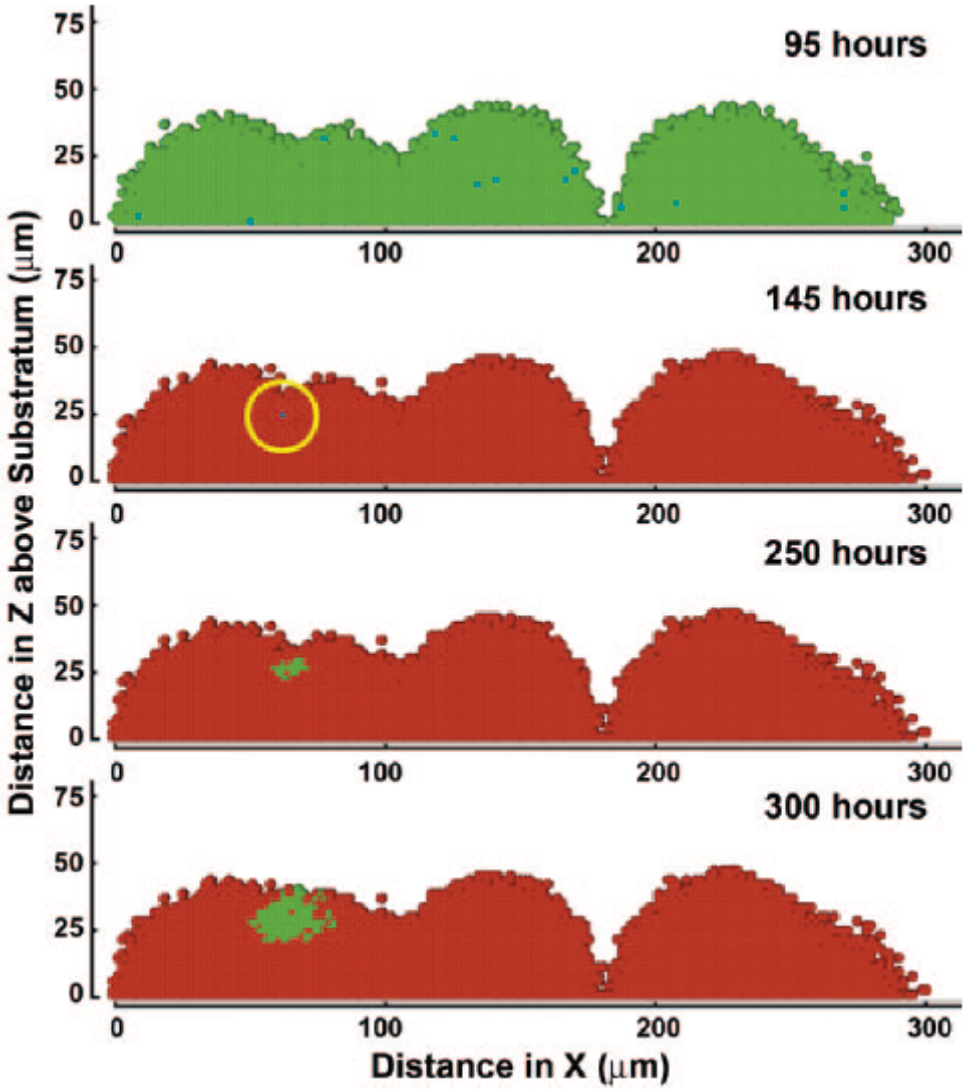

Figure 2-10. Cross section of a persister protected biofilm. The cross sections are taken at 95, 145, 250, and 300 hours. The figure shows that a single persister cell, circled in yellow in hour 145, can reseed the colony with new growth after an antimicrobial treatment has ended.

Dispersing cells from a biofilm protected by persister formation should not change the overall susceptibility. That is, of course, unless there exists a period of time between the dispersal of the biofilm and the application of the antimicrobial that is sufficient to allow the reversion of the persister cells to live cells. If the antimicrobial

challenge is applied quickly, however, the live cells will remain vulnerable and persister cells should remain mostly invulnerable. Thus, the dispersed cells would be expected to exhibit susceptibility similar to that of the intact biofilm. While experimenters rarely analyze the susceptibility of dispersed biofilm cells, when they do they find that the dispersed cells are usually more susceptible than the intact biofilm.

Conclusions

A 3D computer model of biofilm dynamics has been developed as a tool for investigating mechanisms of protection from antimicrobial agents in biofilms. All four of the hypothetical mechanisms explored in this study did provide protection according to model simulations. It is not appropriate to compare the relative degree of protection afforded by each of these mechanisms because these results depend on the choice of key parameters whose true values are unknown. What can be compared are the qualitative features of the behavior predicted by the simulations since these features are relatively insensitive to the choice of specific parameter values. Features that differed between the four protective mechanisms were the shape of the survival versus time curve and the spatial patterns of survival and cell type distribution (Table 2-4).

Table 2-4. Characteristics of alternative protective mechanisms.

Mechanism	Shape of killing curve	Distribution of cell types	Susceptibility of dispersed cells
Slow Penetration	Approximately bilinear, killing accelerating with time	Sharply stratified with dead cells on the outside and live cells inside	Same as planktonic
Stress Response	Approximately linear	Sharply stratified with dead cells on the outside and live cells inside	Equal to or less than planktonic, depending on how fast adapted cells return to an unadapted state
Substrate Limitation	Approximately linear	Noisily stratified with dead cells mostly on the outside and live cells mostly inside	Equal to or less than planktonic, depending on how fast inactive cells return to an active state
Persisters	Approximately bilinear, killing decelerating with time	Clonal survival of pockets of live cells at random locations within the biofilm	Same as intact biofilm

These results may be helpful in designing laboratory experiments to elucidate protective mechanisms in biofilms. We suggest that the most powerful approach to this problem would be to measure, in the same experimental system, all three of the aspects tabulated in Table 2-4, i.e., the shape of killing curves, the spatial pattern of antimicrobial action within the biofilm, and the relative susceptibility of resuspended biofilm cells. Though there are extant methods for measuring each of these features, we are aware of no single study in which all three have been performed concurrently.

One of the ways in which the work described in this article differs from previous modeling studies of antimicrobial action on biofilms is in the incorporation of stochastic elements in the model. Processes that have been simulated with random or probabilistic components in the current study include the initial seeding of the substratum, the direction in which biomass is displaced when growth occurs, and the transformation of live cells to dead cells in the presence of an antimicrobial. The result is that no two

simulations produce exactly the same quantitative result. The variability between simulations with identical input parameter values captures some of the variation that is measured by experimenters working with real biofilms. The stochastic elements of the model provide the ability to repeat experiments and statistically analyze the results just as an experimenter would in a real-world lab investigation.

References

1. Anderl, J. N., M. J. Franklin, and P. S. Stewart. 2000. Role of antibiotic penetration limitation in *Klebsiella pneumoniae* biofilm resistance to ampicillin and ciprofloxacin. Antimicrob. Agents Chemother. 44:1818-1824.

2. Anderl, J. N., J. Zahller, F. Roe, and P. S. Stewart. 2003. Role of nutrient limitation and stationary-phase existence in *Klebsiella pneumoniae* biofilm resistance to ampicillin and ciprofloxacin. Antimicrob. Agents Chemother. 47(4): 1251-6.

3. Baillie, G. S. and L. J. Douglas. 1998. Effect of growth rate on resistance of *Candida albicans* biofilms to antifungal agents. Antimicrob. Agents Chemother. 42(8): 1900-5.

4. Barker, G. C., and M. J. Grimson. 1993. A cellular automaton model of microbial growth. Binary 5:132-137.

5. Brooun, A., S. Liu, et al. 2000. A dose-response study of antibiotic resistance in *Pseudomonas aeruginosa* biofilms. Antimicrob. Agents Chemother. 44(3): 640-6.

6. Brown, M. R., D. G. Allison, and P. Gilbert. 1988. Resistance of bacterial biofilms to antibiotics: a growth-rate related effect? J. Antimicrob. Chemother. 22:777-80.

7. Cochran, W.L., G.A. McFeters, and P.S. Stewart. 2000. Reduced susceptibility of thin *Pseudomonas aeruginosa* biofilms to hydrogen peroxide and monochloramine. J. Appl. Microbiol. 88:22-30

8. Cogan, N. G., R. Cortez, and L. Fauci. 2005. Modeling physiological resistance in bacterial biofilms. Bull. Math. Biol. 67:831-853.

9. Colasanti, R. L. 1992. Cellular automata models of microbial colonies. Binary 4:191-193.

10. Darouiche, R. O., A. Dhir, A. J. Miller, G. C. Landon, I. I. Raad, and D. M. Musher. 1994. Vancomycin penetration into biofilm covering infected prostheses and effect on bacteria. J. Infect. Dis. 170:720-723.

11. Das, J. R., M. Bhakoo, M. V. Jones, P. Gilbert. (1998). Changes in the biocide susceptibility of *Staphylococcus epidermidis* and *Escherichia coli* cells associated with rapid attachment to plastic surfaces. J. Appl. Microbiol. 84(5): 852-8.

12. Davies, D. 2003. Understanding biofilm resistance to antibacterial agents. Nature Reviews Drug Discovery 2:114-122.

13. de Beer, D., P. Stoodley, F. Roe, and Z. Lewandowski. 1994. Effects of biofilm structures on oxygen distribution and mass-transport. Biotechnol. Bioeng. 43:1131-1138.

14. Dibdin, G. H., S. J. Assinder, W. W. Nichols, and P. A. Lambert. 1996. Mathematical model of beta-lactam penetration into a biofilm of *Pseudomonas aeruginosa* while undergoing simultaneous inactivation by released beta-lactamases. J. Antimicrob. Chemother. 38:757-769.

15. Dodds, M. G., K. J. Grobe, and P. S. Stewart. 2000. Modeling biofilm antimicrobial resistance. Biotechnol. Bioeng. 68:456-465.

16. Duguid, I. G., E. Evans, M. R. Brown, and P. Gilbert. 1992. Effect of biofilm culture upon the susceptibility of Staphylococcus epidermidis to tobramycin. J. Antimicrob. Chemother. 30(6): 803-10.

17. Dunne, W. M., E. O. Mason, and S. L. Kaplan. 1993. Diffusion of rifampin and vancomycin through a *Staphylococcus epidermidis* biofilm. Antimicrob. Agents Chemother. 37:2522-2526.

18. Eberl, H. J., C. Picioreanu, J. J. Heijnen, and M. C. M. van Loosdrecht. 2000. A three-dimensional numerical study on the correlation of spatial structure, hydrodynamic conditions, and mass transfer and conversion in bioflms. Chem Eng Sci 55:6209-6222.

19. Evans, D. J., D. G. Allison, M. R. Brown, P. Gilbert. 1990. Effect of growth-rate on resistance of gram-negative biofilms to cetrimide. J. Antimicrob. Chemother. 26(4): 473-8.

20. Evans, D. J., D. G. Allison, M. R. Brown, P. Gilbert. 1991. Susceptibility of *Pseudomonas aeruginosa* and *Escherichia coli* biofilms towards ciprofloxacin: effect of specific growth rate. J. Antimicrob. Chemother. 27(2): 177-84.

21. Goto, T., Y. Nakame, et al. 1999. In vitro bactericidal activities of beta-lactamases, amikacin, and fluoroquinolones against *Pseudomonas aeruginosa* biofilm in artificial urine. Urology 53(5): 1058-62.

22. Hunt, S. M., M. A. Hamilton, J. T. Sears, G. Harkin, and J. Reno. 2003. A computer investigation of chemically mediated detachment in bacterial biofilms. Microbiol. 149:1155-63.

23. Hunt, S. M., M. A. Hamilton, and P. S. Stewart. 2005. A 3D model of antimicrobial action on biofilms. Wat. Sci. Technol. 52:143-148.

24. Kreft, J. U., G. Booth, and J. W. T. Wimpenny. 1998. BacSim, a simulator for individual-based modelling of bacterial colony growth. Microbiol. 144:3275-3287.

25. Lewis, K. 2001. Riddle of biofilm resistance. Antimicrob. Agents Chemother. 45:999-1007.

26. Mah, T. C., and G. A. O'Toole. 2001. Mechanisms of biofilm resistance to antimicrobial agents. Trends Microbiol. 9:34-39.

27. Nichols, W. W., M. J. Evans, M. P. E. Slack, and H. L. Walmsley. 1989. The penetration of antibiotics into aggregates of mucoid and non-mucoid *Pseudomonas aeruginosa*. J. Gen. Microbiol. 135:1291-1303.

28. Noguera, D. R., G. Pizarro, D. A. Stahl, and B. E. Rittmann. 1999. Simulation of multispecies biofilm development in three dimensions. Wat. Sci. Tech. 39:123-130.

29. Picioreanu, C., M. C. M. van Loosdrecht, and J. J. Heijnen. 1998. A new combined differential-discrete cellular automaton approach for biofilm modeling: Application for growth in gel beads. Biotechnol. Bioeng. 57:718-731.

30. Picioreanu, C., M. C. M. van Loosdrecht, and J. J. Heijnen. 1999. Discrete-differential modelling of biofilm structure. Wat. Sci. Tech. 39:115-122.

31. Pyle, B. H. and G. A. McFeters. 1990. Iodine susceptibility of pseudomonads grown attached to stainless steel surfaces. Biofouling 2: 113-20.

32. Roberts, M. E., and P. S. Stewart. 2004. Modeling antibiotic tolerance in biofilms by accounting for nutrient limitation. Antimicrob. Agents Chemother. 48:48-52.

33. Shigeta, M., G. Tanaka, H. Komatsuzawa, M. Sugai, H. Suginaka, and T. Usui. 1997. Permeation of antimicrobial agents through *Pseudomonas aeruginosa* biofilms: A simple method. Chemotherapy 43:340-345.

34. Spoering, A. L. and K. Lewis. 2001. Biofilms and planktonic cells of Pseudomonas aeruginosa have similar resistance to killing by antimicrobials. J. Bacteriol. 183(23): 6746-51.

35. Sternberg, C., B. B. Christensen, T. Johansen, A. Toftgaard Nielsen, J. B. Andersen, M. Givskov, and S. Molin. 1999. Distribution of bacterial growth activity in flow-chamber biofilms. Appl. Environ. Microbiol. 65:4108-17.

36. Stewart, P. S. 1994. Biofilm accumulation model that predicts antibiotic resistance of *Pseudomonas aeruginosa* biofilms. Antimicrob. Agents Chemother. 38:1052-1058.

37. Stewart, P. S. 1996. Theoretical aspects of antibiotic diffusion into microbial biofilms. Antimicrob. Agents Chemother. 40:2517-2522.

38. Stewart, P. S. 2002. Mechanisms of antibiotic resistance in bacterial biofilms. Int. J. Med. Microbiol. 292:107-113

39. Stewart, P. S., and J. W. Costerton. 2001. Antibiotic resistance of bacteria in biofilms. Lancet 358:135-138.

40. Stewart, P. S., M. A. Hamilton, B. R. Goldstein, and B. T. Schneider. 1996. Modeling biocide action against biofilms. Biotechnol. Bioeng. 49:445-455.

41. Stewart, P. S., G. A. McFeters and C.-T. Huang. 2000. Biofilm control by antimicrobial agents. P. 373-405. In J.D. Bryers (ed.), Biofilms II Process Analysis and Applications. Wiley-Liss, New York.

42. Stewart, P. S., J. Rayner, F. Roe, and W. M. Rees. 2001. Biofilm penetration and disinfection efficacy of alkaline hypochlorite and chlorosulfamates. J. Appl. Microbiol. 91:525-32.

43. Suci, P. A., M. W. Mittelman, F. P. Yu, and G. G. Geesey. 1994. Investigation of ciprofloxacin penetration into *Pseudomonas-aeruginosa* biofilms. Antimicrob. Agents Chemother. 38:2125-2133.

44. Szomolay, B., I. Klapper, J. Dockery, and P. S. Stewart. 2005. Adaptive responses to antimicrobial agents in biofilms. Environ. Microbiol. 7:1186-1191.

45. Walters, M. C., 3rd, F. Roe, A. Bugnicourt, M. F. Franklin, and P. S. Stewart. 2003. Contributions of antibiotic penetration, oxygen limitation, and low metabolic activity

to tolerance of *Pseudomonas aeruginosa* biofilms to ciprofloxacin and tobramycin. Antimicrob. Agents Chemother. 47(1): 317-23.

46. Wentland, E. J., P. S. Stewart, C. T. Huang, and G. A. McFeters. 1996. Spatial variations in growth rate within *Klebsiella pneumoniae* colonies and biofilm. Biotechnol. Progr. 12:316-321.

47. Wimpenny, J. W. T., and R. Colasanti. 1997. A unifying hypothesis for the structure of microbial biofilms based on cellular automaton models. FEMS Microbiol. Ecol. 22:1-16.

48. Xu, K. D., P. S. Stewart, F. Xia, C. T. Huang, and G. A. McFeters. 1998. Spatial physiological heterogeneity in *Pseudomonas aeruginosa* biofilm is determined by oxygen availability. Appl. Environ. Microbiol. 64:4035-9.

49. Zheng, Z. L., and P. S. Stewart. 2002. Penetration of rifampin through *Staphylococcus epidermidis* biofilms. Antimicrob. Agents Chemother. 46:900-903.

CHAPTER 3

A 3D COMPUTER MODEL ANALYSIS OF THREE HYPOTHETICAL BIOFILM DETACHMENT MECHANISMS

Reproduced with permission from Chambless, J. D., and P. S. Stewart. 2007. A three-dimensional computer model analysis of three hypothetical biofilm detachment mechanisms. Biotechnology and Bioengineering 97:1573-1584.

Summary

Three hypothetical mechanisms of detachment were incorporated into a three-dimensional computer model of biofilm development. The model integrated processes of substrate utilization, substrate diffusion, growth, cell advection, and detachment in a cellular automata framework. The purpose of this investigation was to characterize each of the mechanisms with respect to four criteria: the resulting biofilm structure, the existence of a steady state, the propensity for sloughing events, and the dynamics during starvation. The three detachment mechanisms analyzed represented various physical and biological influences hypothesized to affect biofilm detachment. The first invoked the concept of fluid shear removing biomass that protrudes far above the surface and is therefore subjected to relatively large drag forces. The second pathway linked detachment to changes in the local availability of a nutrient. The third pathway simulated an erosive process in which individual cells are lost from the surface of a biofilm cell cluster. The detachment mechanisms demonstrated diverse behaviors with respect to the four analysis criteria. The height dependant mechanism produced flat, steady state biofilms that lacked sloughing events. Detachment based on substrate limitation produced significant

sloughing events. The resulting biofilm structures included distinct, hollow clusters separated by channels. The erosion mechanism produced neither a non-zero steady state nor sloughing events. A mechanism combining all three detachment mechanisms produced mushroom-like structures. The dynamics of biofilm decay during starvation were distinct for each detachment mechanism. These results show that detachment is a critical determinant of biofilm structure and of the dynamics of biofilm accumulation and loss.

Introduction

Planktonic microorganisms are typically easily understood. They do not employ complicated or diverse methods of growth, are easily eradicated with antimicrobials or biocides, and do not demonstrate sophisticated mechanisms of dispersal. However, these same microorganisms often will attach to wetted surfaces and form biofilms. Biofilm formation affords protection from antimicrobial challenges (36, 58), the potential for metabolic cooperation between species (22), and relative stability of the physical and chemical environment. Likewise, microorganisms also will detach from biofilms and return to the planktonic state. Detachment, or dispersal, is an important process that allows an organism the possibility of traveling to and colonizing a new location. Detachment also balances growth and so determines the net accumulation of biomass on the surface. Detachment is surely a critical determinant of microbial ecology and activity in many natural and engineered environments where biofilms form (51, 57).

The motivation behind research on biofilm detachment varies widely. Detachment studies can focus on discovering new approaches for controlling detrimental biofilms (65,

72), improving biological reactor design for treating wastewater (15, 20, 41, 66), or developing insight into the metastasis of infections within the human body (16, 30, 70).

The biological, chemical, and physical factors that drive detachment are complex and incompletely understood. Some of the phenomena or cues that are probably involved in detachment mechanisms include: degradation of the extracellular polymeric substances (EPS) constituting the biofilm matrix (1, 28), presence of excess nutrients (53), absence of sufficient nutrients (18, 26, 27, 54) or oxygen (62), production of an autocidal protein (37), production of biosurfactants (6, 10, 55), quorum sensing (12, 49, 50, 67), regulation by the secondary messenger cyclic di-GMP (19, 61), nitrosative stress (4), hydraulic shear and normal forces (21, 34, 38), cation crosslinking (3, 9, 64), sloughing (2, 24, 60), and erosive action (5, 17, 39). Judging from the length and variety of phenomena hypothesized as factors in biofilm detachment, one can anticipate that there are multiple detachment mechanisms, each of which may be multifactorial.

The absence of a single pathway to understanding biofilm detachment is reflected in the wide variety of mathematical submodels that have been proposed to describe detachment. It is worth noting that a number of important multidimensional biofilm models neglect detachment entirely (13, 32, 40, 44, 71). Others neglect cells that move out of the model domain (43, 46) or consider detachment to be subsumed in a general decay process (11, 48).

The earliest detachment models were those based on concepts of fluid shear (42, 52) in which the rate of detachment increases with the distance above the substratum (7, 63, 68). A common form assumes that detachment rate is proportional to the square of the

height above the substratum, a functionality that has the practical advantage of ensuring a steady state (57). Shear models of detachment in which a key variable is height continue to be widely and successfully employed in biofilm modeling (e.g. (73, 74)). One particularly elegant model computationally solved the fluid hydrodynamics around the biofilm, calculated internal stresses in the biofilm treating the biofilm as an elastic solid, and allowed for biofilm detachment via adhesive or cohesive failure (47).

A few biofilm models have made detachment rates dependent on the local concentration of a metabolic substrate or product. Several studies specifically link detachment to nutrient deprivation (8, 26, 35). Hunt et al. (25) investigated biofilm dynamics using a detachment function that depended on the concentration of a metabolic product, an approach that simulates the hypothetical accumulation of a quorum sensing signal as an impetus for detachment. Xavier et al. (72) implemented a detachment function that allowed for an externally added agent to degrade the mechanical cohesiveness of the biofilm matrix and thereby increase local detachment.

Some multidimensional biofilm models have prescribed an erosive detachment mechanism in which individual cells are lost from the surface of the biofilm (23, 33). We note that 1D models of biofilm formation have never employed surface erosion models of detachment that are independent of height. The likely reason for this is that a purely erosive model cannot produce a non-zero steady state. The rate of erosion from a flat surface is constant. A biofilm that begins to grow when the simulation starts will continue to grow indefinitely. A biofilm that begins to erode away at the outset will decay away to

a bare substratum. A relevant question is whether the same outcomes are expected in biofilm models of higher dimensionality.

In this study, we have focused on three conceptually distinct pathways of detachment. The first invokes the concept of fluid shear removing biomass that protrudes far above the surface and is therefore subjected to relatively large drag forces. The second pathway links detachment to changes in the local availability of a nutrient. The third pathway attempts to simulate an erosive process in which individual cells are lost from the surface of a biofilm cell cluster. Each detachment mechanism was investigated computationally using a hybrid cellular automata model called BacLAB. The purpose of this study was to characterize each of the hypothetical mechanisms with respect to four criteria: the resulting biofilm structure, the existence of a steady state, the propensity for sloughing events, and the behavior during starvation. The overall goal of this project was to compare the qualitative behaviors predicted in simulations using the three detachment mechanisms and to demonstrate that the choice of detachment mechanism can, by itself, profoundly influence biofilm structure and dynamics.

Materials and Methods

Description of the BacLAB Model

The BacLAB computer model used in this investigation has been described in three prior publications (8, 25, 26). The model integrated processes of substrate utilization, substrate diffusion, microbial growth, advective displacement of biomass, and detachment in a cellular automata framework. The distribution of the soluble substrate was modeled using discretized differential equations describing simultaneous reaction

and diffusion while the individual microorganisms that compose the biofilm were modeled discretely using a cellular automata algorithm. A cellular automaton is an independent unit, here equated to a microbial cell and its associated matrix material, which follows certain behavioral rules. In BacLAB, a biofilm cell can occupy fixed nodes on a regular 3D grid. When a cell has consumed sufficient substrate to divide, a daughter cell is generated and placed in an adjoining node. Growth can lead to the displacement of neighboring cells when there is no empty adjoining node to receive the daughter. This displacement is analogous to the process of biomass advection as articulated by Wanner and Gujer (68). A cell can detach, in which case it is removed entirely from the model space. When a biofilm cell (or cluster of cells) no longer has an unbroken chain of occupied automata nodes leading back to the substratum, the cell (or cluster) is removed from the model space and considered to have detached. In this way it is possible for a single detaching cell to precipitate the release of an aggregate of cells. Neither fluid flow nor the extracellular polymeric substances of the biofilm were explicitly included in the model. Cellular automata models can produce realistic, structurally heterogeneous biofilms (8, 14, 26, 40, 45). In these computer simulations, biofilm structure and activity evolve from the interactions between cells, emulating how bacterial cells organize themselves into biofilms. Parameter values are summarized in Table 3-1. The following subsection explains the conceptual basis, and mathematical implementation, of each detachment mechanism explored in this study. Please note that the parameters described in Table 3-1 do not represent any specific bacterial species; however, these parameters are the same order of magnitude for a typical bacterial species.

Table 3-1. Summary of parameters used in the BacLAB model.

Parameter	Symbol	Value	Unit(s)
Maximum specific growth rate	$\mu_{S,max}$	0.3	h^{-1}
Time step	Δt	1.0	h
Bulk substrate concentration	$C_{S,bulk}$	8.0	g m^{-3}
Diffusivity of substrate in aqueous phase (including the liquid, channels, and voids	$D_{S,aq}$	7.2 x 10^{-6}	m^2 h^{-1}
Relative effective diffusivity of substrate in biofilm	$D_{S,e}$ / $D_{S,aq}$	0.55	
Substrate Monod half saturation coefficient	K_M	0.1	g m^{-3}
Average cell mass	m_{avg}	1.75 x 10^{-13}	g
Initial number of colonies	N_c	28	
Number of nodes in x-direction	N_x	300	
Number of nodes in y-direction	N_y	300	
Radius of initial colonies	R_c	8.55 x 10^{-6}	m
Biomass yield (g_X) per gram of substrate (g_S)	Y_{XS}	0.24	g_X g_S^{-1}

Mechanism Descriptions

Each detachment mechanism modeled here was based conceptually on a single factor hypothesized to influence detachment. The mechanisms were modeled individually to characterize their behavior with respect to the four criteria mentioned above. An additional analysis examined a mathematical description of detachment that combined the three individual mechanisms.

Shear Detachment: This mechanism is the classic model of biofilm detachment and reflects, in an empirical fashion, the influence of fluid shear (7, 21, 38, 57). As the clusters of a biofilm grow taller, they are subjected to elevated shear forces from the movement of the bulk liquid. In order to simulate this effect, the probability of a cell detaching was made proportional to the square of its height above the substratum. The choice of squared dependence on height is empirical. We made this choice because this

formulation has been used both in prior seminal 1D modeling studies (68) and in more recent 3D treatments (73, 74). A squared dependence on height has the advantage of ensuring a steady state (57). In mathematical terms the shear detachment relationship is given by:

$$P = K_S \cdot \Delta t \cdot \left(\frac{z}{Z_{\max}} \right)^2 \quad (1)$$

where P is the probability of a given cell detaching, Δt is the length of each timestep, K_S is the detachment coefficient, z is the height of the biofilm cell, and Z_{max} is the maximum height allowed by the model. The inclusion of Z_{max} forces the growth of the biofilm to stay within the confines of the model space.

One of the conceptual barriers to using Eqn. 1 is that a cell deep in the interior of a cell cluster can detach. The probability of detachment depends only on height above the substratum, not on position within the biofilm structure. One can question how a cell can be "sheared" from the interior of a cell cluster without disturbing its neighbors. This is plainly not physically realistic at the individual cell level. On the other hand, a cell in the interior of a cell cluster can be removed by shear if it is stripped by fluid forces as part of an aggregate of cells. Modeling often involves simplifications that capture global properties of a phenomenon in ways that avoid undue complexity. The concept that cells that are further from the substratum are more likely to be detached is a reasonable concept, and Eqn. 1 implements this concept in a simple fashion.

Substrate Limited Detachment: The substrate limited mechanism simulates the possibility of deterioration of the biofilm in regions that are subjected to prolonged

substrate limitation (50). This deterioration, and subsequent detachment, could be due to phenomena such as cell lysis or degradation of the extracellular matrix of the biofilm. We have not attempted to simulate the specifics of this pathway, as these remain uncertain. A simple timing function for cell detachment was implemented. When the local concentration of substrate around a biofilm cell dropped below a user-specified minimum ($C_{S,min}$) for an extended period of time (t_{detach}), the cell detached from the biofilm. We began our analysis with this version of the substrate limited detachment model because this is the detachment mechanisms that was implemented in two previous BacLAB studies (8, 26). Later we describe a probabilistic variation of the substrate limited detachment model.

The substrate limited detachment mechanism can be expected to lead to detachment occurring from the interior of cell clusters where substrate concentrations are lowest. Here again is a physical paradox. How can a loose cell escape when it is surrounded by intact biofilm? It is perhaps most realistic to consider the early hollowing that occurs in a cell cluster to be due to cell lysis rather than detachment (59, 69). Later in the process, when the hollowed interior communicates with the bulk fluid, true detachment would be possible.

Erosion Detachment: The third mechanism addresses erosion. This mechanism focuses on the possibility of single cell detachment from the surfaces of the biofilm. In order to model this effect, the detachment probability of a cell was made inversely proportional to the number of neighboring cells. The equation used to determine detachment probabilities in this mechanism was:

$$P = K_e \cdot \Delta t \cdot \left(1 - \frac{n}{N_{\max}}\right) \quad (2)$$

where P is the probability of detachment of an individual cell, Δt is the length of each timestep , K_e is the detachment coefficient, n is the cell's neighbor count, and N_{max} is the maximum number of neighbors possible. From this equation it is easily seen that only cells located at the biofilm-bulk fluid interface were able to detach. A condition for detachment within this mechanism is that the cell be surrounded by a minimum number of unoccupied nodes before detaching. A cell must have at least nine vacant nodes surrounding it, the equivalent of one completely exposed face, before detachment can occur.

The erosion detachment mechanism does not incorporate any influence of the exposure of the local biofilm surface to fluid shear. A cell at the top of a tall cell cluster that has five neighboring cells has the same probability of detaching as does a cell near the base of the biofilm that has five neighbors.

The parameters related to each of the three detachment mechanisms are summarized in Table 3-2.

Table 3-2. Parameter values related to each detachment mechanism.

Parameter	Symbol	Value	Unit(s)
Maximum height allowed by model	Z_{max}	$341 \cdot 10^{-6}$	m
Starvation threshold concentration	$C_{s,min}$	0.1	g m^{-3}
Maximum number of neighbor cells	N_{max}	28	

Model Analysis

For each detachment mechanism, three experimental sets of simulations were performed: (1) the first set established the mechanism's ability to produce a steady state, and provided the resulting biofilm structure, using several rates of detachment, (2) the second set determined the propensity for sloughing events, and (3) the third set provided the results required to elucidate the behavior during starvation. The simulations in the first set of experiments were each controlled by a different rate of detachment respective to the particular mechanism. The number of simulations per experiment varied for each mechanism. A mechanism is said to have a steady state if it reaches a stable total cell density at some point during the simulation, and perturbations from this level are less than five percent of the total density over the next 100 hours. For the second set of experiments, a single detachment rate was chosen from the first set and six replicate simulations were performed to determine the propensity for sloughing events. The definition of a sloughing event is the same as that used in our previous paper (26), i.e. greater than 50% of biomass removed in one time step. The third and final set of experiments used the same detachment rate as the second set, and also consisted of six replicates. Starvation conditions in this final set of experiments were applied when the biofilm reached a steady state by removing all substrate from the model space for the remainder of the simulation. Replicate simulations are employed due to the stochastic nature of the mechanisms and the model. Differences between replicate simulations arise, despite identical model parameter values, because of the random initial distribution of cells on the substratum, the random nature of cell displacement resulting from growth of

neighboring cells, and the probabilistically driven detachment functions. Each simulation in each of the experimental sets ran for 500 hours.

Two of the three mechanisms, erosion and shear, execute cell removal via a comparison between a calculated detachment probability and a random number. During each time step, all cells in the simulation generate a random number from a uniform distribution on the interval [0, 1]. If the calculated detachment probability is greater than this random number, and each of the other mechanism-specific conditions necessary for detachment are satisfied, the cell detaches from the biofilm. The final mechanism, substrate limitation, draws on a simple cause and effect relationship. Essentially, cells detach from the biofilm after they have been starved of substrate for a particular period of time.

Results

The purpose of this investigation was to characterize each of three hypothetical detachment mechanisms with respect to four criteria: the resulting biofilm structure, the existence of a steady state, the propensity for sloughing events, and the behavior during starvation. The results of this analysis are presented in this section.

Shear Detachment

Structure: Simulations of the shear detachment mechanism consistently produced flat slab biofilms (Figure 3-1). Such features as clusters, towers, and channels were never observed in the steady-state structures. The height of the biofilm at steady state could be controlled by the value of the detachment coefficient (K_S).

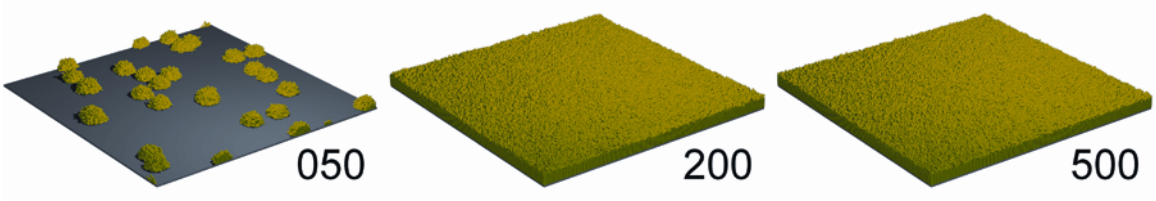

Figure 3-1. Typical simulation of biofilm development using the shear detachment mechanism. Microcolonies initially present merged into a confluent flat slab biofilm. This mechanism consistently produced biofilm structures lacking complex morphological features. Time is indicated in hours.

Steady State: A clear steady state was consistently achieved in simulations tracking the overall biofilm cell count versus time (Figure 3-2A).

Sloughing: Replicate simulations using a single value of the shear detachment coefficient exhibited a high degree of similarity, even though the initial cell count and colony placement were randomly determined (Figure 3-2B). The biofilm grew exponentially until cells began to reach a particular height. Biofilm accumulation stalled at this height, creating a flat slab of cells. This mechanism showed no signs of sloughing.

Starvation: Biofilms generated by the shear detachment mechanism decayed in a uniform fashion when substrate was removed from the system (Figure 3-2C). At hour 200 the model space was cleared of all substrate, and the biofilm immediately began to decay. As could be anticipated from a mechanism involving height–squared detachment, the decay was approximately quadratic. Again, no major sloughing events were observed, only a slow but steady decrease in the cell count. From the diminishing slope of the curve, it seems that this mechanism would predict extremely long starvation times in order to completely remove the biofilm. An additional simulation was performed to test this hypothesis. The end result showed that this mechanism did not exhibit complete

removal even after 1300 hours of substrate starvation.

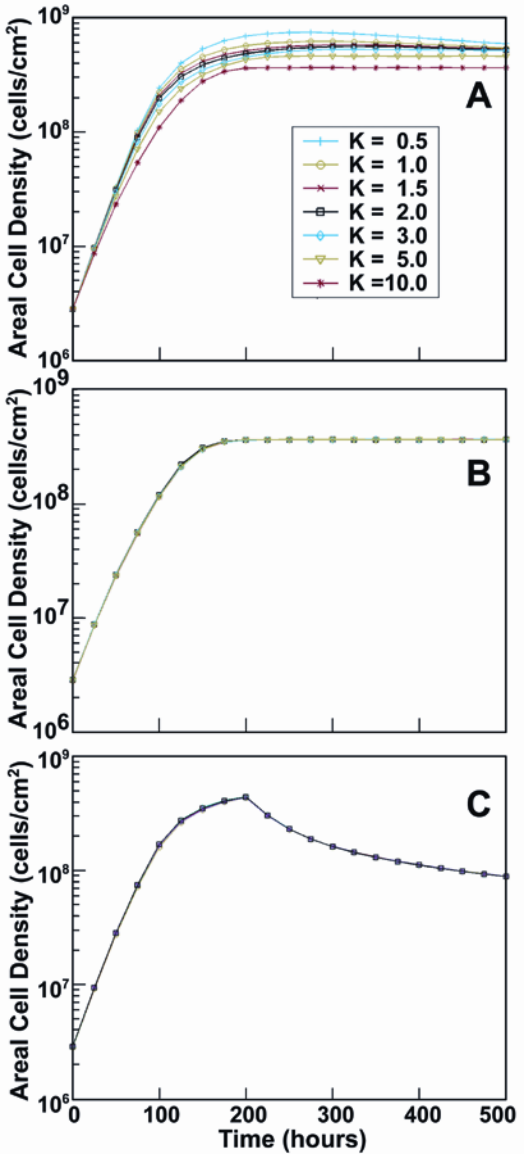

Figure 3-2. Seven simulations of the shear mechanism with seven different values of the detachment rate coefficient each provided a steady state cell density (A). Six replicate simulations of the shear mechanism with K_S = 5.0 showed zero sloughing events (B). Starvation conditions were introduced at hour 200 for each of six replicate simulations (C). This resulted in a decelerating, quadratic rate of decay that never completely removed the biofilm from the substratum.

Substrate Limitation

Structure: The substrate limitation mechanism produced structures (Figure 3-3) that were analogous to the swarming and hollow clusters found in some experimental studies (6, 29, 49, 56). Substrate limitation in the lower regions of the biofilm caused cells to detach, leaving hollow, towering clusters that were loosely tethered to the substratum. Hollow regions in time expanded to the point that they communicated with the bulk fluid. As the biofilms continued to grow taller and thus create diminished substrate concentrations near the substratum, nearly all cells in the lower strata of the biofilm detached due to limited availability of nutrients.

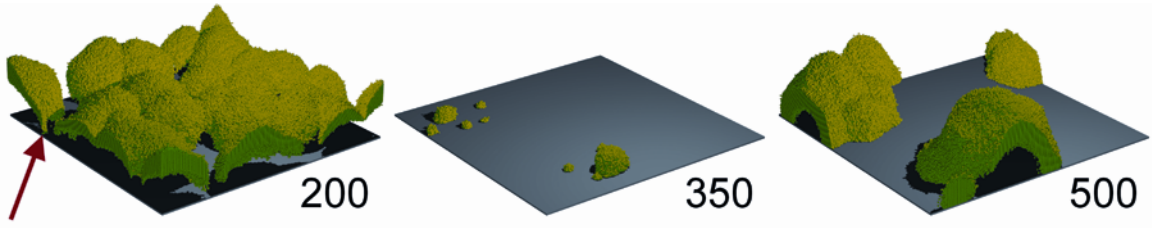

Figure 3-3. Typical simulation of biofilm development using the substrate limitation mechanism. These simulations produced towering, hollow structures that were loosely anchored to the substratum (red arrow) and that were prone to sloughing events. Biofilm growth renewed after sloughing events. Time is indicated in hours.

Steady State: Several detachment times (t_{detach}) were simulated with this mechanism, each one demonstrating a pseudo steady state (Figure 3-4A). Please recall that t_{detach} is the period the local substrate concentration around a cell must be continuously below the minimum threshold concentration, $C_{S,min}$, before the cell detaches. A simulation described as “pseudo steady state” possessed a minimum of two stationary phase cell densities, separated by 100 hours, which were within five percent of each other. The 100 hour separation could occur at any point in the stationary phase, and may

even span a major sloughing event.

Sloughing: Replicate simulations using a single detachment time of 24 hours each produced one or more major sloughing events, though the size and timing of the events were unpredictable (Figure 3-4B). Bear in mind that the model's stochastic components allowed differences to arise in replicate simulations with equal parameters. The substrate limitation mechanism was the only mechanism to provide significant variability among the replicate simulations. An important observation is that none of the sloughing events led to complete removal of the biofilm.

Starvation: At hour 200 of each simulation shown in Figure 3-4C the model space was cleared of all substrate. The biofilm soon began to decay, and 24 h later, for each simulation, all cells simultaneously detached. Complete detachment precludes any chance of renewed growth if substrate were to be reintroduced.

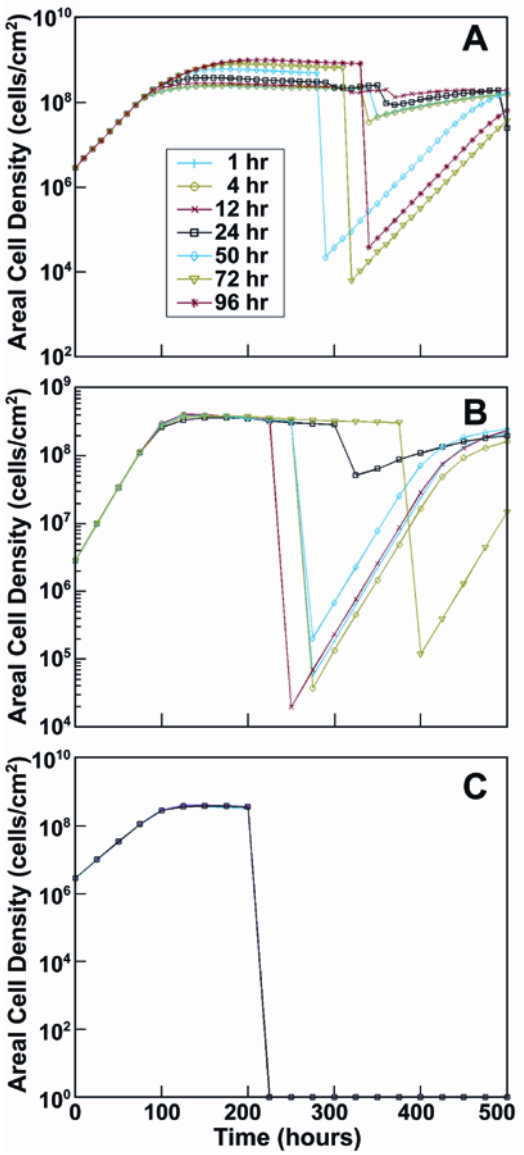

Figure 3-4. Seven simulations of the substrate limitation mechanism with seven different values of the detachment rate coefficient provided a pseudo steady state cell density despite the occurrence of sloughing events (A). Six replicate simulations using a single detachment time of 24 hours each produced one or more major sloughing events, though the nature and timing of the event were unpredictable (B). Twenty four hours after starvation conditions were imposed at 200 h, all cells simultaneously detached from the substratum (C), precluding the opportunity for regrowth.

This extensive, sudden detachment may not be realistic. In order to further address this issue, we performed six additional simulations in which the detachment was

not based on a timing function, but was instead probabilistically driven via a comparison between local substrate concentrations and the bulk substrate concentration. This version of the mechanism posited a higher probability of detachment for cells that were starved of substrate, as compared to those that had ample local substrate available. The equation describing this mechanism is:

$$P = K_{sub} \cdot \Delta t \cdot \left(1 - \frac{C_S}{C_{S,bulk}} \right) \tag{3}$$

where P is the probability of a cell detaching, K_{Sub} is the detachment coefficient, Δt is the length of each timestep, C_S is the local substrate concentration for the cell, and $C_{S,bulk}$ is the bulk substrate concentration. This version of the substrate limited detachment still led to a steep loss of cell density during starvation, but the detachment was less abrupt (Figure 3-5).

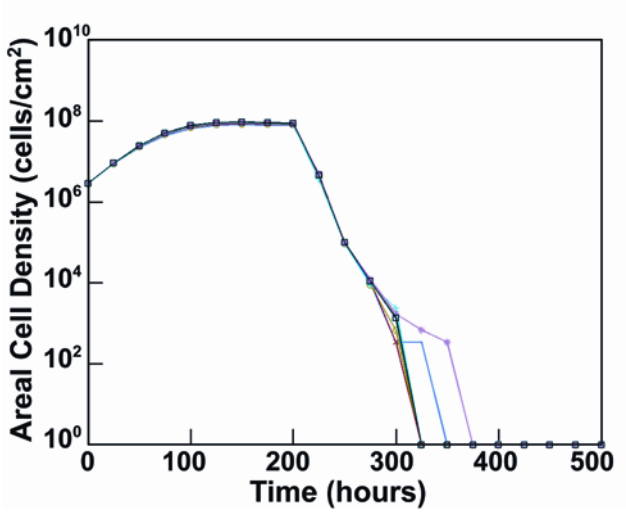

Figure 3-5. Response of biofilm formed using an alternative version of the substrate limitation detachment mechanism to starvation conditions. Six simulations of the substrate limitation mechanism were performed in which the detachment was not based on a timing function, but instead probabilistically tied to local substrate concentrations. Starvation conditions imposed at 200 h still lead to a steep loss of cell density, though less abrupt than the version presented in Figure 3-4C.

Erosion

Structure: The erosion mechanism produced tall, towering structures similar to those of the substrate limited mechanism, but did not demonstrate any signs of cluster hollowing (Figure 3-6). Hollowing would not be expected since the inner cells are completely surrounded by neighbors, and, based on equation (2), have a detachment probability of zero. The structures resemble confocal microscope images of *P. aeruginosa* biofilms taken in some experimental studies (31).

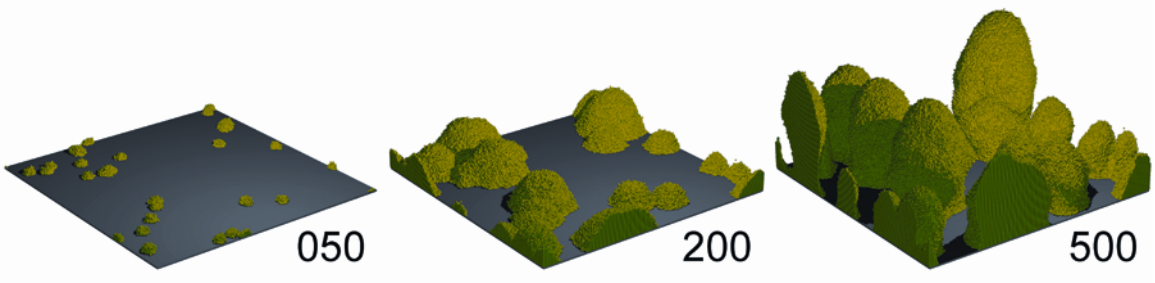

Figure 3-6. Typical simulation of biofilm development using the erosion mechanism. This detachment mechanism produced distinct towering structures. Unlike the clusters produced by the substrate limitation mechanism, no signs of cluster hollowing were observed. Time is indicated in hours.

Steady State: The erosion mechanism did not produce a non-zero steady state. If the erosive detachment coefficient K_e was too large, the biofilm decayed completely; if it was too small, the biofilm achieved unrestricted growth (Figure 3-7). Despite the intriguing structures produced by this mechanism, we did not attempt to analyze erosion detachment any further due to the inability of the mechanism to produce a steady state.

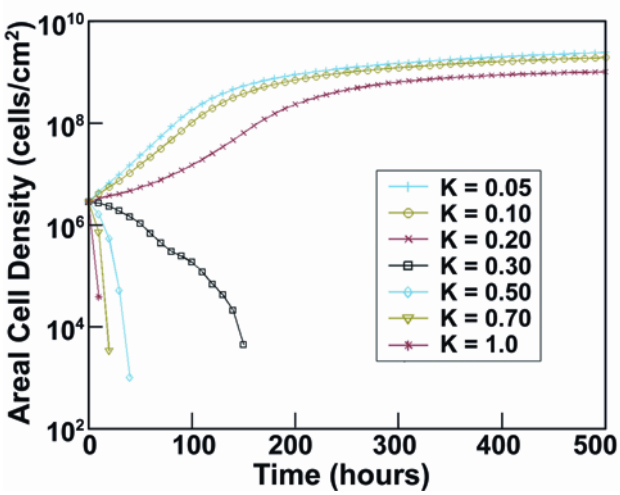

Figure 3-7. Seven simulations of biofilm development using the erosion detachment mechanism with different values of the detachment rate coefficient. The erosion mechanism did not produce a non-zero steady state. Some simulations decayed away to bare substratum while others achieved unrestricted growth.

Combined Detachment Mechanism

After performing the starvation experiments with the probabilistic substrate limited mechanism, and in the interest of demonstrating that the erosion mechanism could be a contributing factor in biofilm detachment, we set out to learn what behavior would result from a combined mechanism that included the erosion, shear, and probabilistic substrate limitation mechanisms. The combined detachment was based on the summation of each separate mechanisms' probability of detachment, as shown in equation (3-4):

$$P = \Delta t \cdot \left[K_S \cdot \left(\frac{z}{Z_{\max}} \right)^2 + K_e \cdot \left(1 - \frac{n}{N_{\max}} \right) + K_{sub} \cdot \left(1 - \frac{C_S}{C_{S,bulk}} \right) \right] \quad (3\text{-}4)$$

where each parameter definition is consistent with those in the previous three equations. The authors would like to acknowledge that typically, combining probabilities would mean a multiplicative combination, and not an additive one. Such a combination would not meet the goal of a combined detachment mechanism, however. Depletion of substrate caused local concentrations to approach zero in some regions of the biofilm due to the parameter values used. Physical limits require the minimum values of z and n to equal one; this would give an inappropriate weight to the substrate portion of the combination if the probabilities were multiplied. The additive model is best viewed as a purely empirical means of combining the three detachment mechanisms. All the conditional elements of the previous, separate simulations also applied in these simulations. In order to adequately combine these mechanisms, a single modification of the detachment probability was executed; namely, the detachment probability resulting

from erosion was set equal to -1 if the cell did not meet the minimum vacant nodes criteria. Essentially, this modification provided a neighbor-based "cohesiveness" adjustment to the probability of detachment that severely decreased the likelihood of a cell detaching when it was surrounded by many neighboring cells. Also, to keep the number of simulations at an acceptable level the detachment coefficients were not varied individually; i.e. all coefficients were equal during each particular simulation. Each simulation in each experimental set ran for 700 hours.

Structure: Combining the three mechanisms generated tall, mushroom-like structures (Figure 3-8), somewhat similar to those of the erosion mechanism. The mechanism featured towering clusters, minor sloughing events, and a "necking" phenomenon exemplified by thin stalks supporting large, spheroidal cell masses.

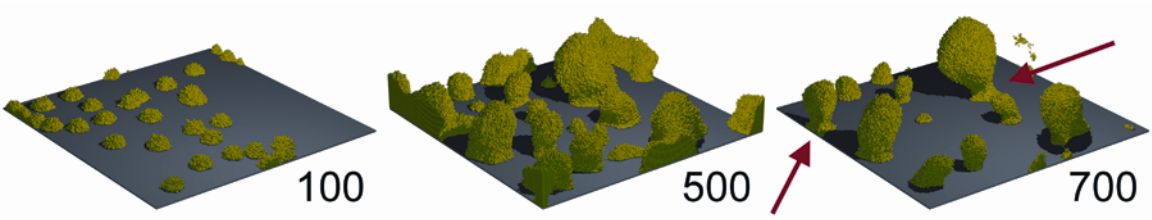

Figure 3-8. Typical simulation of biofilm development using the combined detachment mechanism. These simulations generated tall, mushroom-like structures that featured towering clusters, minor sloughing events, and a "necking" phenomenon exemplified by thin stalks supporting large, spherical cell masses (red arrows). Time is indicated in hours.

Steady State: Eight simulations were performed in this first experimental set, five of which reached a steady state (Figure 3-9A). Simulations with coefficients equal to or greater than 0.35 decayed away before a stable cell count could be achieved. The simulation using a coefficient of 0.05 exceeded the upper limit of the model space,

causing it to terminate before reaching 700 hours.

Sloughing: Replicate simulations using detachment coefficients equal to 0.125 provided two instances of a sloughing event that removed 50% of the total biomass (Figure 3-9B). Sloughing occurred in this mechanism due to the "necking" phenomenon, where the large mass of cells at the top of a cluster was released when the neck of the cluster pinched off (Figure 3-10). Each simulation seemed to reach a maximum cell density, followed by a slow, natural decay resulting from an increase in substrate-limited- and erosion-driven cell removal at the bases of the biofilm clusters.

Starvation: Due to the late-occurring steady state of this mechanism, the starvation conditions were imposed at hour 400 instead of hour 200. With a detachment coefficient of 0.125 the shape of the starvation curve was concave down, indicating an accelerating rate of attrition. (Figure 3-9C). Detachment during the starvation period caused several small sloughing events, along with the overall shrinking of all cell clusters. Complete cell removal was accomplished for each simulation within 330 hours of the onset of starvation conditions.

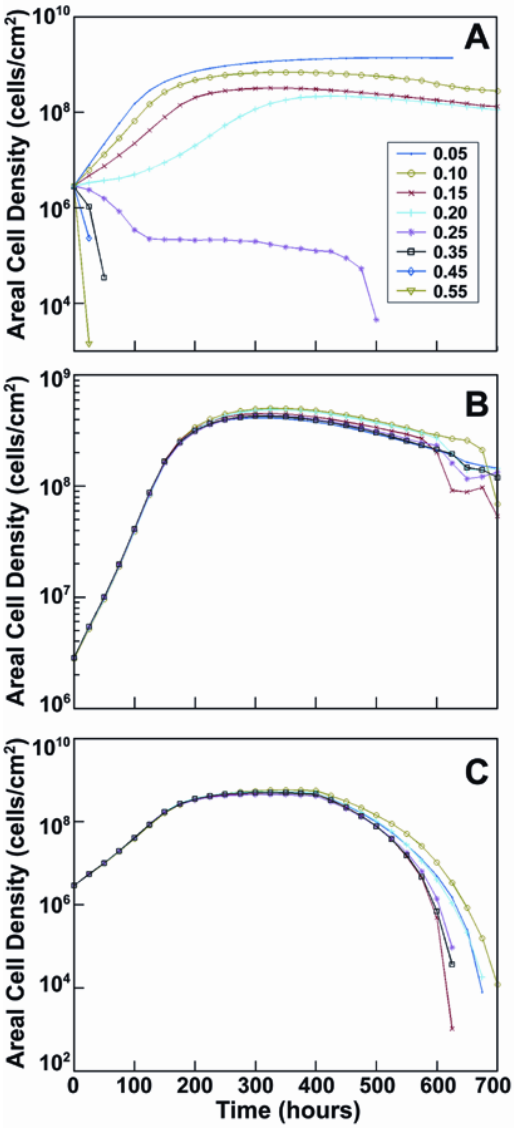

Figure 3-9. Eight simulations of the combined detachment mechanism with different values of the detachment rate coefficient. Five simulations reached a steady state, whereas simulations with coefficients greater than 0.25 decayed away (A). Two of the six replicate simulations using detachment coefficients equal to 0.125 produced a sloughing event of greater than 50% of the total biomass (B). Starvation conditions imposed at 400 h lead to concave down curvature in the cell density versus time trajectory, indicating an accelerating rate of attrition. All cells were eventually removed from the model space.

Discussion and Conclusion

We have analyzed the simulated behavior resulting from four different mathematical descriptions of detachment incorporated in a 3D cellular automata biofilm model in which all other parameter values were held constant. Each detachment mechanism resulted in distinct structural and dynamic features (Table 3-3). One obvious conclusion is that the choice of specific detachment pathway alone can significantly influence biofilm structure and dynamic behavior. We are not aware of prior biofilm modeling studies that have performed such a side-by-side comparative analysis of different detachment models in which other parameter values are fixed.

Table 3-3. Summary of results for each mechanism.

Mechanism	**Structure**	**Existence of Steady State**	**Propensity for Sloughing**	**Starvation Behavior**
Shear	Flat slabs	Steady state achieved, regardless of the detachment coefficient	None	Quadratic, decelerating decay
Substrate Limitation	Towering clusters with hollow interiors, loosely anchored to the substratum	Pseudo-steady state, equal cell densities often separated by substantial sloughing events	Sloughing with seemingly random timing and size	All cells detached 24 hours into starvation period
Erosion	Towering clusters with slight necking effects	No non-trivial steady state	Not tested	Not tested
Combined	Towering clusters with necking effects and base shrinkage	Steady state achieved with detachment coefficients less than or equal to $0.25h^{-1}$	Two sloughing events observed in six replicate simulations	Accelerating rate of decay leading to complete removal

Perhaps the most similar prior work to our study is that of Xavier et al. (72). In that investigation, the authors demonstrated that a change in the magnitude of a single detachment rate coefficient could completely change the steady-state structure and dynamics of the biofilm. Hermanowicz (23) also reported modest changes in biofilm structure predicted by a 2D model as the magnitude of a detachment coefficient was varied. The Xavier et al. report underscores the possibility that very different biofilm structures can arise with a single detachment mechanism. Thus while we have demonstrated here that the specific detachment mechanism is important, there are other features of the system, such as the degree of external mass transfer resistance, that also influence biofilm structure.

It is surprising that many of the prior multidimensional biofilm modeling studies do not directly address the question of whether the model produces a steady state. A number of these studies do not include detachment at all (13, 32, 40, 44, 71); a steady state is impossible. Others do not simulate detachment but rely on a subtractive decay process to balance growth (11, 48). It is our contention that models in which detachment occurs purely by surface erosion and is made independent of the distance above the substratum (e.g., (23, 33); and our erosion mechanism) cannot attain a non-zero steady state. This is based on the expectation that the surface area to volume ratio of biomass in the biofilm is greatest in the early stages of cell attachment and erosion will be proportionally large at this early stage. If the biofilm enlarges from this stage, it will continue to do so. There are two elegant, multidimensional modeling studies that address long-term behavior and demonstrate the potential for a noisy steady-state (47, 72).

We have characterized the dynamic behavior of simulated biofilms in response to starvation, an analysis of which we are aware of no precedent in the literature. In starvation mode, growth is eliminated and the dynamic behavior is determined by detachment and decay processes alone. We suggest that this may be an informative experimental design for gathering clues about the nature of the detachment process. For example, it might be possible to discriminate between detachment dominated by a shear pathway and detachment dominated by a substrate limitation pathway with a starvation experiment. In starvation mode, our simulations suggest that the rate of biomass loss continually slows with a shear mechanism, whereas the rate continually increases with a substrate limitation mechanism.

We conclude with a few additional remarks about the three primary detachment mechanisms investigated in this work, beginning with the shear mechanism. The explanation for the lack of sloughing events observed with this detachment pathway is presumably that the detachment probability of individual cells near the substratum is so small, due to their low height, that the chance of an entire group of these cells simultaneously detaching is miniscule. A biofilm in which detachment is governed by a height-dependant shear mechanism could be particularly difficult to remove completely using antimicrobial and physical treatments. As the biofilm gets thinner, the rate of detachment slows and the residual biomass will persist.

The substrate limitation detachment mechanism produced hollow cell clusters and, later, cell clusters that were held to the substratum through thin contacts at the periphery of cluster. As the biofilm matures, cells in the deep interior of cell clusters are

the first to experience prolonged substrate limitation and hence the first to detach. It may be appropriate to think of these lost cells as having lysed rather than detached since there is no path for physical release of cells from the interior of the cluster to the bulk fluid at the early stages of the hollowing process. As the biofilm continues to mature, however, the hollow interior expands until it communicates with the bulk fluid. Cells at the edge of the cell cluster, including those very close to the substratum have more substrate and are somewhat less likely to detach. This leads to the formation of umbrella-shaped structures that are loosely tethered at a few contact points around the edge of the cell cluster. The substrate limitation mechanism gives rise to sloughing events when these structures finally detach as one unit. Significant sloughing events were only observed when substrate limitation was included in the detachment model.

The erosion mechanism implemented in this study was independent of height above the substratum. This is likely an inadequate and unrealistic formulation. As discussed above, a purely erosive mechanism does not lead to non-zero steady states. When implemented in combination with height dependence, erosion detachment can lead to necked towers or mushrooms as described by Xavier et al. (74) and as shown in Figure 3-10. This shape arises when a cell cluster becomes tall enough that the lower portions of the cluster are substrate limited and therefore little new growth occurs. In these mid-portions of the cluster, erosion will cause the cluster to thin, generating a mushroom. Even though models generate mushroom-shaped structures resembling those seen by experimenters, this does not prove that this is the actual mechanism of formation of such structures.

It is interesting to note that in the erosion simulations the division between a coefficient value that lead to biofilm accumulation versus a coefficient value that forced complete decay occurred at a numerical value close to the maximum specific growth rate. For instance, when the maximum growth rate was 0.30 h^{-1}, K_e values greater than or equal to 0.30 h^{-1} all decayed to the trivial steady state. Time did not permit further analysis to determine if the point of this bifurcation in behavior was dependant on the value of the maximum growth rate.

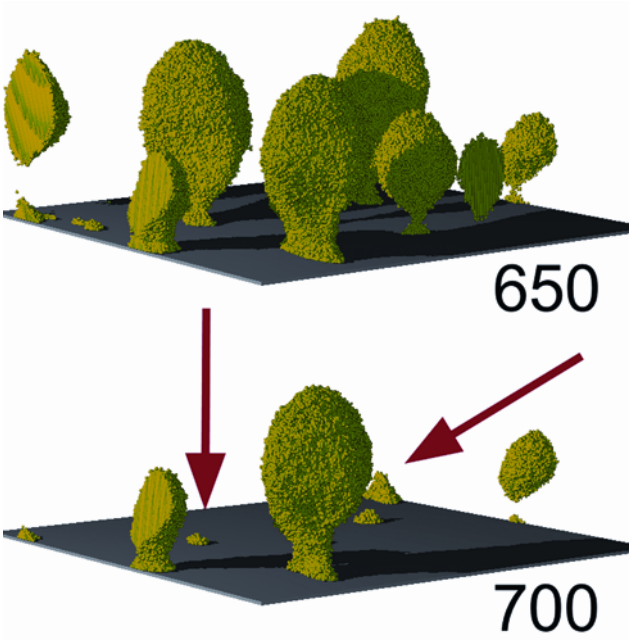

Figure 3-10. Example of a sloughing event in a simulation using the combined detachment mechanism. Sloughing occurred in this mechanism due to the "necking" phenomenon, where the large mass of cells at the top of a cluster was released when the neck of the cluster pinched off (location of detached cluster indicated by red arrows). Time is indicated in hours.

References

1. Allison, D. G., B. Ruiz, C. SanJose, A. Jaspe, and P. Gilbert. 1998. Extracellular products as mediators of the formation and detachment of *Pseudomonas fluorescens* biofilms. Fems Microbiology Letters 167:179-184.

2. Applegate, D. H., and J. D. Bryers. 1991. Effects of carbon and oxygen limitations and calcium concentrations on biofilm removal processes. Biotechnology and Bioengineering 37:17-25.

3. Banin, E., K. M. Brady, and E. P. Greenberg. 2006. Chelator-induced dispersal and killing of *Pseudomonas aeruginosa* cells in a biofilm. Applied and Environmental Microbiology 72:2064-2069.

4. Barraud, N., D. J. Hassett, S. H. Hwang, S. A. Rice, S. Kjelleberg, and J. S. Webb. 2006. Involvement of nitric oxide in biofilm dispersal of Pseudomonas aeruginosa. Journal of Bacteriology 188:7344-7353.

5. Bester, E., G. Wolfaardt, L. Joubert, K. Garny, and S. Saftic. 2005. Planktonic-cell yield of a pseudomonad biofilm. Applied and Environmental Microbiology 71:7792-7798.

6. Boles, B. R., M. Thoendel, and P. K. Singh. 2005. Rhamnolipids mediate detachment of Pseudomonas aeruginosa from biofilms. Molecular Microbiology 57:1210-1223.

7. Bryers, J. D. 1984. Biofilm formation and chemostat dynamics - pure and mixed culture considerations. Biotechnology and Bioengineering 26:948-958.

8. Chambless, J. D., S. M. Hunt, and P. S. Stewart. 2006. A three-dimensional computer model of four hypothetical mechanisms protecting biofilms from antimicrobials. Applied and Environmental Microbiology 72:2005-2013.

9. Chen, X., and P. S. Stewart. 2002. Role of electrostatic interactions in cohesion of bacterial biofilms. Applied Microbiology and Biotechnology 59:718-720.

10. Davey, M. E., N. C. Caiazza, and G. A. O'Toole. 2003. Rhamnolipid surfactant production affects biofilm architecture in Pseudomonas aeruginosa PAO1. Journal of Bacteriology 185:1027-1036.

11. Dockery, J., and I. Klapper. 2002. Finger formation in biofilm layers. Siam Journal on Applied Mathematics 62:853-869.

12. Dow, J. M., L. Crossman, K. Findlay, Y. Q. He, J. X. Feng, and J. L. Tang. 2003. Biofilm dispersal in *Xanthomonas campestris* is controlled by cell-cell signaling and is required for full virulence to plants. Proceedings of the National Academy of Sciences of the United States of America 100:10995-11000.

13. Eberl, H. D., D. Parker, and M. C. M. van Loosdrecht. 2001. A new deterministic spatio-temporal continuum model for biofilm development. Computational and Mathematical Methods in Medicine 3:161-175.

14. Eberl, H. J., C. Picioreanu, J. J. Heijnen, and M. C. M. van Loosdrecht. 2000. A three-dimensional numerical study on the correlation of spatial structure, hydrodynamic conditions, and mass transfer and conversion in biofilms. Chemical Engineering Science 55:6209-6222.

15. Eker, S., and F. Kargi. 2006. Biological treatment of para-chlorophenol containing synthetic wastewater using rotating brush biofilm reactor. Journal of Hazardous Materials 135:365-371.

16. Fux, C. A., S. Wilson, and P. Stoodley. 2004. Detachment characteristics and oxacillin resistance of Staphyloccocus aureus biofilm emboli in an in vitro catheter infection model. Journal of Bacteriology 186:4486-4491.

17. Gikas, P., and A. G. Livingston. 2006. Investigation of biofilm growth and attrition in a three-phase airlift bioreactor using (SO42-)-S-35 as a radiolabelled tracer. Journal of Chemical Technology and Biotechnology 81:858-865.

18. Gjermansen, M., P. Ragas, C. Sternberg, S. Molin, and T. Tolker-Nielsen. 2005. Characterization of starvation-induced dispersion in Pseudomonas putida biofilms. Environmental Microbiology 7:894-906.

19. Gjermansen, M., P. Ragas, and T. Tolker-Nielsen. 2006. Proteins with GGDEF and EAL domains regulate Pseudomonas putida biofilm formation and dispersal. Fems Microbiology Letters 265:215-224.

20. Gonzalez-Brambila, M., O. Monroy, and F. Lopez-Isunza. 2006. Experimental and theoretical study of membrane-aerated biofilm reactor behavior under different modes of oxygen supply for the treatment of synthetic wastewater. Chemical Engineering Science 61:5268-5281.

21. Guillemot, G., G. Vaca-Medina, H. Martin-Yken, A. Vernhet, P. Schmitz, and M. Mercier-Bonin. 2006. Shear-flow induced detachment of *Saccharomyces cerevisiae* from stainless steel: Influence of yeast and solid surface properties. Colloids and Surfaces B-Biointerfaces 49:126-135.

22. Hall-Stoodley, L., and P. Stoodley. 2002. Developmental regulation of microbial biofilms. Curr Opin Biotechnol 13:228-33.

23. Hermanowicz, S. W. 2001. A simple 2D biofilm model yields a variety of morphological features. Mathematical Biosciences 169:1-14.

24. Howell, J. A., and B. Atkinson. 1976. Sloughing of microbial film in trickling filters. Water Research 10:307-315.

25. Hunt, S. M., M. A. Hamilton, J. T. Sears, G. Harkin, and J. Reno. 2003. A computer investigation of chemically mediated detachment in bacterial biofilms. Microbiology-Sgm 149:1155-1163.

26. Hunt, S. M., E. M. Werner, B. C. Huang, M. A. Hamilton, and P. S. Stewart. 2004. Hypothesis for the role of nutrient starvation in biofilm detachment. Applied and Environmental Microbiology 70:7418-7425.

27. Jackson, D. W., K. Suzuki, L. Oakford, J. W. Simecka, M. E. Hart, and T. Romeo. 2002. Biofilm formation and dispersal under the influence of the global regulator CsrA of *Escherichia coli*. Journal of Bacteriology 184:290-301.

28. Kaplan, J. B., M. F. Meyenhofer, and D. H. Fine. 2003. Biofilm growth and detachment of *Actinobacillus actinomycetemcomitans*. Journal of Bacteriology 185:1399-1404.

29. Kaplan, J. B., C. Ragunath, N. Ramasubbu, and D. H. Fine. 2003. Detachment of *Actinobacillus actinomycetemcomitans* biofilm cells by an endogenous beta-hexosaminidase activity. Journal of Bacteriology 185:4693-4698.

30. Khardori, N., and M. Yassien. 1995. Biofilms in device-related infections. Journal of Industrial Microbiology 15:141-147.

31. Klausen, M., A. Aaes-Jorgensen, S. Molin, and T. Tolker-Nielsen. 2003. Involvement of bacterial migration in the development of complex multicellular structures in *Pseudomonas aeruginosa* biofilms. Molecular Microbiology 50:61-68.

32. Kreft, J. U., C. Picioreanu, J. W. T. Wimpenny, and M. C. M. van Loosdrecht. 2001. Individual-based modelling of biofilms. Microbiology-Sgm 147:2897-2912.

33. Laspidou, C. S., and B. E. Rittmann. 2004. Modeling the development of biofilm density including active bacteria, inert biomass, and extracellular polymeric substances. Water Research 38:3349-3361.

34. Liu, Y., and J. H. Tay. 2001. Detachment forces and their influence on the structure and metabolic behaviour of biofilms. World Journal of Microbiology & Biotechnology 17:111-117.

35. Luna, E., G. Dominguez-Zacarias, C. P. Ferreira, and J. X. Velasco-Hernandez. 2004. Detachment and diffusive-convective transport in an evolving heterogeneous two-dimensional biofilm hybrid model. Physical Review E 70:8.

36. Mah, T. F. C., and G. A. O'Toole. 2001. Mechanisms of biofilm resistance to antimicrobial agents. Trends in Microbiology 9:34-39.

37. Mai-Prochnow, A., J. S. Webb, B. C. Ferrari, and S. Kjelleberg. 2006. Ecological advantages of autolysis during the development and dispersal of *Pseudoalteromonas tunicata* biofilms. Applied and Environmental Microbiology 72:5414-5420.

38. Manz, B., F. Volke, D. Goll, and H. Horn. 2005. Investigation of biofilm structure, flow patterns and detachment with magnetic resonance imaging. Water Science and Technology 52:1-6.

39. Nicolella, C., S. Chiarle, R. DiFelice, and M. Rovatti. 1997. Mechanisms of biofilm detachment in fluidized bed reactors. Water Science and Technology 36:229-235.

40. Noguera, D. R., G. Pizarro, D. A. Stahl, and B. E. Rittmann. 1999. Simulation of multispecies biofilm development in three dimensions. Water Science and Technology 39:123-130.

41. Odegaard, H. 2006. Innovations in wastewater treatment: the moving bed biofilm process. Water Science and Technology 53:17-33.

42. Peyton, B. M., and W. G. Characklis. 1993. A statistical-analysis of the effect of substrate utilization and shear-stress on the kinetics of biofilm detachment. Biotechnology and Bioengineering 41:728-735.

43. Picioreanu, C., J. U. Kreft, and M. C. M. van Loosdrecht. 2004. Particle-based multidimensional multispecies Biofilm model. Applied and Environmental Microbiology 70:3024-3040.

44. Picioreanu, C., M. C. M. van Loosdrecht, and J. J. Heijnen. 1999. Discrete-differential modelling of biofilm structure. Water Science and Technology 39:115-122.

45. Picioreanu, C., M. C. M. van Loosdrecht, and J. J. Heijnen. 1998. Mathematical modeling of biofilm structure with a hybrid differential-discrete cellular automaton approach. Biotechnology and Bioengineering 58:101-116.

46. Picioreanu, C., M. C. M. van Loosdrecht, and J. J. Heijnen. 1998. A new combined differential-discrete cellular automaton approach for biofilm modeling: Application for growth in gel beads. Biotechnology and Bioengineering 57:718-731.

47. Picioreanu, C., M. C. M. van Loosdrecht, and J. J. Heijnen. 2001. Two-dimensional model of biofilm detachment caused by internal stress from liquid flow. Biotechnology and Bioengineering 72:205-218.

48. Pizarro, G., D. Griffeath, and D. R. Noguera. 2001. Quantitative cellular automaton model for biofilms. Journal of Environmental Engineering-Asce 127:782-789.

49. Purevdorj-Gage, B., W. J. Costerton, and P. Stoodley. 2005. Phenotypic differentiation and seeding dispersal in non-mucoid and mucoid *Pseudomonas aeruginosa* biofilms. Microbiology-Sgm 151:1569-1576.

50. Rice, S. A., K. S. Koh, S. Y. Queck, M. Labbate, K. W. Lam, and S. Kjelleberg. 2005. Biofilm formation and sloughing in *Serratia marcescens* are controlled by quorum sensing and nutrient cues. Journal of Bacteriology 187:3477-3485.

51. Rittmann, B. E. 1989. Detachment from biofilms, p. 49-58. *In* W. G. Characklis and P. A. Wilderer (ed.), Structure and function of biofilms. John Wiley & Sons, New York.

52. Rittmann, B. E. 1982. The effect of shear-stress on biofilm loss rate. Biotechnology and Bioengineering 24:501-506.

53. Sauer, K., M. C. Cullen, A. H. Rickard, L. A. H. Zeef, D. G. Davies, and P. Gilbert. 2004. Characterization of nutrient-induced dispersion in *Pseudomonas aeruginosa* PAO1 biofilm. Journal of Bacteriology 186:7312-7326.

54. Sawyer, L. K., and S. W. Hermanowicz. 1998. Detachment of biofilm bacteria due to variations in nutrient supply. Water Science and Technology 37:211-214.

55. Schoolin, S. R., U. K. Charaf, D. G. Allison, and P. Gilbert. 2004. A role for rhamnolipid in biofilm dispersion. Biofilms 1:91-99.

56. Stapper, A. P., G. Narasimhan, D. E. Ohman, J. Barakat, M. Hentzer, S. Molin, A. Kharazmi, N. Hoiby, and K. Mathee. 2004. Alginate production affects *Pseudomonas aeruginosa* biofilm development and architecture, but is not essential for biofilm formation. Journal of Medical Microbiology 53:679-690.

57. Stewart, P. S. 1993. A model of biofilm development. Biotechnology and Bioengineering 41:111-117.

58. Stewart, P. S., and J. W. Costerton. 2001. Antibiotic resistance of bacteria in biofilms. Lancet 358:135-138.

59. Stewart, P. S., S. A. Rani, E. Gjersing, S. L. Codd, Z. Zheng, and B. Pitts. 2007. Observations of cell cluster hollowing in *Staphylococcus epidermidis* biofilms. Letters in Applied Microbiology 44:454-457.

60. Telgmann, U., H. Horn, and E. Morgenroth. 2004. Influence of growth history on sloughing and erosion from biofilms. Water Research 38:3671-3684.

61. Thormann, K. M., S. Duttler, R. M. Saville, M. Hyodo, S. Shukla, Y. Hayakawa, and A. M. Spormann. 2006. Control of formation and cellular detachment from *Shewanella oneidensis* MR-1 biofilms by cyclic di-GMP. Journal of Bacteriology 188:2681-2691.

62. Thormann, K. M., R. M. Saville, S. Shukla, and A. M. Spormann. 2005. Induction of rapid detachment in *Shewanella oneidensis* MR-1 biofilms. Journal of Bacteriology 187:1014-1021.

63. Trulear, M. G., and W. G. Characklis. 1982. Dynamics of biofilm processes. Journal Water Pollution Control Federation 54:1288-1301.

64. Turakhia, M. H., K. E. Cooksey, and W. G. Characklis. 1983. Influence of a calcium-specific chelant on biofilm removal. Applied and Environmental Microbiology 46:1236-1238.

65. van der Borden, A. J., H. C. van der Mei, and H. Busscher. 2005. Electric block current induced detachment from surgical stainless steel and decreased viability of *Staphylococcus epidermidis*. Biomaterials 26:6731-6735.

66. van Loosdrecht, M. C. M., and S. Salem. 2006. Biological treatment of sludge digester liquids. Water Science and Technology 53:11-20.

67. Vuong, C., S. Kocianova, Y. F. Yao, A. B. Carmody, and M. Otto. 2004. Increased colonization of indwelling medical devices by quorum-sensing mutants of *Staphylococcus epidermidis* in vivo. Journal of Infectious Diseases 190:1498-1505.

68. Wanner, O., and W. Gujer. 1986. A multispecies biofilm model. Biotechnology and Bioengineering 28:314-328.

69. Webb, J. S., L. S. Thompson, S. James, T. Charlton, T. Tolker-Nielsen, B. Koch, M. Givskov, and S. Kjelleberg. 2003. Cell death in *Pseudomonas aeruginosa* biofilm development. Journal of Bacteriology 185:4585-4592.

70. Wilson, S., M. A. Hamilton, G. C. Hamilton, M. R. Schumann, and P. Stoodley. 2004. Statistical quantification of detachment rates and size distributions of cell clumps from wild-type (PAO1) and cell signaling mutant (JP1) *Pseudomonas aeruginosa* biofilms. Applied and Environmental Microbiology 70:5847-5852.

71. Wimpenny, J. W. T., and R. Colasanti. 1997. A unifying hypothesis for the structure of microbial biofilms based on cellular automaton models. Fems Microbiology Ecology 22:1-16.

72. Xavier, J. B., C. Picioreanu, S. A. Rani, M. C. M. van Loosdrecht, and P. S. Stewart. 2005. Biofilm-control strategies based on enzymic disruption of the extracellular polymeric substance matrix - a modelling study. Microbiology-Sgm 151:3817-3832.

73. Xavier, J. B., C. Picioreanu, and M. C. M. van Loosdrecht. 2005. A framework for multidimensional modelling of activity and structure of multispecies biofilms. Environmental Microbiology 7:1085-1103.

74. Xavier, J. D., C. Picioreanu, and M. C. M. van Loosdrecht. 2005. A general description of detachment for multidimensional modelling of biofilms. Biotechnology and Bioengineering 91:651-669.

CHAPTER 4

PERSISTER CELL FORMATION AND RESUSCITATION IN BIOFILMS: A 3D COMPUTER MODEL

Summary

Four different combinations of random and substrate-dependant persister mechanisms have been simulated through the use of a three dimensional hybrid cellular automata biofilm model. The purpose of this study was to determine and compare the effects of differing formation and resuscitation strategies on persister-related protection of biofilms. Simulations ran for 900 simulated hours. An antimicrobial dose lasting 48 hours was introduced at hour 375, after the colony had reached an established steady state. We evaluated each mechanism with respect to structure, live cell density, persister cell density, log reduction of live cells, and persister spatial distribution. The current study intimates that substrate resuscitation mechanisms have an advantage over random resuscitation mechanisms due to their much slower rate of persister resuscitation. After performing all of the simulations and analysis, it now seems intuitive that if persisters remain dormant for very extended periods, then the biofilm as a whole will be much more tolerant to antimicrobial challenges. If, however, the persisters remain too long in their dormant state, detachment forces may eventually remove them before they resuscitate. Nevertheless, we are unaware of a similar conclusion explicitly stated in any previous modeling study.

Introduction

Antimicrobial control of biofilms has been extensively researched, but is still poorly understood. Several competing theories attempt to explain biofilm recalcitrance through biofilm activity (5, 27), biofilm inactivity (1), genetic mutation (12), or phenotypic variation (24), among other phenomenon.

Phenotypic variants, often in the form of dormant cells that survive an antimicrobial treatment (30), can make up 0.1% to 1% of a biofilm population (13, 16). The existence of these cells, termed persisters, has been hypothesized to explain several characteristics of biofilm recalcitrance that cannot be adequately addressed with any other single survival mechanism. The most common, signature attribute of persister protection is biphasic killing, an example of which is shown in Figure 4-1. Very often, when dosing a biofilm with an antimicrobial, killing occurs in two stages (11): a sudden, sharp reduction in live cells, followed by a much slower loss in a subpopulation of live cells. Such a limitation of antimicrobial effectiveness occurs despite the continued dosing at a constant, or even increasing, concentration (2)

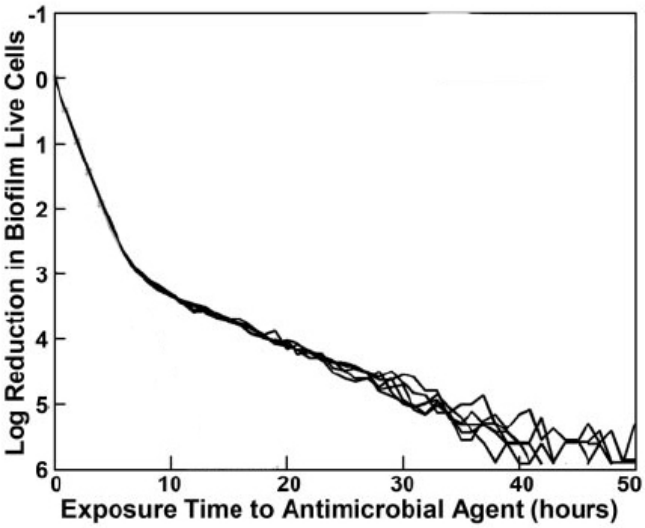

Figure 4-1. Representation of a biphasic killing curve on a log scale. The y-axis is log reduction of bacterial population and the x-axis is time, in hours, during the antimicrobial dose.

Non-inheritable tolerance is another effect often seen by researchers (13). Usually, if a biofilm population becomes resistant to an antimicrobial and is able to survive a treatment, these cells pass this resistance on to successive generations. The end result is a biofilm population that is unhindered by that same antimicrobial. However, when this effect is not observed, and the tolerant cells, when removed and resuspended, are killed to the same degree as the original population, another explanation is required. It is believed that persister cells are not a different genotype, but instead a separate phenotypic state that live cells enter into and revert from. Such an attribute would give rise to these populations that seem to only have a small percentage survive the same antimicrobial challenge in successive generations.

Much research has involved the hypothesis that biofilms, due inherently to their structure and morphology, create a barrier to the diffusion of an antimicrobial or react

sufficiently with the antimicrobial to create gradients in the depths of the biofilm. Seemingly, reduced antimicrobial penetration could allow biofilm cells deep within the biofilm clusters to survive an antimicrobial treatment. Unfortunately this hypothesis is unable to explain the tolerance of very young biofilm colonies whose thickness does not pose any obstruction to full antimicrobial penetration (5, 8). A study showing the quick penetration of antimicrobials into biofilms has been performed previously by the Stewart lab (28).

The formation of a persister is thought to be a reversible phenomenon (16). Events leading to cell switching are the basis of a burgeoning field of research. The simplest explanation, it would seem, is that persisters are simply a product of substrate limitation, resulting in slower growing biofilm cells (1, 19, 23). Some studies have used this characteristic to isolate what they deemed were true persister cells (1, 30). Others have shown that stochastic fluctuations in chromosomal toxin/antitoxin module levels, such as the *hipA* gene, inhibit macromolecular cell functions, thereby shutting down the cell and making it impervious to antimicrobials that target these cellular functions (7, 16, 19, 22, 30). Similarly, Vasquez-Laslop et al. (33) conducted a study that found proteins unrelated to the toxin/antitoxin model, which become toxic when ectopically expressed, that increase the number of persisters formed within a biofilm. Attachment, an essential early step in biofilm formation, has also been hypothesized to initiate persister formation in fungal biofilms (21). Additionally, persister formation has been tied to the density of the biofilm population (17) and responsive switching due to the bacterium's environment (20).

Several previous articles have attempted to explain the rise, existence, and protective effects of a persister, or protected, population within biofilms through modeling studies. In 2005, Szomolay et al. (32) hypothesized that reaction-diffusion limited penetration of antimicrobial agents caused ineffective exposure deep within biofilm colonies. They postulated that if antimicrobial concentrations are high enough to be sensed, but low enough to control the interior cells, an adaptive response (namely, live cells switching to an adapted state) could take place. Their model results showed that despite having the same adaptive response, planktonic cells could not tolerate an antimicrobial challenge as well as a biofilm. The advantage arises from reaction and/or diffusion interactions within the biofilm that slow the penetration of the antimicrobial, thus allowing the interior biofilm cells a chance to respond to the dose before the antimicrobial concentration is high enough to kill the interior cells.

Wiuff et al. (35) examined three hypotheses regarding biofilm recalcitrance, one of which occurs due to the random creation of a tolerant phenotypic variant during cell division. The new cell could grow and divide, but did not necessarily pass its tolerance on to the next generation. This is akin to a persister cell model, with the exception that the persister cells in this work are created during cell division, and not due to the predominately hypothesized switching process. Persisters, once formed, never reverted to a normal live cell. The researchers found that modifying the rate that a daughter cell is a tolerant cell will modify the rate at which the biofilm is able to withstand an antimicrobial challenge.

A 2005 article provided one of the first models for persister formation based on substrate depletion (29). The study describes a deterministic, material balance model of batch and chemostat bacterial cultures where live, dead, and persister cells were present. Persister cell formation was proportional to the total live cell concentration, and reversion was proportional to the local substrate concentrations. The authors posited that persister-forming biofilms could be better protected from antimicrobial challenges than persister-forming planktonic cultures due to the limited substrate available in the deeper regions of the biofilm. The study concluded that substrate depletion could account for the accumulation of persisters in the depths of the biofilm. This accumulation was shown to afford greater protection to biofilms than planktonic cultures.

Our own group studied the effects of four hypothetical protection mechanisms for biofilms in a recent work, which included a hypothesis on the persister phenotype (3). Persisters were randomly formed and resuscitated in a three-dimensional cellular automata model. The study was a comparison of the four mechanisms in an attempt to evaluate survival as a function of exposure time, along with the overall spatial patterns of survival. The study produced randomly spaced persister cells which reseeded the biofilm after an antimicrobial dose. Clonal pockets of biofilm cells resulted from these persister cells, and were able to regrow the biofilm.

A deterministic biofilm model was used to obtain guidelines for optimal dosing strategies of persister-forming biofilm infections (6). The model linked persister formation to antimicrobial concentrations and growth rate, and persister resuscitation to the existence of antimicrobial in the model space. The study showed that if persister

formation is related to growth stage, a generalized optimal dosing strategy can be obtained. Also, it was posited that the type of mechanism that regulates resuscitation is trivially important to the regrowth of the biofilm after an antimicrobial treatment.

In a recently published article, Klapper et al. (18) took a new look at tolerance with the knowledge that asymmetric cell division creates a new daughter cell, but leaves the mother cell unchanged (31). The older (senescent), mother cells were hypothesized to be persister cells. The core assumption of this work was that antimicrobial agents become less effective as cells age. A unique deterministic model was used to explain several of the observed persister characteristics with a simple application of tolerance due to cell age, instead of relying on switching phenomena. The study found that when tolerance is tied to senescence, the modeled biofilms successfully exhibited several of the experimentally observed persister-related and tolerance characteristics.

We have developed two sub-models of persister formation and resuscitation that either rely solely on random probabilities, or rely on random and substrate-dependant probabilities. We feel that an acceptable and thorough description of persister switching would need to be part stochastic and part environmentally driven. Substrate dependence incorporates a method for reversible, responsive switching that is tied to substrate availability, but still stochastically dominated, thereby enabling the inclusion of several observed results regarding persisters. Four different combinations of random and substrate-dependant persister mechanisms have been simulated through the use of a three dimensional hybrid cellular automata biofilm model. The purpose of this study was to determine and compare the effects of differing formation and resuscitation strategies on

persister-related protection of biofilms. It is our hope that this study will contribute to the overall goal of determining persister switching methods and understanding how biofilms may protect themselves via persister-generating mechanisms.

Materials and Methods

BacLAB Model

The BacLAB model used in this investigation has been described in various iterations in previous publications (3, 4, 14, 15). The model integrated processes of substrate utilization, substrate diffusion, microbial growth, advective displacement of biomass, detachment, and phenotypic switching in a cellular automata framework. Diffusion of substrate was performed by solving the discretized reaction-diffusion equation while individual bacteria were modeled via a cellular automata algorithm. Cellular automata models have been shown to produce structurally and functionally realistic biofilms (4, 9, 15, 25, 26). An artificial boundary layer exists at 49µm above the highest cell in the model space, which causes gradients to develop in diffusible materials. Bacterial cells detach from the model space when they no longer have a direct or indirect link to the substratum, or when shear stresses, erosion, or substrate limitation force their removal. Detachment from the model space was accomplished via a mechanism functionally dependant on the local substrate concentrations, the height of the bacterial cell above the substratum, and the number of empty nodes surrounding the bacterial cell. This combined mechanism of detachment is described in detail in Chambless and Stewart (4). Neither fluid flow nor extracellular polymeric substances (EPS) were explicitly modeled within BacLAB; however the detachment mechanism makes use of properties

resultant from an assumed existence of both. In these computer simulations, biofilm dynamics evolve from individual cells interacting with each other and their environment. Parameter values are summarized in Table 4-1. Please note that the parameters described in Table 4-1 do not represent any specific bacterial species; however, these parameters are the same order of magnitude for a typical bacterial species.

Table 4-1. Parameters, symbols, and values used in the BacLAB model.

Parameter	**Symbol**	**Value**	**Unit(s)**
Maximum specific growth rate	$\mu_{S,max}$	0.3	h^{-1}
Time step	Δt	1.0	h
Bulk substrate concentration	$C_{S,bulk}$	8.0	$g\ m^{-3}$
Diffusivity of substrate in the aqueous phase (including the liquid, channels and voids)	$D_{S,aq}$	$7.20 \cdot 10^{-6}$	$m^2\ h^{-1}$
Relative effective diffusivity of substrate in biofilm	$D_{S,e} / D_{S,aq}$	0.55	
Substrate Monod half saturation coefficient	K_M	0.1	$g\ m^{-3}$
Average cell mass	m_{avg}	$1.75 \cdot 10^{-13}$	g
Number of initial colonies	N_c	28	
Number of nodes in x-direction	N_x	300	
Number of nodes in y-direction	N_y	300	
Radius of initial colonies	R_c	$8.55 \cdot 10^{-6}$	m
Biomass yield (g_X) per gram of substrate (g_S)	Y_{XS}	0.24	$g_X\ g_S^{-1}$

Mechanism Descriptions

The four mechanisms tested in this study are named as follows: 1) Random Formation-Random Resuscitation (RR), 2) Random Formation-Substrate Resuscitation (RS), 3) Substrate Formation-Random Resuscitation (SR), and 4) Substrate Formation-Substrate Resuscitation (SS). “Formation” refers to the formation of a persister cell from

a live cell, and "Resuscitation" refers to the resuscitation of a persister cell to a live cell. For example, the combination "Random Formation – Substrate Resuscitation" refers to the case where a live cell will convert to the persister state via a randomly determined probability, and a persister cell will resuscitate into the live state via a probability that depends on the local substrate concentration.

In the "Random" case, whether "Formation" or "Resuscitation", the probabilities for the conversion are constant. The formation of a persister or the resuscitation of a live cell only depends on whether or not a randomly generated number on the scale of 0 to 1 is greater than the corresponding formation (P_{form}) or resuscitation (P_{res}) constant probabilities, respectively.

In the "Substrate Formation" case, the probability of a live cell converting to a persister cell is calculated by the equation:

$$P_{SubIn} = K_{form} \cdot \Delta t \cdot \left(1 - \frac{C_S}{C_{Bulk}}\right) \tag{1}$$

where P_{SubIn} is the *calculated* probability that the live cell will convert, K_{form} is the *maximum* probability that a live cell will convert to a persister cell per timestep, Δt is the size of each timestep, C_S is the local substrate concentration, and C_{Bulk} is the bulk substrate concentration. Mathematically, the equation states that where lower concentrations of substrate prevail, a live cell has a higher probability of converting to a persister cell. The probability of persister formation is zero when substrate is abundant.

In the "Substrate Resuscitation" case, the probability of a persister cell resuscitating to a live cell is calculated by the equation:

$$P_{SubOut} = K_{res} \cdot \Delta t \cdot \left(\frac{C_S}{C_{Bulk}} \right) \quad (2)$$

where P_{SubOut} is the *calculated* probability that the persister cell will resuscitate and K_{res} is the *maximum* probability that a persister cell will resuscitate to a live cell per timestep. Persister cells resuscitate more rapidly when substrate is abundant and resuscitate more slowly when the substrate concentration is low. In both formation and resuscitation cases, the calculated probability is checked against a random number between 0 and 1. If the calculated probability is greater than the random number, the cell switches to the alternate state. All the possible cell switching probabilities are presented in Table 4-2. The probability values are chosen to give a persister population of 1% of the total live cell population.

Table 4-2. Parameters associated with persister formation and resuscitation probabilities.

Parameter	**Symbol**	**Value**
Maximum probability for RR persister formation	P_{form}	0.0015
Maximum probability for RR persister resuscitation	P_{res}	0.15
Maximum probability for SR persister formation (hr^{-1})	K_{form}	0.0015
Maximum probability for SR persister resuscitation (hr^{-1})	K_{res}	0.15
Maximum probability for RS persister formation (hr^{-1})	K_{form}	0.0000857
Maximum probability for RS persister resuscitation (hr^{-1})	K_{res}	0.15
Maximum probability for SS persister formation (hr^{-1})	K_{form}	0.0000857
Maximum probability for SS persister resuscitation (hr^{-1})	K_{res}	0.00857
Calculated probability for Substrate-augmented persister formation	P_{SubIn}	Variable
Calculated probability for Substrate-augmented persister resuscitation	P_{SubOut}	Variable
Local substrate concentration (g/m^3)	C_S	Variable
Bulk Substrate Concentration (g/m^3)	C_{Bulk}	8.0

The disparity between the maximum probabilities for the random and substrate mechanisms arises due to unequal persister densities when the probabilities are equivalent. A substrate-dependant mechanism in our model, due to the current set of parameters and the existence of the boundary layer, will create roughly seventeen times more persisters than a purely random mechanism. In order to create equal numbers of persisters for the sake of comparison, specific probabilities have been reduced to 17.5 times less than the purely random mechanism probabilities.

Model Analysis

One set of six simulations was performed for each persister mechanism and also for the control (no persister cells). The simulations ran for 900 simulated hours. An antimicrobial dose lasting 48 hours was introduced at hour 375, after the colony had reached an established steady state.

Antimicrobial action on live and persister cells occurred by checking the probability that a cell would die during the timestep against a randomly generated number between 0 and 1. For all simulations the probability of live cell death due to the presence of the antimicrobial agent was 0.6838 for a one hour interval. This value corresponds to a 6-log reduction in non-growing suspended cell cultures in a twelve hour treatment period and is calculated by solving the following equality:

$$(1-P)^{12} = 10^{-6} \tag{3}$$

where P is the probability of killing. Mathematically, this equation states that a live bacterial cell within BacLAB has a million-to-one chance of surviving a 12 hour treatment.

Persister cell death due to antimicrobials follows the same procedure with the probability of death at 0.0034 per one hour interval. This leads to a 4% chance of death for each persister cell over the course of a 12 hour treatment. In both cases, if the calculated probability is greater than the randomly generated number, the cell dies.

We have chosen five different metrics for analyzing the results obtained during this study: structure, live cell density, persister cell density, log reduction of live cells, and persister locations. The resulting structures that arise from the random and substrate-dependant mechanisms will be compared to determine the effects of the differing mechanisms. Also, the consequences, if any, that the individual persister mechanisms have on structure, detachment, and regrowth will be evaluated.

The viable cell densities (obtained from the sum of persisters and live cells) will be plotted to show the severity and rapidity of overall cell loss during the antimicrobial treatment, as well as how adept the mechanism is at providing the biofilm with a means of regrowth after the antimicrobial treatment.

Likewise, the persister cell densities will be plotted to show the severity and rapidity of persister loss during the antimicrobial treatment, as well as the behavior of the persister population immediately after the treatment has ended.

Plots of the log reductions of live cells will be used to determine if the mechanisms produce the hallmark biphasic kill curve of a persister-forming biofilm.

Finally, the distribution of persisters with respect to their heights above the substratum will be graphed to determine the effects, if any, of spatial persister aggregation on biofilm survival.

In addition to these five metrics, a figure showing a representative simulation for each mechanism will be provided exhibiting the relationship between live, dead, and persister cells throughout the entire length of a simulation.

The percentage of persisters at the treatment start, viable cell log reductions, and recovery as a function of the viable cell counts before the treatment will be tabulated and compared to determine the effectiveness of each mechanism at protecting the biofilm.

Results

To reiterate, our purpose in this study was to determine and compare the effects of differing formation and resuscitation strategies on persister-related protection of biofilms. The four mechanisms we studied included random and/or substrate-dependent probabilities for persister formation and resuscitation. The four mechanisms were Random Formation-Random Resuscitation (RR), Random Formation-Substrate Resuscitation (RS), Substrate Formation-Random Resuscitation (SR), and Substrate Formation-Substrate Resuscitation (SS). We evaluated each mechanism with respect to structure, live cell density, persister cell density, log reduction of live cells, and persister spatial distribution.

Structure

A structural comparison at 25 hours before (timestep 350) and 77 hours after (timestep 500) the antimicrobial treatment, and at the end of the simulations (timestep 900) for each mechanism (RR=Random In-Random Out, RS=Random In-Substrate Out, SR=Substrate In-Random Out, SS=Substrate In-Substrate Out) is shown in Figure 4-2.

Live cells are shown in green, dead cells in purple, and persister cells in blue. This comparison is an attempt to determine the effect of different persister formation mechanisms on the resulting structure of the biofilm. At time 350, all the structures are very similar. At timestep 500, the SS simulation retains a small cluster (green circle) that appears to have detached from each of the other simulations. This small cluster will detach as well, as can be seen by its absence in timestep 900. Of the six simulations performed for the RR mechanism, the simulation shown is the only one that was able to successfully revive the colony after the antimicrobial treatment. The SR mechanism had no simulations that recovered. Both the RS and SS simulations returned to pre-treatment, or near-pre-treatment, levels by the end of the simulation, though with differing results. The clusters of the RS simulation are isolated; no one cluster is in contact with any other. In comparison, the SS simulation shows paired clusters in most instances. As a comparison, the figure reveals no appreciable effect on structure with the inclusion of persisters at the levels provided in these mechanisms.

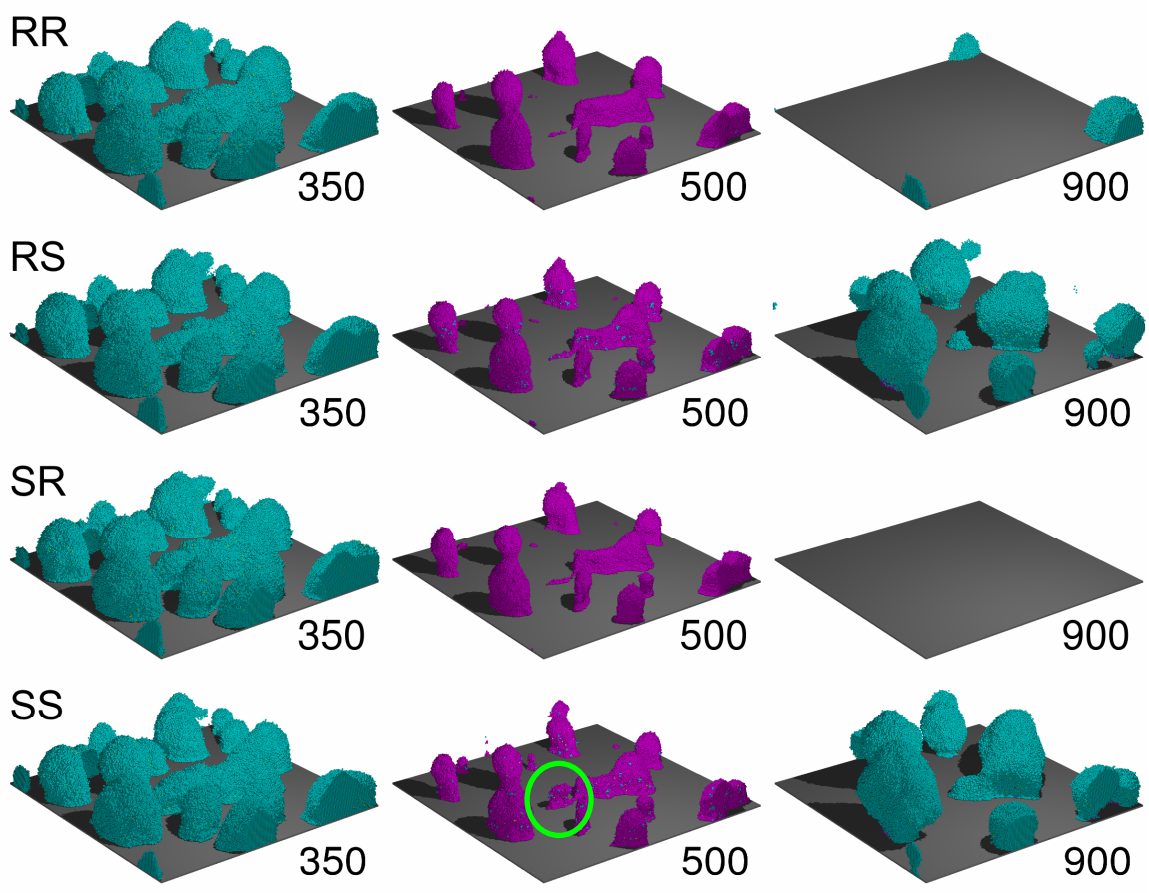

Figure 4-2. Structural comparison of each persister mechanism. Live cells (green), persister cells (blue), and dead cells (purple) are shown at 350 hours (25 hours before the antimicrobial treatment), 500 hours (77 hours after the antimicrobial treatment), and 900 hours (final timestep).

Viable Cell Density

Figure 4-3 shows areal cell densities of viable cells (persister and live cells) during the course of six simulations for each mechanism (RR=Random In-Random Out, RS=Random In-Substrate Out, SR=Substrate In-Random Out, SS=Substrate In-Substrate Out). Control simulations that had no persisters are shown in gray. Each control simulation was eradicated within 12 hours of the start of the treatment. All persister mechanisms were able to provide enough protection to endure the treatment with non-

zero numbers of viable cells at the end of the treatment. The RS and SS mechanisms recovered completely from the treatment, while only one RR simulation moderately recovered and no SR simulations recovered. Each SR simulation was able to survive the treatment with some viable cells intact, but could not muster enough growth to revive the colony. The RR mechanism had one of its six simulations recover and return to a logarithmic growth pattern, but did not reach pre-treatment density before the end of the simulation. Each of its other five simulations survived the treatment, but were unable to permanently restore the population.

All simulations for both the RS and SS mechanisms were able to make complete recoveries and attained pre-treatment, or near pre-treatment, densities within an average of 360 hours and 381 hours, respectively, after the treatment completion. The curves for RS and SS are all clearly biphasic, with the only difference between the two mechanisms being the behavior immediately after the antimicrobial treatment. The RS simulations continued sharply downward, followed by reentry into a logarithmic growth phase after seven hours. The SS simulations continued downward at a slower pace, and likewise returned to a logarithmic growth phase after 45 hours in somewhat of a lag phase.

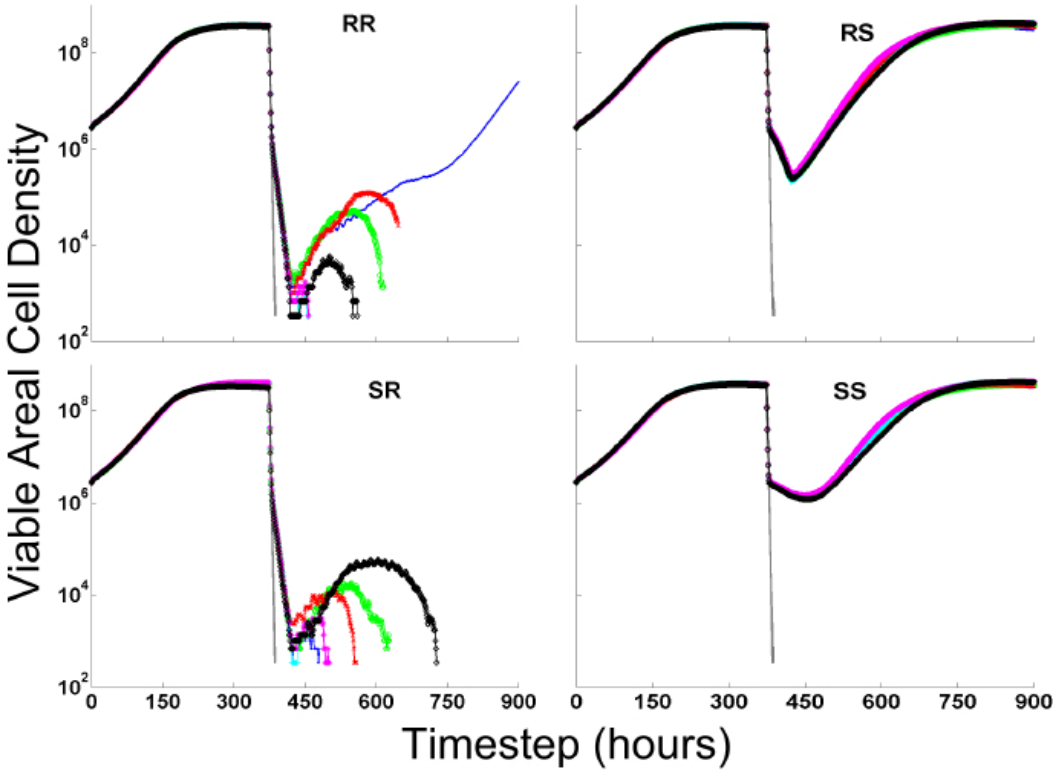

Figure 4-3. Viable areal cell densities (live cells and persister cells) throughout all simulations for each mechanism and also the control simulations (gray curves).

Persister Areal Cell Density

The persister areal cell densities for each mechanism (RR=Random In-Random Out, RS=Random In-Substrate Out, SR=Substrate In-Random Out, SS=Substrate In-Substrate Out) are provided in Figure 4-4 at 50 hours before the antimicrobial treatment, during the 48 hour treatment (bound by the yellow area), and 52 hours after the cessation of the treatment. Note that all simulations included roughly two million persister cells/cm^2 at the start of the antimicrobial treatment.

The RS and SS mechanisms had a much slower loss of persister cells than the SR and RR mechanisms. The mechanisms show a steady (SR,RR) or slightly increasing

(RS,SS) persister density in the 50 hours leading up to the antimicrobial dose. The antimicrobial treatment produced logarithmic loss of persister cells for all mechanisms, though in very different magnitudes. When the persister resuscitation is governed by only random chance (RR, SR), the antimicrobial treatment decimates the persister population to fewer than 350 cells/cm^2 (four-log reduction). When the persister resuscitation is dependent on the local substrate concentrations, the antimicrobial effect caused between a half-log reduction (SS) and a one-log reduction (RS). In these same simulations of Substrate Out mechanisms (RS,SS), persister density continued to decrease logarithmically, at the same rate as that during the treatment, well after the end of the treatment. Persister loss was not biphasic for any mechanism.

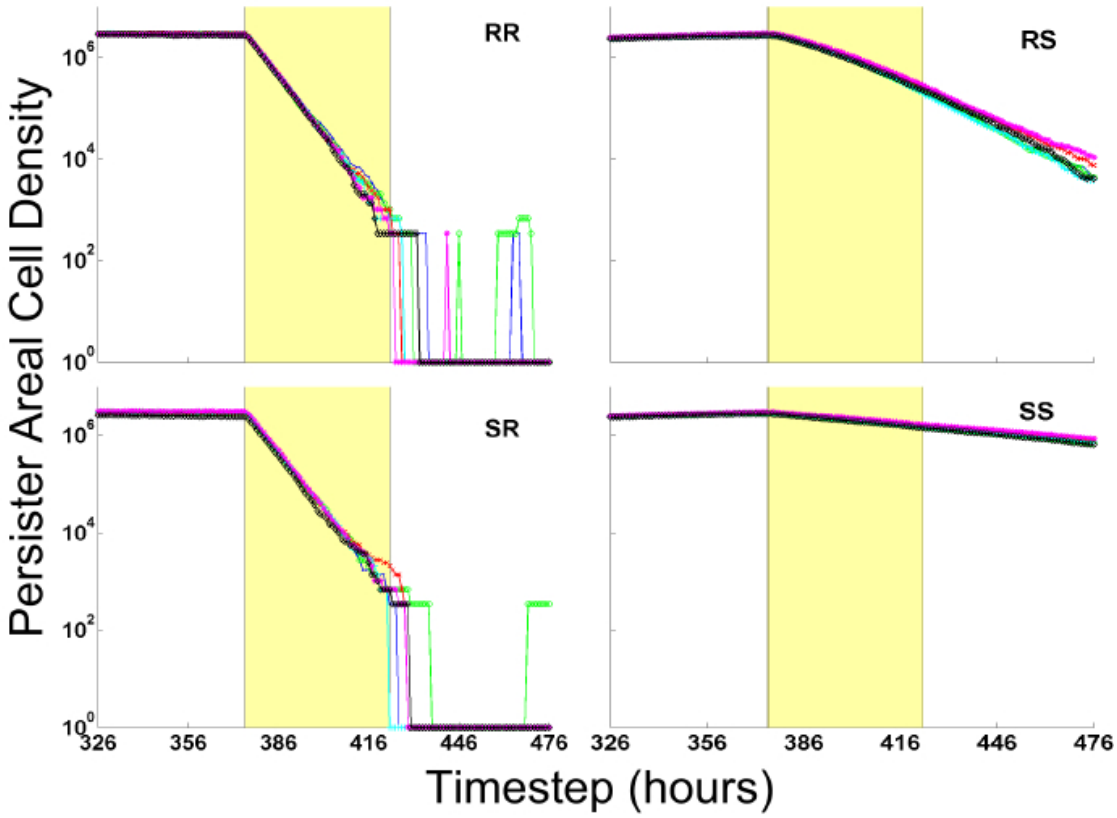

Figure 4-4. Persister areal cell densities for each mechanism preceding, during, and after the antimicrobial dose.

Log Reduction of Live Cells

The live cell log reductions during the antimicrobial treatment (375 hours to 423 hours) for each mechanism (RR=Random In-Random Out, RS=Random In-Substrate Out, SR=Substrate In-Random Out, SS=Substrate In-Substrate Out), along with the corresponding control simulations (gray curves) are shown in Figure 4-5. Note that this figure addresses only log reductions of live cells, and does not include persister cells. Each control simulation was completely eradicated during the first 12 hours of the

antimicrobial treatment. All persister mechanisms provided the hallmark biphasic curve typically attributed to the persister-related response to antimicrobials. The biphasic shape occurs due to the resuscitation of persisters, which supports the live cell count in the later stages of the dose. Initially, rapid killing of cells lead to a three log reduction, or larger, of live cells for each mechanism within the first six to ten hours of the treatment. Following this fast, primary phase of cell loss was a decelerated, secondary loss of live cells. Each set of mechanisms responded differently with respect to the amount of time spent in the two phases of the biphasic loss. In all, reductions of live cells were six-log for RR and SR, four-log for RS, and 4.5-log for SS. The slight, upward slopes for RS and SS at the end of their curves are occurring after the treatment has ended (hours 424 and 425). No significant live cell increases occurred during the treatment itself.

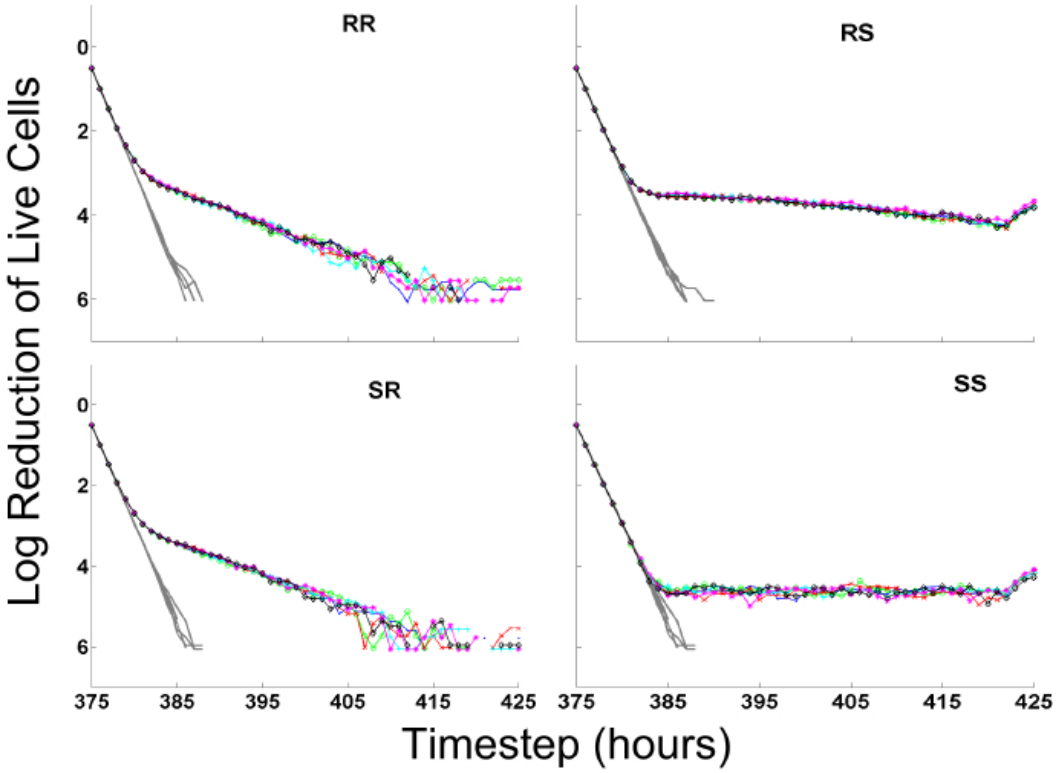

Figure 4-5. Log reductions of live cells for each mechanism and the control simulations during the antimicrobial treatment (timesteps 375 through 423).

Persister Placement and Aggregation

Figure 4-6 gives the distribution of persisters (x-axis) with respect to their height above the substratum (y-axis) at timestep 375, immediately preceding the antimicrobial treatment. The figure shows how persisters were distributed for each mechanism; longer horizontal bars correspond to a higher percentage of the total persister population at that height above the substratum. The RR mechanism showed the most uniform distribution of persisters, with the bulk of the biofilm containing 1.5% to 3% of the persister population. The SR mechanism gave a similar result, but did have increasing percentages closer to the lower, substrate poor regions. Both the RS and SS mechanisms were

different from the RR and SR mechanisms in that the majority of the persister population resided in the lower levels of the biofilm. In these mechanisms, the lower 30um contained roughly 70% of the total persister population, compared to roughly 45% for the RR and SR mechanisms.

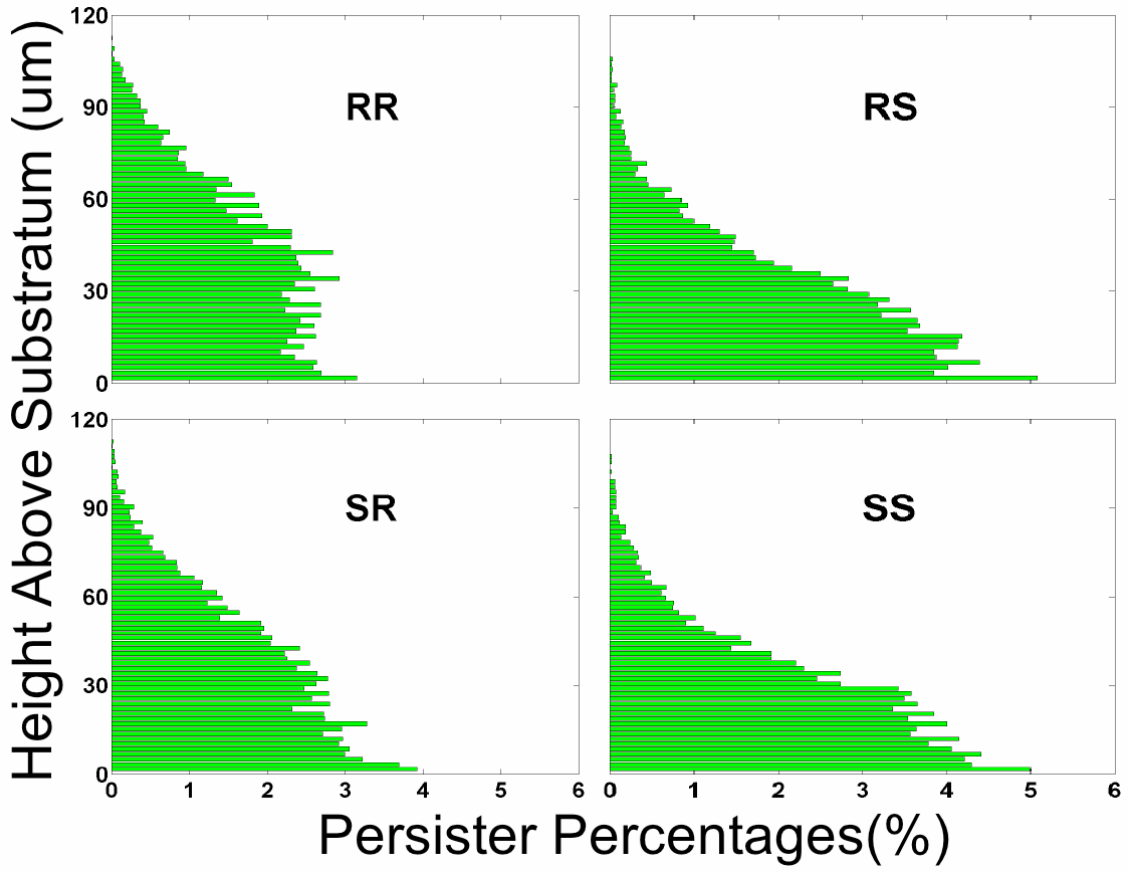

Figure 4-6. A comparison of persister placement between each of the four mechanisms immediately preceding the antimicrobial treatment (timestep 375). The figure shows the vertical distribution of persisters as a percentage of the total persister population.

Representative Areal Cell Densities

Areal cell densities of live (green), persister (blue), and dead (black) cells in Figure 4-7 show the relationship between each of the three types of cells included in the

simulations. Only one representative simulation is shown for each mechanism. Prior to the antimicrobial treatment, each live cell curve was nearly identical. Persister populations were all equal to zero at the start of the simulations. Persister cell formation was accelerated in the Random Out simulations (RR,SR), reaching a steady state of roughly two million cells/cm^2 two hundred hours before the antimicrobial treatment; Substrate Out simulations (RS,SS) reached the same density immediately preceding the treatment. During the first hour of the 48 hour antimicrobial treatment (bound by the yellow area), 68 percent of live cells were immediately converted to dead cells. For the Random Out mechanisms (RR,SR) live cell and persister cell densities dropped precipitously at the start of the treatment to only a few hundred cells. Both the Random Out mechanisms (RR,SR) attempted a repopulation via standard live cell growth, but the small resurgence was not enough to fully revive the colony; with no support from the persister population, all live cells were detached due to erosion. However, both the Substrate Out mechanisms (RS,SS) are able to withstand the treatment, and subsequently restore the population to pre-treatment levels. The sudden increase in live cells two hours after the treatment ended, exhibited by the RS and SS mechanisms, is due to both the resuscitation of persister cells and the normal growth of the remaining live cells.

Dead cells were governed by the same detachment rules as live and persister cells. In RR and SR, as the biofilm became sparse, dead cells were completely removed, primarily due to convective action of the surrounding fluid. Dead cells in RS and SS had a similar removal pattern up to ~200 hours after the treatment ends; however, as live cells

regenerate the biofilm convective effects lessened and dead cell removal slowed significantly. A summary of the results provided in this study can be found in Table 4-3.

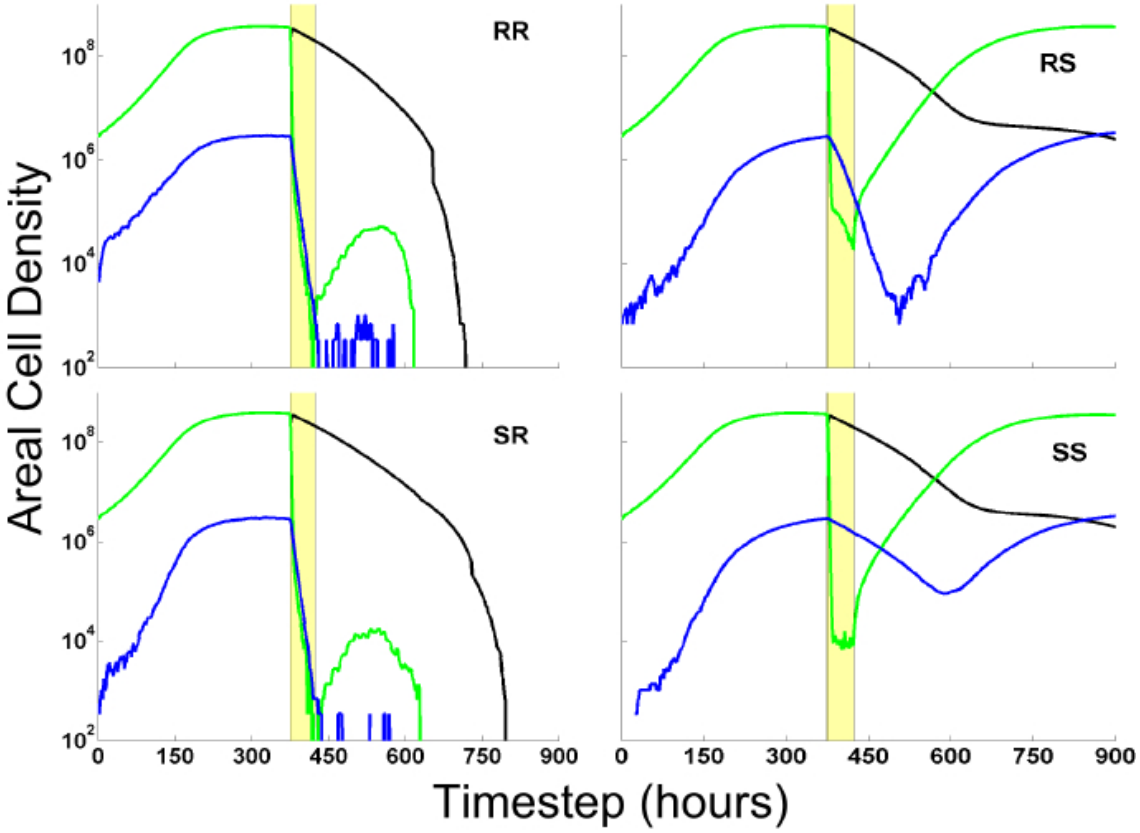

Figure 4-7. A single representative simulation for each mechanism showing live (green curves), persister (blue curves), and dead cell (black curves) areal cell densities. The yellow area represents the duration of the antimicrobial treatment.

Table 4-3. Averages for percent of persisters with respect to live cells immediately prior to antimicrobial treatment, log reductions of viable cells at the termination of the 48 hour dose period, and maximum percent recovery after the end of the antimicrobial treatment with respect to viable cell densities preceding the antimicrobial treatment.

Mechanism	% Persisters at 374 hours	Viable Log Reductions	% Recovery
RR	0.78%	5.64	1%
SR	0.77%	5.75	0%
RS	0.76%	3.16	105%
SS	0.78%	2.38	103%
Control	0.00%	Eradicated	0%

Discussion and Conclusions

The current study intimates that substrate resuscitation mechanisms (RS and SS) have an advantage over random resuscitation mechanisms (SR, RR) due to their much slower rate of persister resuscitation. These substrate-dependent resuscitation mechanisms lead to scenarios where only persisters that are formed at the biofilm/bulk fluid interface are likely to resuscitate at any appreciable rate. Even then, when the boundary layer is in effect, the maximum rate of persister resuscitation is roughly a fourth the rate of a random resuscitation mechanism due to the existence of substrate gradients (Figure 4-8). Persisters in a completely starved state have no chance at resuscitating, thus allowing a substrate resuscitation mechanism the opportunity to build a reserve of persisters in the inner, securely attached, substrate starved regions of the biofilm cluster. This is counter to a random resuscitation mechanism, where there is no significantly concentrated region of persister reserves. These characteristics lead to substrate resuscitation mechanisms where persisters remain in their current state for much longer periods, thus allowing them to easily survive a 48 hour treatment of antimicrobials.

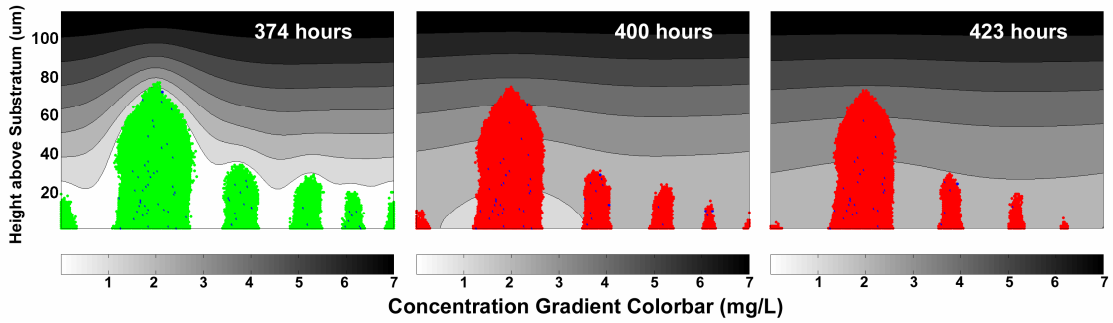

Figure 4-8. The changing concentration gradients before (374 hours), during (400 hours) and at the end of the antimicrobial treatment (423 hours) using the SS mechanism. The figure shows that despite the absence of actively growing cells during the antimicrobial treatment, a concentration gradient still exists due to the boundary layer. The lowest concentration of substrate during the treatment occurs in hour 423, and is slightly greater than 2mg/L.

Also, when an antimicrobial treatment has ceased, mechanisms relying on substrate-dependent persister formation benefit from a flood of substrate into the inner regions of the biofilm as live cells in the outer echelons of the biofilm are killed. Higher substrate levels correlate to lower numbers of live cells going into persisters, thereby allowing more live cells to stay in their actively growing state, repopulating the biofilm faster. However, such an effect could also provide for an optimal occasion to dose the biofilm with a second round of antimicrobials. Without any persisters, it would seem that the biofilm could be eradicated based on these results. No simulations were performed to test this hypothesis.

The two contrasting aspects shown by the RS and SS mechanisms are the lag phase after the initial drop in viable cells during the treatment, and the difference in the speed of recovery (Figure 4-3). The RS simulations began the regrowth almost immediately due to the resuscitation of ~90% of persister cells within 25 hours of treatment end, while only ~29% of persisters in SS resuscitate within the same period.

This is a striking difference that results despite the mechanisms being controlled by the same resuscitation probabilities.

During the antimicrobial treatment, the Substrate Formation-Random Resuscitation mechanism was especially ill-equipped to survive the treatment. Any persisters formed in the lower levels of the biofilm were resuscitating at a constant rate, in addition to the influx of substrate to the previously substrate-poor, persister laden interior of the biofilm. This, in turn, caused the formation of persisters to slow. The complete absence of persister cells for nearly 50 hours after the antimicrobial treatment in the SR simulations was due to the prevalence of substrate in all levels of the colony.

The Random Formation-Random Resuscitation mechanism on the whole can be said to provide protection from the antimicrobial treatment, but in only one case was it able to repopulate the biofilm after the treatment ended. Examination of the persister locations and images of the RR simulations did not lead to any differences between the one simulation that survived the treatment and the other simulations that did not survive. The slight inflection in this one surviving colony's growth curve suggested that this colony could have just as easily shared the same fate as the other RR simulations and surrendered to the detachment forces that prematurely ended the other RR simulations, as well as all of the SR simulations.

For all mechanisms, it did not appear that the method and speed of detachment of dead cells contributed appreciably to the restoration of the colony. In most cases, regrowth occurred sufficiently enough to reseed the biofilm colony, despite the fact that nearly all of the cells in the SR and RR simulations eventually detached. However, the

presence of dead cells after the antimicrobial treatment undoubtedly provided a moderate amount of protection from the convective detachment forces that might otherwise remove some of the live and persister cells in the RS and SS simulations in a similar manner as occurred in the RR and SR simulations.

Detachment did cause massive loss of viable cells after the antimicrobial treatment in the RR and SR mechanisms. Due to the mostly random placement of the persisters, these mechanisms were unable to obtain persister pockets close enough to the substratum to be securely attached during regrowth (Figure 4-6). It may be possible that such a large, cohesive group of viable cells suddenly thrust into the surrounding system could be a source of metastasis within the host organism. It is believed that in some biofilm infections, a successful removal of the biofilm from a particular area, especially around an in-dwelling device, can be followed by the same type of infection appearing in another area entirely (10, 34). We submit that biofilms employing a persister mechanism much like the SR or RR mechanism could lead to such an effect.

Additional Simulations (10%, 100%, and 500%)

An additional set of simulations was performed in order to determine how the absolute values of the maximum probabilities affected biofilm recalcitrance in the BacLAB model. The simulations were performed with the Random Formation-Random Resuscitation mechanism: 1) normal probabilities of formation and resuscitation (0.0015 and 0.15, respectively), 2) probabilities that are 10 percent of the normal values (0.00015 and 0.015, respectively), and 3) probabilities that were 500 percent of the normal values (0.0075 and 0.75, respectively). The results, shown in Figure 4-9, demonstrate how

survival is intrinsically linked to the absolute values of the formation and resuscitation probabilities, and not necessarily the ratio of the two. Most importantly, these results, along with the results from the RS and SS mechanisms, show that any mechanism which severely slows the resuscitation of persisters will provide a very tolerant biofilm. Interestingly, the simulation with probabilities at 10 percent the normal values resembles the Substrate Formation-Substrate Resuscitation mechanism. The SS mechanism essentially had the same, slowed formation and resuscitation probabilities, though the driving force was mechanistically different.

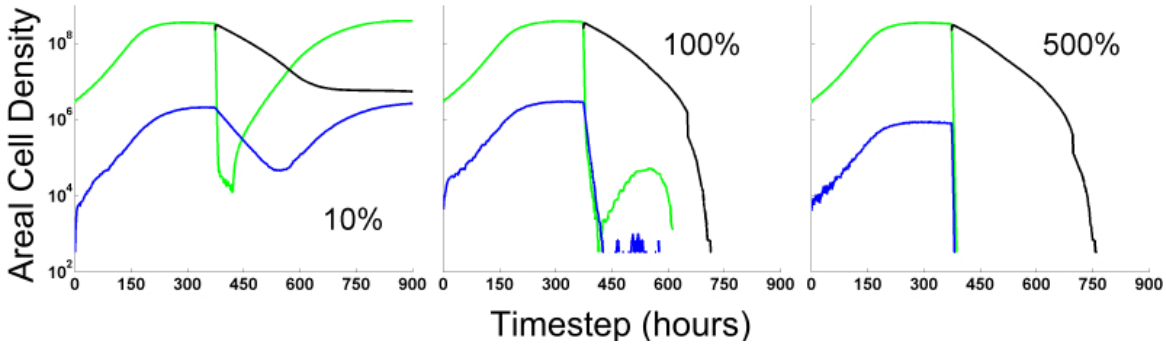

Figure 4-9. Live and Persister Areal Cell Densities with formation and resuscitation probabilities at the normal rate, 10% of the normal rate, and 500% of the normal rate.

After performing all of the simulations and analysis, it now seems intuitive that if persisters remain dormant for very extended periods, then the biofilm as a whole will be much more tolerant to antimicrobial challenges. Nevertheless, we are unaware of a similar conclusion explicitly stated in any previous modeling study. If, however, the persisters remain too long in their dormant state, detachment forces may eventually remove them before they resuscitate. A future study may include an analysis of repopulation versus duration of persister states.

Possibly, if persister switching truly is tied to growth rate, and growth rate slows as a biofilm cell ages, then as a biofilm on the whole ages it will maintain persisters in their persister state longer, particularly in the interior of the clusters where substrate is limited. Another interesting, future study could track cell age as a function of location and the corresponding durations spent in the persister versus live cell state.

References

1. Balaban, N. Q., J. Merrin, R. Chait, L. Kowalik, and S. Leibler. 2004. Bacterial persistence as a phenotypic switch. Science 305:1622-1625.

2. Brooun, A., S. H. Liu, and K. Lewis. 2000. A dose-response study of antibiotic resistance in *Pseudomonas aeruginosa* biofilms. Antimicrobial Agents and Chemotherapy 44:640-646.

3. Chambless, J. D., S. M. Hunt, and P. S. Stewart. 2006. A three-dimensional computer model of four hypothetical mechanisms protecting biofilms from antimicrobials. Applied and Environmental Microbiology 72:2005-2013.

4. Chambless, J. D., and P. S. Stewart. 2007. A three-dimensional computer model analysis of three hypothetical biofilm detachment mechanisms. Biotechnology and Bioengineering 97:1573-1584.

5. Cochran, W. L., G. A. McFeters, and P. S. Stewart. 2000. Reduced susceptibility of thin *Pseudomonas aeruginosa* biofilms to hydrogen peroxide and monochloramine. Journal of Applied Microbiology 88:22-30.

6. Cogan, N. G. 2006. Effects of persister formation on bacterial response to dosing. Journal of Theoretical Biology 238:694-703.

7. Correia, F. F., A. D'Onofrio, T. Rejtar, L. Y. Li, B. L. Karger, K. Makarova, E. V. Koonin, and K. Lewis. 2006. Kinase activity of overexpressed HipA is required for growth arrest and multidrug tolerance in *Escherichia coli*. Journal of Bacteriology 188:8360-8367.

8. Das, J. R., M. Bhakoo, M. V. Jones, and P. Gilbert. 1998. Changes in the biocide susceptibility of *Staphylococcus epidermidis* and *Escherichia coli* cells associated with rapid attachment to plastic surfaces. Journal of Applied Microbiology 84:852-858.

9. Eberl, H. J., C. Picioreanu, J. J. Heijnen, and M. C. M. van Loosdrecht. 2000. A three-dimensional numerical study on the correlation of spatial structure, hydrodynamic conditions, and mass transfer and conversion in biofilms. Chemical Engineering Science 55:6209-6222.

10. Fux, C. A., S. Wilson, and P. Stoodley. 2004. Detachment characteristics and oxacillin resistance of *Staphyloccocus aureus* biofilm emboli in an in vitro catheter infection model. Journal of Bacteriology 186:4486-4491.

11. Guerillot, F., G. Carret, and J. P. Flandrois. 1993. Mathematical-model for comparison of time-killing curves. Antimicrobial Agents and Chemotherapy 37:1685-1689.

12. Halme, A., S. Bumgarner, C. Styles, and G. R. Fink. 2004. Genetic and epigenetic regulation of the FLO gene family generates cell-surface variation in yeast. Cell 116:405-415.

13. Harrison, J. J., R. J. Turner, and H. Ceri. 2005. Persister cells, the biofilm matrix and tolerance to metal cations in biofilm and planktonic *Pseudomonas aeruginosa*. Environmental Microbiology 7:981-994.

14. Hunt, S. M., M. A. Hamilton, J. T. Sears, G. Harkin, and J. Reno. 2003. A computer investigation of chemically mediated detachment in bacterial biofilms. Microbiology-Sgm 149:1155-1163.

15. Hunt, S. M., E. M. Werner, B. C. Huang, M. A. Hamilton, and P. S. Stewart. 2004. Hypothesis for the role of nutrient starvation in biofilm detachment. Applied and Environmental Microbiology 70:7418-7425.

16. Keren, I., N. Kaldalu, A. Spoering, Y. P. Wang, and K. Lewis. 2004. Persister cells and tolerance to antimicrobials. Fems Microbiology Letters 230:13-18.

17. Keren, I., D. Shah, A. Spoering, N. Kaldalu, and K. Lewis. 2004. Specialized persister cells and the mechanism of multidrug tolerance in Escherichia coli. Journal of Bacteriology 186:8172-8180.

18. Klapper, I., P. Gilbert, B. P. Ayati, J. Dockery, and P. S. Stewart. 2007. Senescence can explain microbial persistence. Microbiology 153:3623-3630.

19. Korch, S. B., T. A. Henderson, and T. M. Hill. 2003. Characterization of the hipA7 allele of *Escherichia coli* and evidence that high persistence is governed by *(p)ppGpp* synthesis. Molecular Microbiology 50:1199-1213.

20. Kussell, E., R. Kishony, N. Q. Balaban, and S. Leibler. 2005. Bacterial persistence: A model of survival in changing environments. Genetics 169:1807-1814.

21. LaFleur, M. D., C. A. Kumamoto, and K. Lewis. 2006. Candida albicans biofilms produce antifungal-tolerant persister cells. Antimicrobial Agents and Chemotherapy 50:3839-3846.

22. Lewis, K. 2005. Persister cells and the riddle of biofilm survival. Biochemistry-Moscow 70:267-+.

23. Lewis, K. 2007. Persister cells, dormancy and infectious disease. Nature Reviews Microbiology 5:48-56.

24. Lewis, K. 2001. Riddle of biofilm resistance. Antimicrobial Agents and Chemotherapy 45:999-1007.

25. Noguera, D. R., S. Okabe, and C. Picioreanu. 1999. Biofilm modeling: Present status and future directions. Water Science and Technology 39:273-278.

26. Picioreanu, C., M. C. M. van Loosdrecht, and J. J. Heijnen. 1998. A new combined differential-discrete cellular automaton approach for biofilm modeling: Application for growth in gel beads. Biotechnology and Bioengineering 57:718-731.

27. Ramage, G., S. Bachmann, T. F. Patterson, B. L. Wickes, and J. L. Lopez-Ribot. 2002. Investigation of multidrug efflux pumps in relation to fluconazole resistance in *Candida albicans* biofilms. Journal of Antimicrobial Chemotherapy 49:973-980.

28. Rani, S. A., B. Pitts, and P. S. Stewart. 2005. Rapid diffusion of fluorescent tracers into *Staphylococcus epidermidis* biofilms visualized by time lapse microscopy. Antimicrobial Agents and Chemotherapy 49:728-732.

29. Roberts, M. E., and P. S. Stewart. 2005. Modelling protection from antimicrobial agents in biofilms through the formation of persister cells. Microbiology-Sgm 151:75-80.

30. Shah, D., Z. G. Zhang, A. Khodursky, N. Kaldalu, K. Kurg, and K. Lewis. 2006. Persisters: a distinct physiological state of E-coli. Bmc Microbiology 6:9.

31. Stewart, E. J., R. Madden, G. Paul, and F. Taddei. 2005. Aging and death in an organism that reproduces by morphologically symmetric division. Plos Biology 3:295-300.

32. Szomolay, B., I. Klapper, J. Dockery, and P. S. Stewart. 2005. Adaptive responses to antimicrobial agents in biofilms. Environmental Microbiology 7:1186-1191.

33. Vazquez-Laslop, N., H. Lee, and A. A. Neyfakh. 2006. Increased persistence in *Escherichia coli* caused by controlled expression of toxins or other unrelated proteins. Journal of Bacteriology 188:3494-3497.

34. Wilson, S., M. A. Hamilton, G. C. Hamilton, M. R. Schumann, and P. Stoodley. 2004. Statistical quantification of detachment rates and size distributions of cell clumps from wild-type (PAO1) and cell signaling mutant (JP1) *Pseudomonas aeruginosa* biofilms. Applied and Environmental Microbiology 70:5847-5852.

35. Wiuff, C., R. M. Zappala, R. R. Regoes, K. N. Garner, F. Baquero, and B. R. Levin. 2005. Phenotypic tolerance: Antibiotic enrichment of noninherited resistance in bacterial populations. Antimicrobial Agents and Chemotherapy 49:1483-1494.

CHAPTER 5

CONCLUSIONS

This dissertation presented the results of three separate biofilm computer modeling studies concerned with antimicrobial tolerance of biofilms, biofilm detachment, and persister protection mechanisms of biofilms. The research objectives outlined in Chapter 1 were addressed in the three manuscripts included in Chapters 2, 3, and 4. Included here is a short summary of the results and conclusions from each body chapter, a discussion on the contributions the current dissertation has made to biofilm research, future work and experiments that would also be valuable, and improvements that could be made to the current model.

Summary of Results

In Chapter 2, I performed simulated experiments with the 3D computer model to investigate four mechanisms of protection from antimicrobial agents in biofilms: poor antimicrobial penetration, deployment of adaptive stress responses, physiological heterogeneity in the biofilm population, and the presence of phenotypic variants or persister cells. When compared to simulations of unprotected biofilms, all four hypothetical mechanisms explored in this study provided some level of protection. Taken separately, the mechanisms produced distinct killing curve shapes and non-uniform spatial patterns of survival and cell type distribution.

The investigation described in Chapter 3 incorporated three different detachment mechanisms into the model: fluid shear, detachment resulting from substrate limitation,

and surface level erosion. The three mechanisms, and a combination mechanism comprised of the three separate mechanisms, represented various physical and biological influences hypothesized to affect biofilm detachment. The detachment mechanisms demonstrated diverse behaviors with respect to biofilm structure, the existence of a steady state, the propensity for sloughing events, and the dynamics during starvation. The fluid shear mechanism produced flat, steady state biofilms that lacked sloughing events. Detachment based on substrate limitation produced significant sloughing events. The resulting biofilm structures included distinct, hollow clusters separated by channels. The erosion mechanism produced neither a non-zero steady state nor sloughing events. The combined mechanism produced mushroom-like structures. The results showed that the choice of specific detachment pathway alone can significantly influence biofilm structure and dynamic behavior.

Four different combinations of random and substrate-dependant persister switching mechanisms were described in Chapter 4. The purpose of that study was to determine and compare the effects of differing formation and resuscitation strategies on persister-related protection of biofilms. I found that substrate resuscitation mechanisms had an advantage over random resuscitation mechanisms due to their much slower rate of persister resuscitation. Through further analysis of the results, including two additional simulations where persister switching was both slowed and accelerated, I concluded that biofilms with persisters remaining in the dormant state for extended periods will realize superior antimicrobial tolerance.

It would be interesting to determine if this same conclusion held, had the simulations been performed with the substrate limited detachment mechanism from Chapter 2. Extending the amount of time a cell is in the dormant persister state would certainly increase the survival rate of persisters, no matter what detachment mechanism were employed. The results of Chapter 4 showed that the combined detachment mechanism permitted the accumulation of persisters deep within the biofilm. This, in turn, allowed the persisters to be near enough to the substratum after the antimicrobial dose to secure a solid foundation for regrowth. The crux of the matter, though, is whether or not the persisters are vulnerable to detachment forces while they are non-growing. The combined detachment mechanism continually detaches biofilm cells even when the local substrate concentrations are high, unlike the substrate limited detachment mechanism. If a cell were dormant for a much extended duration, it would seem that erosive forces from the combined mechanism would eventually remove the cell from the model space before it reverted. This would lead one to believe that if some persisters existed near the substratum, and the substrate limited detachment mechanism was in use, the low-level persisters would have ample substrate available for regrowth without being subjected to the erosive forces of the combined mechanism. Ultimately, I believe the combined detachment mechanism fosters the best conditions leading up to regrowth, while the substrate-limited detachment mechanism more enables the actual process of regrowth.

The detachment mechanism used in the study for Chapter 2 affected the results of the penetration mechanism as well. If the combined mechanism were substituted for the substrate limited detachment mechanism in Chapter 2, denser biofilms may result,

possibly making the antimicrobial penetration mechanism one of the better protection strategies instead of the worst. However, all results are still subject to the modeler's estimates for the antimicrobial diffusion and consumption parameters. A moderate decrease in the antimicrobial consumption rate, e.g., could likely bring about the same results despite a denser biofilm.

In a similar vein, if the subject of susceptibility during dispersal were evaluated in the results of Chapter 4 as they were in Chapter 2, the conclusions for each of the persister mechanisms may be dissimilar. Substrate dependent persister mechanisms like those employed in Chapter 4 would create less persisters than the random mechanism of Chapter 2 due to the increased substrate availability in the dispersed state. The abundance of substrate would essentially reduce to zero the live cell conversion to persisters, while persister reversion to live cells would quicken. If an antimicrobial dose occurs long enough after dispersal that no persisters remained, the dispersed culture would be completely susceptible to an antimicrobial challenge.

Overall, the methods used to generate these simulations are inherently flawed since they are subject to the modeler's whim. For instance, the substrate limited detachment mechanism depends on a cell being continuously at or below an arbitrary level of substrate for an arbitrary amount of time before detaching. Is this any more or less defensible than a combined mechanism where detachment is programmatically forbidden from the interior of clusters and erosion only occurs when a cell has fewer than an arbitrary number of neighbors? In nearly all mathematical models lie assumptions, both right and wrong, simple and complex, from which the behavior of the model's

constituents emerge. Therefore, it does not seem appropriate to judge a model based on its methods alone. The evaluation of a model is best determined by its utility in fostering new hypotheses that can be tested in a laboratory setting.

Taken as a whole, the results summarized here lend to the idea that both the method of protection and the method of detachment are important in the overall picture of biofilm recalcitrance. One can be greatly affected by the other in several circumstances.

Contribution to Biofilm Research

One of the most important advantages of the cellular automata approach is that this inherently visual, rule-based structure can be readily communicated to the experimenters concerned with biofilms. That is, the rules that are used to describe the behavior of individual cells can be readily phrased in terms that are accessible to individuals from a broad range of technical backgrounds. One of the valuable contributions I have made working the model is to serve as a vehicle for dialogue between engineers, mathematicians, biologists, medical scientists, and clinicians.

In each investigation conducted in this body of work, more than one hypothetical mechanism was employed to explain different biofilm phenomena. Studies of antimicrobial tolerance (Chapter 2) and persister protection (Chapter 4) both included four hypotheses, while the detachment investigation (Chapter 3) included three. I submit that a multi-faceted approach is the most efficient way to elucidate an understanding of the unknown mechanisms of biofilm persistence and detachment.

One aspect of the detachment study in Chapter 3 characterized the dynamic behavior of simulated biofilms in response to starvation. In starvation mode, growth was

eliminated and the dynamic behavior was determined by detachment and decay processes alone. This was an analysis of which we are aware of no precedent in the literature. We intimate that this could lead to an experimental design for gathering clues about the nature of the detachment process. For example, it may be possible to discriminate between detachment dominated by shear and detachment dominated by substrate limitation with such a starvation experiment.

The results provided in Chapter 2 may be helpful in designing laboratory experiments to elucidate protective mechanisms in biofilms. One suggested experiment allowed for the coincident measure of the shape of killing curves, the spatial pattern of antimicrobial action within the biofilm, and the relative susceptibility of resuspended biofilm cells. Though there are extant methods for measuring each of these features, we were aware of no single study in which all three had been performed concurrently.

Future Work

While I feel that all of my objectives have been met during the course of the investigations presented, the process of accomplishing these objectives has lead to new ideas regarding biofilm tolerance. The two proposed modeling studies listed here could provide additional momentum for determining the role of persister cells in the recalcitrance of biofilms. Both studies would require minor modification to the cell-tracking methods in the model.

Additional Experimentation

- Repopulation versus Persister State Duration – The results shown in Chapter 4 demonstrated a definite link between longer persister dormancy times and the ability of a subpopulation of persisters to reseed a biofilm colony. It would be interesting to run a set of simulations that could help determine the effectiveness limits for the duration of persister dormancy. It seems that longer periods in the persister state increase the probability of a repopulation, but at what point is the dormancy so long that the persisters are washed away by detachment forces? Obviously the effects of simulated detachment mechanisms are dependent on the coefficients that influence their action and will vary to match different flow patterns, rates, etc. Nonetheless, there is a definite interplay between detachment and persister protection, and studying the relationship between detachment and persister dormancy durations could certainly be another intriguing step in this narrative.
- Cell Age, Persisters, and Locations – Are the oldest cells in a biofilm always located in the lowest levels of the biofilm? If persister cells need to be located near the substratum in order to guarantee adhesion during regrowth, then is it a reasonable assumption that old cells are more likely to be persister cells? The concept of older, “senescent”, cells equating to persister cells has been proposed by Klapper, et al. (2007). This second proposed modeling study would build upon their results and attempt to answer these questions by using the 3D model to track

cell age and the corresponding amount of time spent in the persister state as a function of location within the biofilm.

Potential Improvements to the Existing Model

- Multigrid Method – Due to the size of the model's lattice (typically 300 x 300 x 200 = 18 million nodes), a significant portion (greater than 95%) of the time required to complete a simulation is devoted to simultaneously solving the fast-Fourier transform of the reaction-diffusion equation for each individual node and for each diffusing solute. With current computer hardware and only one diffusible component in the model space, a simulation can be completed in roughly 24 hours. When performing the antimicrobial penetration experiments in Chapter 2, the same simulations required nearly 36 hours. It may be possible to considerably reduce this time requirement by incorporating a nonlinear multigrid method that decreases the number of iterations necessary for each solution of the reaction-diffusion equation (Press, et al. 1997). Other modeling groups have shown that the multigrid method scales linearly with the size of the system being modeled (N), as opposed to N^2 for a fixed-grid method like the one presently in use (Picioreanu, et al. 2004).
- Fluid Dynamics - The erosion and shear mechanisms rely on detachment probability equations as a substitute for modeling the convective forces applied to a true biofilm. Including a computational fluid dynamics package that could solve the fluid flow problem around the biofilm would benefit the model. Detachment could then be a function of the local shear stress acting on individual cells.

Implementation would require checking the local forces on each cell against a cellular-level parameter describing “cohesiveness”.

- Graphical User Interface - An improvement that would immediately affect biofilm researchers interested in biofilm modeling would be to incorporate an interactive, graphical interface that provides real-time model tracking and 3D visuals of the model space. At this time, the model is modified, compiled, and executed entirely via a DOS-style terminal. Parameters and options must be hard-coded into the model itself or included in an input file, neither of which can be altered during a simulation. Such a setup necessitates a moderate understanding of terminal commands, and a significant familiarity with the model’s code. Restructuring the model with a user interface could eliminate these barriers, and allow more traditional physical science researchers to easily incorporate a computer model component into their research cycle. Also, as improvements in computer hardware continue to decrease the effective run-time for a simulation, the stochastic aspect of the model and real-time user interaction could create innumerable sets of customized results.
- Web Accessible - The ability to access research tools via a local network or over the internet is becoming a necessity. Such a transfer for the current model may advance biofilm model usage and the dissemination of knowledge about biofilms. Examples of online biofilm research tools are the Center for Biofilm Engineering’s *Biofilms Hypertextbook* (http://www.erc.montana.edu/biofilmbook/) and the *Monospecies 2D Biofilm*

Model provided by Delft University's Environmental Biotechnology Group (http://www.biofilms.bt.tudelft.nl/frameworkMaterial/monospecies2d.html). Coupling a web accessible 3D biofilm model with the site traffic of the Center's website could produce a very popular, powerful tool for biofilm exploration and may even foster research partnerships.

References

1. Klapper I, Gilbert P, Ayati BP, Dockery J, Stewart PS. 2007. Senescence can explain microbial persistence. Microbiology 153(11):3623-30.

2. Picioreanu C, Kreft JU, van Loosdrecht MCM. 2004. Particle-Based Multidimensional Multispecies Biofilm Model. Applied and Environmental Microicrobiology 70(5):3024-3040.

3. Press, WH, SA Teukolsky, WT Vetterling, and BP Flannery. 1997. Numerical recipes in C: the art of scientific computing, 2nd ed. Cambridge University Press, New York, N.Y.